SHORELINE VARIATION AND BEACH ROTATION OF PAUANUI BEACH

A thesis submitted in partial fulfilment
of the requirements for the degree

of

Master of Science
in Earth and Ocean Sciences

By

Renée A. Foster

THE UNIVERSITY OF
WAIKATO
Te Whare Wānanga o Waikato

University Of Waikato
2012

Abstract

Shoreline variation over short, medium and long term time scales is well studied and documented. Rotation studies however have only focused on the phenomenon occurring on embayed beaches. This type morphological change is known to be caused by variations in wave climate such as wave approach direction and energy flux. Rotation studies on other beach classifications are limited, specifically on the potential of harbour adjacent beaches to rotate. Given the highly variable nature of estuaries and their impact on sediment supply to these flanking beaches, rotation could be exacerbated and aggravate existing localised erosion as a result. This thesis uses a video imagery shoreline dataset to determine the shoreline variation and beach rotation of Pauanui Beach, a harbour adjacent beach. Comparisons are then made to neighbouring Tairua Beach, an embayed beach.

The shoreline over 2002, 2003 and 2004 displayed variation at short, medium and long term scales. Large wave events exceeding 4 m in significant wave height eroded beach profiles until accretion occurred during lull periods. Alongshore uniformity of this erosion pattern was not consistent throughout the timeseries at both beaches indicating the phenomenon of beach rotation. Pauanui transects moved in unison with each other, while an out of phase relationship existed between the Tairua transects. Seasonal changes in wave climate also influenced shoreline change however consistent cycles were not evident at both Pauanui and Tairua until 2004 where summer accretion and winter erosion dominated. The effects of ENSO were also observable in the long term where the shoreline gradually accreted with the long term negative ENSO index. Pauanui accretion quantity was much larger than Tairua over the same period. Rotation phenomenon at Pauanui was caused by a strong variation in cross shore shoreline position while Tairua demonstrated a strong out of phase behaviour at either end of the beach. Wave models were generated to determine the effect of islands inshore of the generating conditions. Shadowing effects were highly

noticeable on the wave climate projected onto the beach, affecting the rotation and mean shoreline position. Alongshore currents were generated which affected the sediment transport to these rotated areas of beach.

Based on these results, the two beaches responded similarly during erosion, accretion and rotation events. Alongshore uniformity does not exist alongshore of the two beaches as wave climate variations are created by the offshore island.

Acknowledgements

First and foremost I would like to extend my gratitude to my supervisor Dr Karin Bryan. Your constant support, help and kindness has been fantastic during this, at times, tedious and challenging period. Your passion for the coastal area is inspiring and I have enjoyed getting to know you. Thank you for all the opportunities you have given me throughout, it has been enjoyable.

I would also like to thank Dr Giovanni Coco from NIWA for initially giving me the opportunity to take on this project, as well as Dr Iain MacDonald for taking on the role as my secondary supervisor. Your generous support and ever extended helping hand is much appreciated. Thank you.

To my fellow students in the Coastal Marine Group, thank you for all the laughs, support and ongoing help, and to those who let me assist on your field work and get out of the dungeon, it was a great change of pace! Thanks for letting me take the opportunity to take part in your research. It was great to get to know you all.

I need to say an incredible thank you to all those organisations that helped fund my thesis. Waikato Masters Research Scholarship, Environment Waikato and the Department of Conservation (Dr Stella Frances Scholarship), and the Broad Memorial Fund.

My biggest thank you goes to my family. Mum and Dad you have been amazing, thank you for your encouragement and ever extended helping hands. I could not have done it without you. Alyssa, thanks for being there when I needed you, you're the best. Ben, your positive enthusiasm, patience (especially when showing you crazy gibberish graphs) and support has been overwhelming, thanks for everything, it means a lot.

Table of Contents

List of Figures

List of Tables

Chapter One -

Introduction

1.1 INTRODUCTION

Shoreline variation is a phenomenon that can severely threaten coastal property during extreme erosive or rotation phases. Shoreline variation over short, medium and long term time scales is well studied and documented regularly in literature. Rotation has also been well studied although only on embayed beaches. Rotation refers to the movement landward or seaward of either beach end caused by the erosion or accretion of sediment respectively (Figure 1.1). Severe movement can trigger the need for detailed coastal management especially if private or public dwellings are put under pressure. This type of morphological change has been well studied on embayed beaches and is known to be caused by variations in wave climate such as wave approach direction and energy flux (Bryan *et al.,* 2009; Klein *et al.,* 2002; Ranasinghe *et al.,* 2004; Ruiz de Algeria-Arzaburu & Masselink, 2010; Thomas, *et al.,* 2010; Thomas *et al.*, 2011). Rotation studies on other beach classifications are limited, specifically on the potential of harbour adjacent beaches to rotate and the associated hydrodynamic forcing. Given the highly variable nature of estuaries and the impact on sediment supply to these flanking beaches, rotation could be exacerbated and aggravate existing localised erosion.

Anthropogenic activities such as deforestation and the development of transport infrastructure, are assisting in elevating the quantity of sediment, pollutants and nutrients released into estuaries through increased run-off (Hart & Bryan, 2008). Longer retention times of sediment within the estuary effectively blocks the natural transport systems to inlet flanking beaches and can actively starve the nearshore zone. Pauanui Beach is one of these harbour adjacent beaches as the Tairua Estuary inlet terminates at the northern end of the beach. Minimal

research currently exists focusing on the Pauanui-Tairua Beach system, therefore little detail is known about beach variability over long time periods. Local authority Waikato Regional Council has monitored areas of the beach with profiling since 1975, however the dataset does not provide appropriate temporal and spatial resolution needed for detecting in-depth processes and patterns. With the introduction of two Cam-Era video image stations in 1999, long term image datasets have been created that cover the entire spatial length of Pauanui Beach. Analysis into this dataset has been extremely limited until the present and knowledge about phenomenon occurring over large time scales is relatively unknown.

This thesis therefore aims to determine the shoreline variability and the erosion and accretion phenomenon known as beach rotation at Pauanui Beach. Several research initiatives already exist on neighbouring Tairua Beach, thus providing a comparative case study. Tairua is an embayed beach that also experiences beach rotation and is known to be influenced by shadowing from offshore Shoe Island (Gallop, 2009). It needs to be determined whether Pauanui is also affected by this shadowing effect generating rotation by alongshore variation in energy flux, or whether rotation is caused by other phenomenon such as wave generated alongshore currents caused by waves propagating at an angle to the beach.

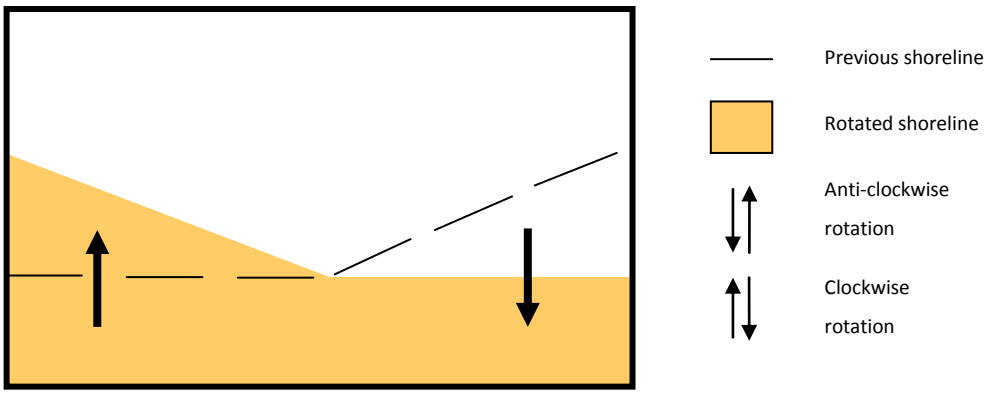

Figure 1.1: Schematic diagram indicating the rotation process.

1.2 STUDY SITE

Pauanui Beach is the focal point for research throughout this thesis, however a comparative study will be conducted on nearby Tairua Beach. Tairua has been well studied particularly in recent years with many articles detailing rip current dynamics, beach rotation and shoreline and barline coupling (Bogle *et al.*, 2000; Bryan *et al.,* 2009; Gallop *et al.*, 2009).

1.2.1 Pauanui Beach

Located on the eastern coast of the Coromandel Peninsula is the sand dune barrier beach Pauanui. At approximately 2.9 km long, the beach is blocked from the south by Pauanui Mountain headland and sheltered from the north by Paku Hill. Tairua Harbour discharges at this northern end (Figure 1.2) while a small tributary stream exits at the southern end. The surrounding catchment is approximately 282.35 ha (hectares) with the area of the Tairua Harbour at high tide to be approximately 6.12 $x10^6$ m^2; a relatively small harbour size compared to the catchment (Wood, 2010). Pauanui consists of fine sand sized sediment (246 µm) and has an intermediate beach classification, although it is slightly more dissipative due to its low beach slope angle (Wood, 2010). Waves dominate from more north-easterly and easterly directions with significant wave heights being around 1.5 m. This can exceed 6 m during storm conditions. It is also probable that the beach is affected in some degree by shadowing from Shoe Island, offshore to the north east.

1.2.2 Tairua Beach

The tombolo embayed beach Tairua is separated from Pauanui Beach by Paku Hill and the Tairua Harbour entrance. The beach is approximately 1.6 km long consisting of medium to coarse sand sized 427 µm (Gallop *et al.*, 2009). Beach orientation is 53^0 resulting in a more northerly direction than Pauanui Beach's orientation (Wood, 2010). Tairua varies between longshore bar and trough beach state and transverse-bar and rip beach state (Bogle *et al.,* 2001). Classification varies according to the patterning and coupling of the shoreline and sandbar. These features are then compared to the Wright and Short model descriptions where

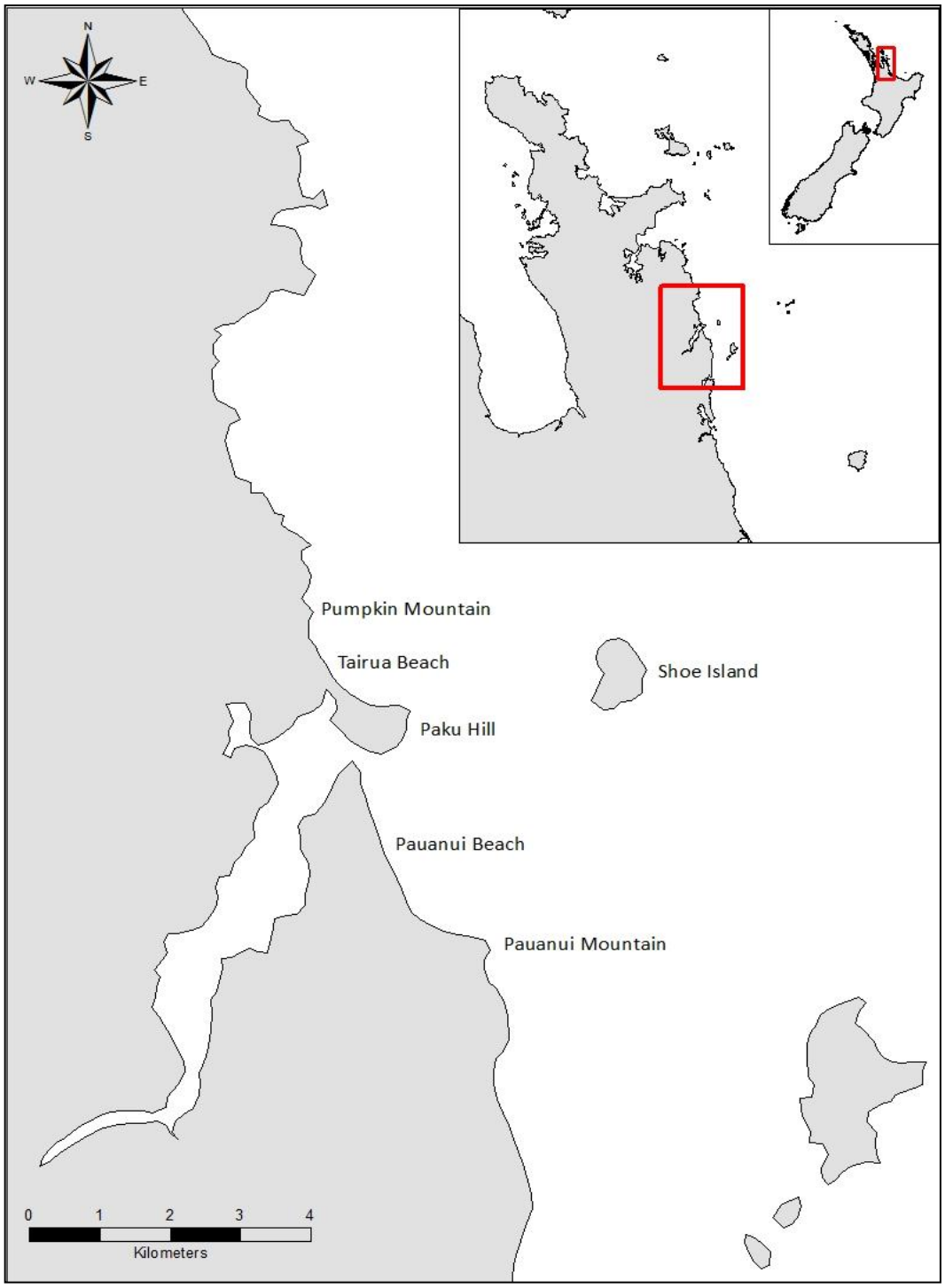

Figure 1.2: Pauanui and Tairua Beaches are located on the eastern Coromandel Peninsula, North Island, New Zealand. Tairua Beach is located to the north of Pauanui Beach while the Tairua Estuary terminates at the northern end of Pauanui. Offshore Shoe Island and Slipper Island are to the north-east and south east respectively of Pauanui Beach.

the ability to determine the correct beach state from the two states is tested (Wood, 2010). Longshore bar and trough state occurs during higher wave energy at Tairua and results in the shoreline and barline being largely separated. There is also a decrease in the linear patterning that is shown in relation to each other. A transverse-bar and rip state instead occurs during normal summer conditions (Bogle *et al.,* 2000) and is determined when the shoreline and barline are closer to each other. Tairua has a steep beach face making it reflective at times with a neap tidal range of 1.2 m and spring tidal range of 2 m. Cam-Era monitoring systems are also set up at Tairua on Paku Hill at a 70.5 m above chart datum in a northward facing direction. Tairua Beach experiences the same wave and meteorological conditions as Pauanui (Salmon, 2008).

1.3 THESIS OBJECTIVES

Objectives of the thesis are to determine the morphological response of Pauanui Beach in relation to its hydrodynamic forcing, by identifying and measuring the shoreline variability. Variability is defined as the lack of uniformity the surf and swash zones experience over time as they are continually changing in response to factors such as wave climates and meteorological conditions. Processes of erosion and accretion are ultimately generated as a result, thus causing beach rotation.

Following identification and analysis of the shoreline at Pauanui, results will be compared to the previously studied Tairua Beach. Comparisons will be made to determine similarities of short term and long term cyclical patterns experienced at the two different beaches. This is of interest to establish whether these patterns are similar on the two beaches or not, as they experience very similar wave climates but are of different classification as presented by the Wright and Short (1984) model.

Therefore, the objectives of this thesis are to:

1. *Develop numerical analysis techniques using a series of purposely designed algorithms to extract shoreline variations from video images through RGB colour intensities within the time-averaged video image. These shorelines will be used to characterise erosion, accretion and rotation on Pauanui Beach.*

2. *Determine beach erosion, accretion and rotation change by analysing a beach profiling dataset. Results will then be used to verify video image results.*

3. *Develop a SWAN wave model of the Tairua-Pauanui Embayment, using WWIII wave hindcast data as input conditions, in order to model the potential wave climate experienced at the Pauanui-Tairua area during the period over which the video dataset extends.*

4. *Compare results found at Pauanui to those already researched at Tairua to determine similarities (or not) between the two beaches that are within close proximity to each other and experience similar wave climates, but are classified differently.*

1.4 THESIS OUTLINE

The following outline briefly describes each proposed adjoining chapter from this point onwards.

Chapter Two – Video Imaging and the Cam-Era Dataset

Background information is detailed on video imaging techniques and the requirements undertaken to ensure the Cam-Era dataset is accurate for analysis. Methods in how to correct for camera movement and image rectification are described along with the process to identify the shoreline.

Chapter Three – Shoreline Patterning and Beach Rotation

Following the identification of the shoreline, in depth analysis is completed on the dataset to understand patterning and rotation events. Shoreline results from the video images are also compared and validated against a beach profiling dataset in this chapter. Focusing on storm events and major rotation shifts, wave climate modelling can be completed to potentially understand this behaviour.

Chapter Four – Wave Climate Modelling

Chapter Four examines the development of wave modelling in order to determine the wave climate at the Pauanui and Tairua area. Offshore island interactions with wave climate are explained, including the alongshore energy flux along the beach. Models are run in conjunction with shoreline rotation and storm events.

Chapter Five – Tairua Beach Comparison

Analysis completed on the Pauanui dataset is then done on the Tairua dataset. Comparisons of beach rotation and modelled wave climates are used to determine whether the beaches behave similarly.

Chapter Six – Conclusion

Overall summary of the results within previous chapters is detailed in Chapter Six. Suggestions for further research associated to this study are also elaborated within this chapter.

Chapter Two -

Video Imaging and the Cam-Era Dataset

2.1 INTRODUCTION

This chapter describes the video imaging monitoring system, image dataset, and pre-processing techniques. Images, once collected by the Cam-Era system, have to be amended and processed for any discrepancies such as camera movement or poor image visibility prior to analysis. Each individual processing step is elaborated on and examples provided.

2.2 VIDEO IMAGING BACKGROUND

Beach morphology is highly dynamic and it continuously changes over a wide range of spatial and temporal scales (Lippmann & Holman, 1990; Plant & Holman, 1997). Beach elevation change of 1 m to 10 m can occur within weeks to months while change of less than a metre can occur within minutes (Plant & Holman, 1997). Morphological changes, although highly variable, generally follow a pattern whether seasonal or annual (Lippmann & Holman, 1990). It is important to focus and understand these cycles in order to characterise any potential risk to property in the future. Conventional techniques like beach profiling and *in situ* instrumentation may not generate enough detail on long term patterns and the overall variability at the large temporal and spatial scales needed (Holland *et al.,* 1997; Plant & Holman, 1997; Smit *et al.*, 2007). Older instrumentation such as the deployment of instruments into the nearshore zone, specifically the surf zone, can return negative results. Instruments may become exposed and vulnerable to high energy storm conditions that potentially causing damage (Lippmann & Holman, 1989), instruments also are put at risk of being vandalised by the general public. Due to the *in situ* location, more than one instrument

would be required if large scale monitoring were to occur, increasing the potential damage risk as well as overall expense.

Monitoring near-shore coastal environments with video imaging is an increasingly popular alternative to traditional oceanographic measuring techniques. Imaging technology provides large scale coverage of beaches and surf zones with long term timeseries capabilities, without the interference of the harsh marine environment (Alexander & Holman, 2004). Long term image data provide details of varying morphodynamic patterning needed for increased understanding of coastal processes used within coastal management (Turner *et al.*, 2006). Video monitoring programs consist of a camera located above a certain beach location to record a timeseries of images every day light hour (Alexander & Holman, 2004). Some locations have multiple cameras overlooking several adjoining areas of the beach; these images are then merged to increase the monitoring spatial scale and resolution (Alexander & Holman, 2004). Timeseries photographs are gathered over a specific period usually between 10 and 15 minutes and are then processed by averaging every image to create a time exposure image (Lippmann & Holman, 1989). Any features associated with individual waves are removed in this type of image and features that are coupled with underlying bathymetry are amplified through white colours generated by wave breaking (Plant *et al.,* 2007). Processing can then occur which can be used to monitor changes in morphology and hydrodynamics within nearshore zones through identifying shorelines and barlines for example (Alexander & Holman 2004). This is done through the design of algorithms that target specific analysis areas.

2.3 Cam-Era DATASET

Cam-Era video monitoring developed by NIWA (National Institute of Water and Atmospheric Research) is a similar system to the commonly-used ARGUS video monitoring. Video technology is used to systematically monitor two beaches along the Coromandel Peninsula (Pauanui and Tairua) that are both within close proximity to each other. Pauanui and Tairua have been monitored for similar

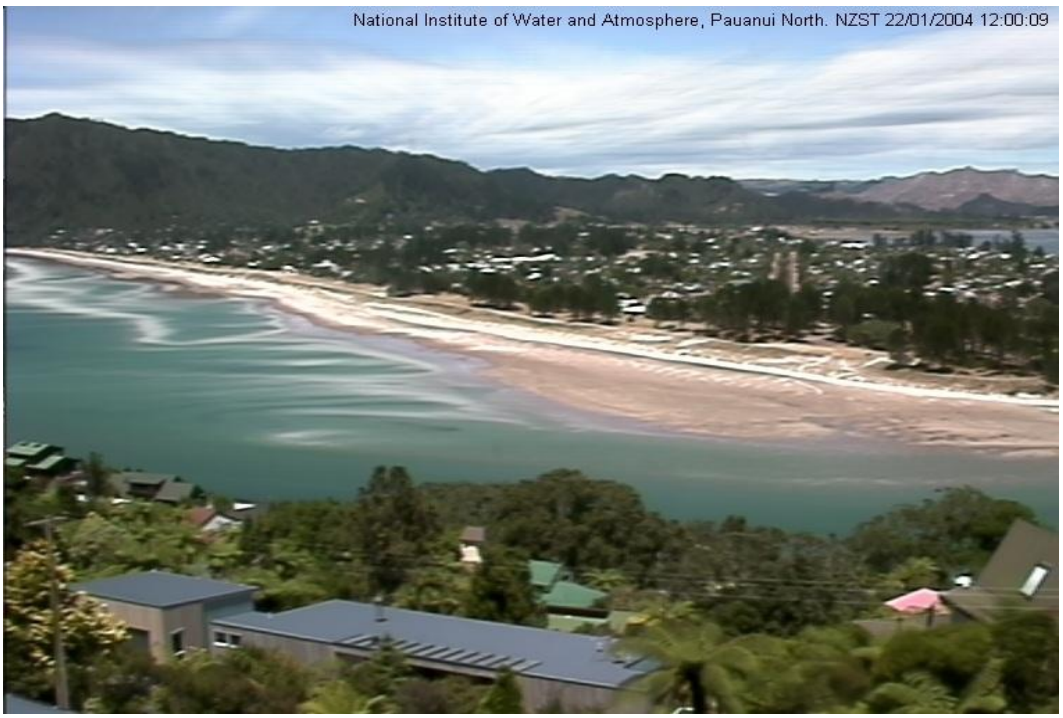

Figure 2.1: 15 minute time averaged image taken at the northern Pauanui Cam-Era video imaging station on Paku Hill (22/01/2004 at 12.00 pm).

Figure 2.2: 15 minute time averaged image taken at the southern Pauanui Cam-Era video imaging station on Pauanui Mountain (22/01/2004 at 12.00 pm).

time periods. The Cam-Era system is permanently positioned at the northern and southern ends of Pauanui Beach, as well as the southern end of Tairua Beach. The Tairua camera and one of the Pauanui cameras (Figure 2.1) are mounted to various houses on Paku hill at 70.5 m and 76.1 m above chart datum respectively, while the southernmost camera located on Pauanui mountain is located at an elevation of 122 m (Figure 2.2) (Salmon, 2008). Each camera is programmed to collect image snapshots every 1.57 seconds over a 15 minute time period. Snapshots are then averaged together by the onsite computer to create a time exposure image which is then sent via internet to the Hamilton NIWA laboratory and archived. Images are then displayed on the World Wide Web for the public to view.

Time constraints of this study meant a three year timeseries was selected from the 10 year dataset. Both northern and southern directed images comprise the overall dataset and initially it was assumed that these two images could be merged together for analysis. Upon merging it was determined that the southern camera alone provided a more detailed spatial resolution alongshore. The northern camera instead provided a detailed monitoring of the estuary mouth and was deemed unnecessary for this analysis. Therefore shoreline data was extracted from images collected by the Pauanui south camera, located on Pauanui Mountain.

2.4 IMAGE PROCESSING

2.4.1 Camera positions and movement

Video monitoring systems are permanently fixed to reduce major camera position shifts. Shifts in the cameras tilt, azimuth and swing angles alter the known camera parameters and positions which are used in rectification processes. Minute shifts can occur occasionally by exposure to weather phenomenon, however any major movement is likely to be caused by vandalism. Any movement to the mentioned angle positions need to be accounted for and corrected. If these movements are not, the rectification process is deemed incorrect and the grid co-ordinates assigned to the image, untrue.

Major shifts from trees or shrubs, vandalism or extreme weather, require field surveying of new GPS co-ordinates at known benchmarks and the re-positioning of the camera. However, minor changes can be overcome manually with designed algorithms. In order to check whether movement has occurred, algorithms are designed to visually display accurate ground control positions and the outline of Paku Hill. Control points are known locations of objects that are thought to not move throughout time, such as buildings, rooftops or trees. Movement is evident if the accurate control point positions do not match the location of the same control points within the image (Figure 2.3). Algorithms are designed to manually display these correct known points for comparison. The same algorithms allow for manual selection of the new locations if movement has taken place.

Some variety was noticeable in the northern located camera, while considerable movement was evident at times in the southern located camera. This correction must be accurate to reduce large error rates in measurement co-ordinates once added to the image during rectification.

Figure 2.3: Shown is an example when the tilt angle of the camera has changed slightly. Pink crosses indicate newly selected ground control points. Yellow crosses locate corrected image ground control points, and the location of Paku Hill.

2.4.2 Rectification

Image rectification refers to the transformation of an images two dimensional co-ordinates (*x, y*) into three dimensional, real world co-ordinates (X, Y, Z) (Aarninkhof *et al.* 2003; Lippmann & Holman, 1989). This process provides accurate spatial positioning of image features in metres, ensuring precise quantitative data can be extracted. The rectification algorithms associate a measured grid to the image by incorporating the known co-ordinates of ground control points and camera parameters (Holland *et al.,* 1997; Holman *et al.,* 1991; Salmon 2008). Camera parameters include internal characteristics, for example lens and camera type which are all used to determine resolution, distortion or focal length (Holland *et al.,* 1997). Any variation in camera position or system affects this rectified co-ordinate system by offsetting the known digitised points. Measurements extracted without these variations being resolved are inaccurate.

Raw images are captured at an oblique angle to the beach and are therefore not in a plan view. Rectification transformed these images from this original placement to a 'birds-eye-view' of the beach (Figure 2.4), using mean sea level (MSL) data associated with the time each image was collected. Tidal information from NIWA provided MSL data and allowed for the separation of images into shore versus bar images. The shorelines were most evident at 1 m above MSL (used for this study) while barlines are most evident at 0.5 m below MSL.

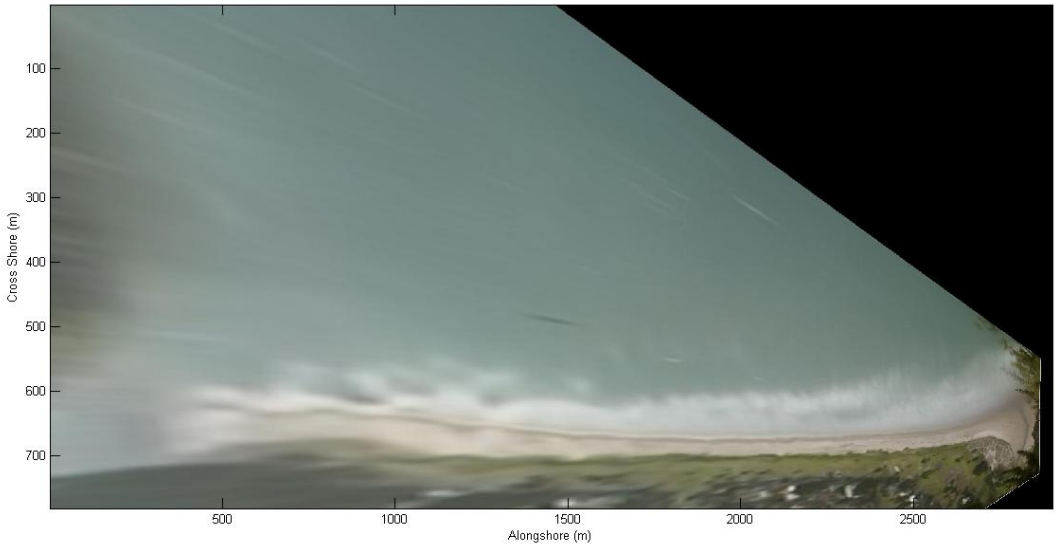

Figure 2.4: Rectified Pauanui South image taken on 02/03/2004 at 4.00 pm.

2.4.3 Image quality

Prior to shoreline detection, quality control of each image was completed. Weather may decrease visibility spatially, particularly during storm events and this is captured by the camera. It is not uncommon that the beach cannot be seen due to severe cloud or fog cover (Figure 2.5). Image quality may also succumb to raindrop distortion where cameras capture rain drops on the outer camera housing in front of the lens. These types of images are worthless during shoreline extraction and are therefore ignored.

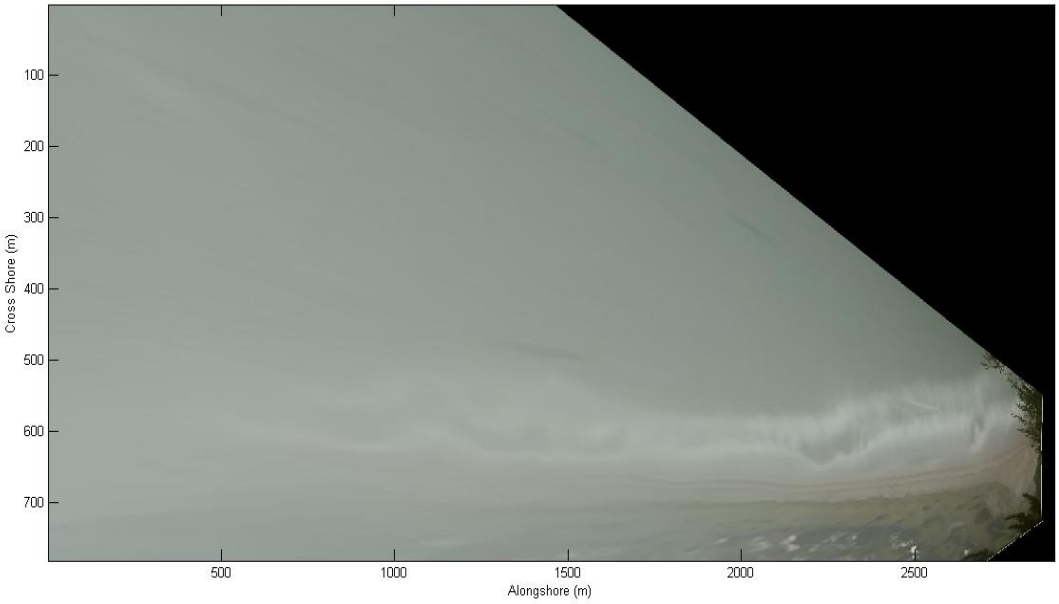

Figure 2.5: Poor quality rectified Pauanui South image taken on 06/02/2004 at 9.00 am.

2.5 SHORELINE DETECTION ALGORITHMS

The shoreline is defined as the margin between the surf zone and swash zone at high tide. The rectification process isolates images which meet the defined shoreline criteria using MSL information, taken from associated tidal data. Several shoreline detection techniques exist to identify and extract shoreline data, however this study uses the RGB colour ratio technique used and developed by Gallop (2009) and Salmon (2008).

Shoreline identification and extraction was completed by computer programme using the images three colour channels, red, green and blue (RGB). Selecting two zones, one each on land and sea, the ratio of red to green colour was determined. This ratio was used as a representation of the entire sand or water zone for that particular image. Sand areas due to the higher shell content should have a higher ratio of red colour, while water areas should have higher ratios of green (Gallop, 2009; Salmon, 2008). The shorelines were then identified as the margin between these two ratio values. However to prevent the programme searching the entire image for the shoreline, two outer limits (dcut1 and dcut2) were set (Figure 2.6). These limits extended seaward from the shoreline, and the other followed the vegetation line along the dune.

Colour intensities vary from image to image by factors such as weather or light availability. Ratio zones therefore have to be selected individually for each image to ensure the correct shoreline is identified. These variations in colour intensities also occur in the alongshore due to the spatial resolution of the camera. Objects in the far distance are not as colour definitive as objects closer to the camera. Manual correction of the shoreline must exist to prevent the false projection of the shoreline.

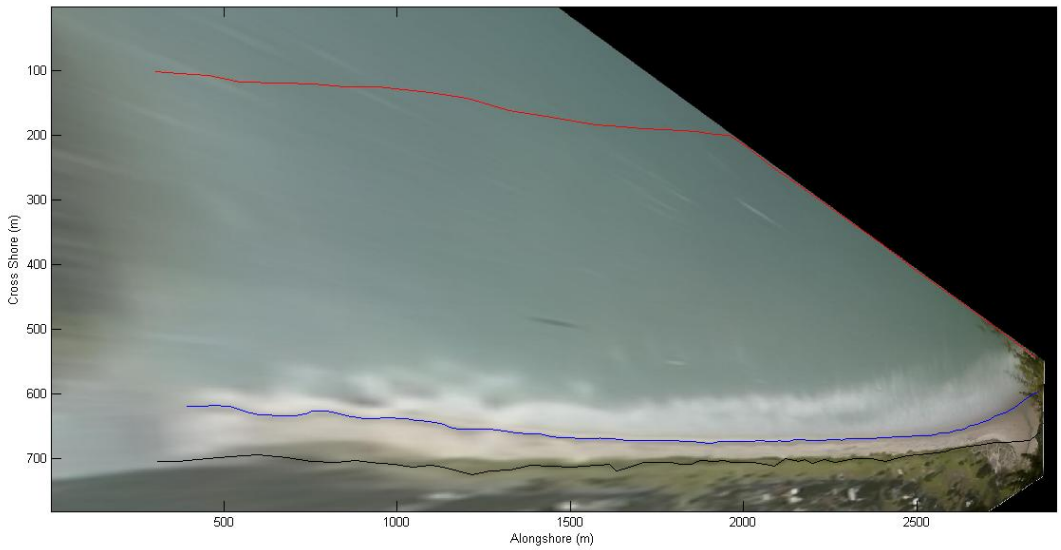

Figure 2.6: Rectified Pauanui South image taken at 02/03/2004 at 4.00 pm. Blue line is the identified shoreline found by the ratio of red to green light. Red (dcut1) and black (dcut2) lines are the outer limits for the programme to search within to identify the shoreline location.

2.6 SUMMARY

- Video imagery provides large spatial and temporal scale resolution to dataset collection. This has resulted in image monitoring becoming a popular alternative to *in situ* instrumentation (Aarninkhof *et al.*, 2003). Several processing techniques are completed on image datasets prior to analysis in order to reduce error.

- Several images experienced movement, the majority only minor, likely caused by variations in temperature or wind. Images had to be corrected with the re-selection of six new ground control points. Points were identified as trees, roads, or roof tops.

- Quality control removed any images deemed unusable due to the interference of weather phenomenon decreasing visibility, or technical malfunction producing a blank image.

- During rectification processes, correct images were transformed into a plan view and amalgamated with a measurement co-ordinate system.

- Upon merging the two images from the north and south, it was deemed unnecessary to use the northern-most camera. The southern Pauanui camera provided the best spatial resolution of the whole beach and became the focus of analysis.

- Shoreline identification and extraction was completed using the RGB colour ratio technique which tended to favour images with strong colour or higher resolution areas within the image (closer to the camera).

- Manual correction of the shoreline occurred to fix shoreline spikes and gaps in order to create a complete shoreline.

- Similar techniques have been completed on the Tairua dataset also used in this analysis.

Chapter Three -

Shoreline Patterning and Beach Rotation

3.1 INTRODUCTION

This chapter identifies the shoreline variability experienced at Pauanui Beach between 2002 and 2004. Detail is put into the erosion and accretion of the beach as shown by the shoreline dataset, as well as the beach rotation. Variation is then separated into three main temporal categories; short term, seasonal and inter-annual time scales.

3.2 BEACH MORPHOLOGY BACKGROUND

New Zealand beaches since the 1950s have experienced increasing levels of coastal development. Higher populations are flocking to the coastal zone (Hart & Bryan, 2008) tempted by the high economic gain coastal properties present, as well as the lavish coastal lifestyle. These developmental pressures have triggered a rise in demand for long term recreational and environmental protection in these areas (Bittencourt *et al.,* 1997; Dean, 2002). Threats of severe coastal erosion can cutback and lower beach faces reducing property and recreational areas, decrease habitat availability and threaten the natural storm surge buffer zone (Bird, 2008; Dean, 2002). Erosion occurs when beaches lose more sediment than what is gained (Bird, 2008), effectively starving the beach of sediment and moving the beach further away from equilibrium. Increased wave action during storms inducing offshore sediment movement, a decline in sediment supply from terrigenous sources, blocked littoral drift, wave reflection scour or run off are all potential causes of this starvation (Bird, 2008). Although a natural process, coastal erosion only becomes a hazard to human lives when property or livelihoods are put at risk. Considering development is predicted to continue for

decades to come, understanding and managing the potential risk within the zone is highlighted even more (Hart & Bryan, 2008).

Beach systems are subject to storm and climatic forcing mechanisms which trigger erosive and accretion processes, varying the shoreline position and beach volume (Wright *et al.,* 1985). Wright and Short (1984) originally noted the ongoing variation in beach morphology following a three year study of Australian beaches and developed a beach state classification model. Six classifications were created detailing the beach morphology occurring as a result of experienced hydrodynamics (Figure 3.1). The frequency of significant wave and climatic conditions mean beach states seldom remain at equilibrium for considerable time periods. Beaches may digress from their major classification depending on the wave forcing projected (Bittencourt *et al.,* 1997; Woodroffe, 2002), however will gradually convert back to their original form under normal hydrodynamic conditions. This recovered state still may not mean the beach is at equilibrium. Equilibrium will only occur if the low energy wave climate is consistent for a considerable time period (Bittencourt *et al.,* 1997).

Variation is subject to several processes that occur over a range of temporal scales (Klein *et al.,* 2002). Measuring shoreline change can prove difficult due to short term, seasonal and long term/interannual time scales. Storm events for example occur rapidly and can be well quantified due to the sudden significant change in beach profiles. However, monitoring the processes governing this disfiguration via *in situ* instrumentation brings high risk due to the large damage potential associated to high energy surf environments, and the overall data collection reliability (Bogle *et al.,* 2000; Plant & Holman, 1997; Smit *et al.*, 2007). In comparison, coastal evolution of several hundreds of metres occurs at interannual and interdecadal scales. Complexities in visualising and monitoring the extreme slow rate of change are therefore created. Technological advancements in video imagery have provided low cost, long temporal and spatial monitoring availability that can quantify this gradual change. Prior to this development, manual beach surveying was undertaken to generate a suitable timeseries able to identify this scale change. Survey techniques do not provide

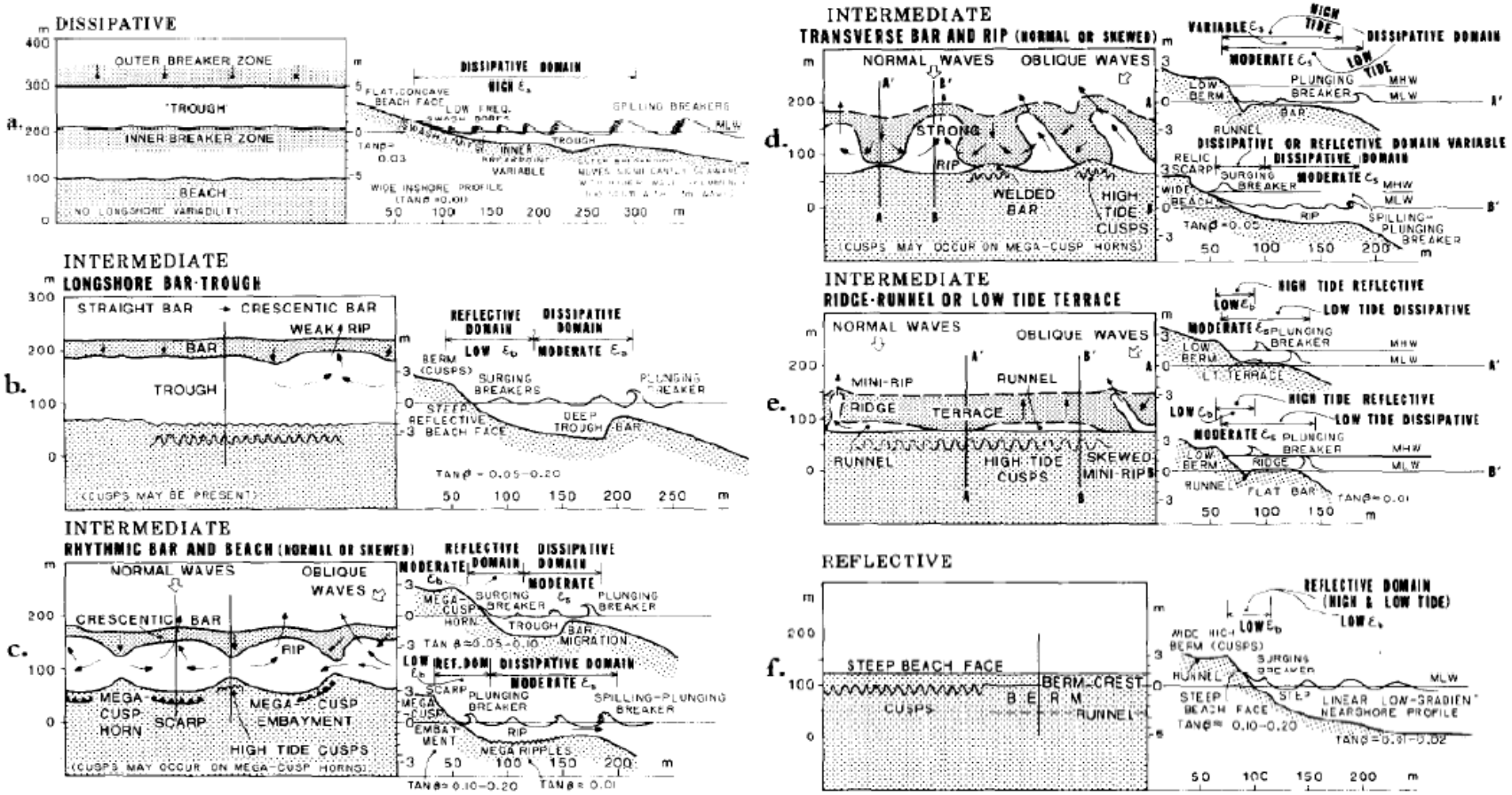

Figure 3.1: Six beach classifications and their specific morphologic features (Wright & Short, 1984).

high resolution data spatially or temporally (Plant & Holman, 1997; Smit *et al.*, 2007), but patterns may be evident if the sampling interval and timeseries is of reasonable length. Coastal management practices utilise these patterns identified by generating indicator levels or zones. Indicators can then be used for predictive capabilities and management strategies such as setting development setback limits.

3.2.1 Short term morphodynamics

Rapid changes in wave climate may cause considerable visual changes to beach profiles. Sudden alterations in wave heights and wave directions onto beaches caused by meteorological conditions adjust the previously experienced alongshore processes (Yates *et al.,* 2009). Sediment that was once accumulating alongshore causing the profile to accrete and advance seaward may abruptly reverse and begin to retreat landward due to erosion (Yates *et al.,* 2011). Short term events like storms influence erosive profiles with increased wave energy (Wright *et al.,* 1985). Physical change may be perceived as being considerable due to the ability to visually quantify the variation almost instantaneously. This rapid erosion however is generally followed by a recovery period during wave energy reductions, where beaches eventually regain previously lost sediment (Yates *et al.,* 2011). This recovery phase may extend over weeks or years depending on the accretion rate. Rates can be much slower than the original erosion rate or faster than the erosion rate allowing sediment to return as rapidly as it disappeared (Komar, 1998). This type of short term shoreline change may not compare to the total shoreline misplacement over longer time periods where change rates, although very slow, are extremely persistent and recovery can extend over decades.

3.2.2 Medium term morphodynamics

Storm events can cause considerable visual change over short time periods. Beaches may recover and accrete quite rapidly; however during periods of

increased storm activity, this recovery may be suppressed. Winter months experience more storms and increases in wave height and energy compared to summer months, which instead experiences less frequent storms and reduced wave heights and energy (Dubois, 1988; Komar, 1998). During erosive periods sediment from the berm is transported offshore to accumulate on the offshore bar (Dubois, 1988; Komar, 1998). This creates what is known as a "winter profile" or "bar profile" (Komar, 1998). When beaches begin to accrete, sediment that was stored in the bar gradually makes its way back onto the beach face in the form of a berm (Dubois, 1988). This creates what is known as a "summer profile" or "berm profile" (Komar, 1998). Erosive winter months may present the notion of continual beach face erosion with on-going shoreline variability. However if beaches have lost the majority of available sediment within the system during the first large storm event, erosion will decrease considerably (Bryan *et al.,* 2009; Haslett, 2009; Wood, 2010). Equilibrium wave energy is required to continue eroding at the initial erosive rate. As sediment becomes scarce, the required wave energy needed to erode increases. Despite the slower response rate of accretion versus erosion, the beach will accrete due to wave energy being under the equilibrium (Haslett, 2009; Wood, 2010).

3.2.3 Long term morphodynamics

It is well recognised that beaches are an evolutionary system that change over long time periods. Storm and seasonal events affect beaches in the short to medium time scales through rapid shoreline movement. However long term/interannual variation relates to the climatic and oscillatory phenomenon that controls the shoreline evolution over decades to centuries. Although rates of change are considerably low compared to short and medium term processes, the variation can be extreme. ENSO (El Niño Southern Oscillation) and IPO (Interdecadal Pacific Oscillation) are atmospheric variations that affect wave height and direction experienced on beaches (Thomas *et al.,* 2010). ENSO brings either El Niño or La Niña conditions while IPO determines the cyclical patterns of which they occur, whether on a decadal or century scale (Ranasinghe *et al.,*

2004). When ENSO is negative, El Niño climatic conditions are favoured (de Lange, 2000). This brings offshore west/south-west winds to the eastern Coromandel Peninsula. Beaches begin to accrete due to the offshore directed wind (de Lange, 2000). Positive ENSO is the opposite, favouring La Niña conditions instead. Increasing northerly winds blow onshore and generate erosive conditions for northerly/easterly facing beaches (de Lange, 2000). During the 1970s beaches in New Zealand's north-east experienced these strong erosion patterns that are associated with La Niña. As a result, coastal monitoring techniques were developed to help understand the long term erosion and accretion cycle experienced on these beaches as a result of ENSO.

3.3 BEACH ROTATION BACKGROUND

Beach rotation is the inverted erosion and accretion pattern of two ends of a beach. Rotation is a common occurrence on headland embayed beaches, and is caused by variations in wave climate (Bryan *et al.*, 2009; Klein *et al.,* 2002; Ranasinghe *et al.,* 2004; Short & Trembanis, 2004; Thomas *et al.,* 2011). Embayed beaches display strong curvature and naturally develop asymmetric shapes in the lee of headlands (Klein *et al.,* 2002). Rotation periodically changes this shape through shifts in the alongshore sediment transport, resulting in the opposite ends being out of phase with each other. If the northern end accretes, the southern end erodes and vice versa. Shore and coastline modification is associated to this phenomenon; however no loss or gain of sediment to the system is required (Klein *et al.,* 2002). Research has found rotation to be a medium term process that is linked to El Niño and La Niña cycles (Bryan *et al.,* 2009; Ranasinghe *et al.,* 2004; Thomas *et al.,* 2010). Climatic phase shifts bring varying wave climates, specifically in wave height and direction (de Lange, 2000; Ranasinghe *et al.,* 2004; Thomas *et al.,* 2010; Thomas *et al.,* 2011) which interact with the alongshore sediment transport. Ranasinghe (*et al.*, 2004) and Short and Trembanis (2004) found that rotation on east coast Australian beaches was influenced by the SOI (Southern Oscillation Index – El Niño/La Niña). Phase shifts varied the wave climate bringing more storms during La Niña cycles than El Niño.

Beaches responded with a clockwise rotation (northern end accretes while southern end erodes) during El Niño, and the opposite, anticlockwise rotation (northern end erodes while the southern end accretes) during La Niña.

Little research exists detailing rotation on any other beach type other than embayed beaches. Wood (2010) noted in his research of eastern Coromandel Peninsula beaches that Pauanui Beach displayed a high rotation coefficient, despite the fact that it is not an embayed beach. Further detailing into this phenomenon was disregarded based on the beach being classified as adjacent to a harbour (Wood, 2010). This research tries to distinguish the rotation experienced on a beach adjacent to a harbour that is not embayed, for later comparison with neighbouring Tairua Beach that is embayed in Chapter Five.

3.4 SHORELINE VARIATION RESULTS

3.4.1 Short term shoreline variation

3.4.1.1 Storm events

Using a wave hindcast dataset (of which details are described in Chapter Four) storm events which exceeded a 4 m significant wave height were isolated for analysis with the relative shoreline position. Details and parameters of the identified storms throughout the study period are presented in Table 3-1. Both 2002 and 2004 had two storms exceeding the threshold criteria, while 2003 had an increased level of five. Wave approach directions ranged between 23^0 and 90^0 which correspond to north-east and east directions respectively. Figure 3.2 shows the mean shoreline movement (seaward towards top, landward towards bottom) plotted against time and significant wave height. Maximum shoreline cutback can be reached over considerably short time periods, ranging between hours and days (Munoz-Perez & Medina, 2010). Therefore Figure 3.2 allows for these short term patterns to be visually distinguished. Initially there is an obvious inverse relationship between the shoreline movement and large wave events. During storm events the shoreline cuts back, then gradually recovers and

Table 3-1: Parameters for identified storms where significant wave height (Hs) exceeded 4m, taken from a WWIII (Wave Watch III) 50 m wave hindcast dataset. Hs is the maximum significant wave height during the storm, Tp, Dir and Dsp are the peak wave period, wave approach direction and wave directional spread respectively at the same instance as Hs.

	2002		2003					2004	
	Storm one	Storm two	Storm three	Storm four	Storm five	Storm six	Storm seven	storm eight	storm nine
Date	June 20th 9am	July 11th 9pm	January 8th 6pm	February 26th 12pm	April 16th 3am	July 28th 12am	August 20th 9am	February 28th 9am	July 17th 12pm
Hs (m)	5.2	4.1	4.4	5	4.6	4.4	4.7	4.3	4.3
Tp (s)	10.2	8.4	10.2	11.2	13.5	13.5	10.1	9.2	11.2
Dir (^{0})	79	65	82	87	63	90	87	23	44
Dsp (^{0})	27.2	28.8	24.8	22.7	22.7	34.6	24.7	24.5	26.8

accretes during periods where there is a lull in large wave events. Prior to the January 2003 storm of 4.4 m (Hs) for example, the shoreline was in an accreted state. The shoreline was cutback a total of 31.87 m over a 4 day period, an erosion rate of 0.33 m/hr. Shoreline advance of 34.4m occurred over approximately 27 days during a period of reduced wave height; a considerably longer time period than what it took to erode the beach profile initially. The accretion rate was much lower than the erosion rate experienced prior, with sediment accumulating at 0.05 m/hr. It must be noted that this event had the largest total erosion and erosion rate over the entire study period, along with the longest accretion period, largest accretion total, and smallest accretion rate over the entire period. Similar patterns were experienced for storms two, six, seven, eight and nine. Remaining storms one, four and five, all highlighted smaller accretion periods than the previous erosion period instead. Storms one and five not only had smaller times for sediment accumulation, but the total accretion outweighed the total amount eroded prior. These two storms also had the largest wave heights throughout the study period, 5.5 m and 5 m. Overall there was a delayed reaction between the beach response and the change in wave

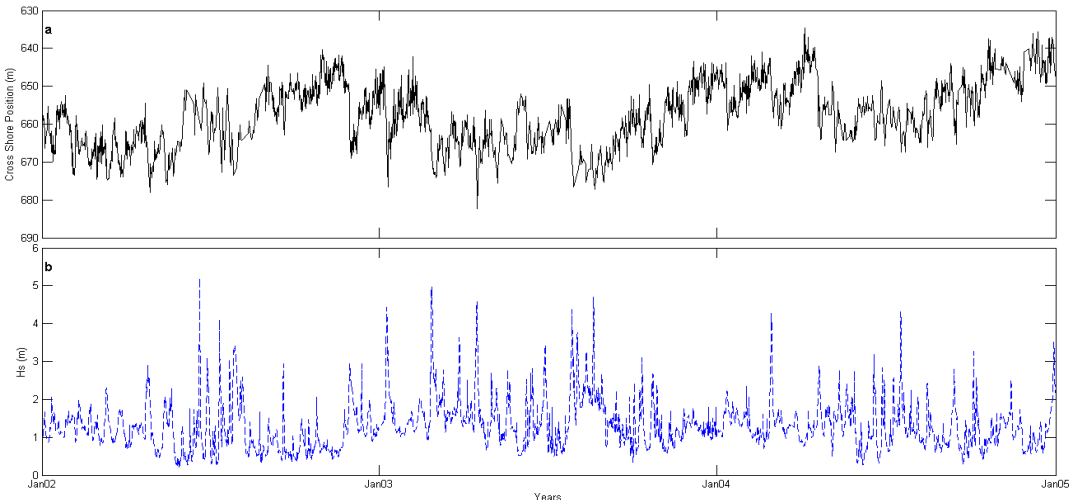

Figure 3.2: a) Mean shoreline position over the dataset period 2002-2004. Seaward (landward) movement is towards the top (bottom) of the graph indicating accretion (erosion). b) deep water significant wave height against time over the same time period.

climate across all storms. On average, a 2 day lag existed from when the maximum significant wave height was experienced, and the maximum beach reduction occurred. Table 3-2 summarises the shoreline movement, specifically the erosion and accretion phenomenon associated with the identified storms in Table 3-1, and that are visible above 4 m Hs in Figure 3.2.

Storm one: *The largest significant wave height maximum throughout the survey period was experienced during this event (5.5 m) with waves approaching from the east. Prior to the wave event the shoreline position was within 4.7 m of the three year average shoreline position 656.92 m. Landward movement of the shoreline during the storm resulted in a 9.45 m retreat over a 150 hour period Following the decline in storm activity, the beach began to accrete. The total accretion period prior to another cutback event was 49 hours, which did not provide enough time for full recovery. However a total shoreline advance of 12.48 m occurred, producing a higher accretion rate than erosion (0.06 m/hr versus 0.25 m/hr). Therefore the accretion period was much smaller than the erosion which would allow significant time for the shoreline to recover. Instead the shoreline advanced 12.48 m over the accretion period resulting in net accretion and shoreline gain.*

Storm two: *Prior to the noted storm, the shoreline was in an accreted state above the three year average. As a result of the increasing wave energy the shoreline was eroded at a rate of 0.21 m/hr, over 108 hours. This meant shoreline retreat of 22.11 m occurred alongshore Pauanui. The following accretion period lasted 149 hours, a longer time frame than the erosive phase. An overall accretion rate of 0.15 m/hr was produced with the total accretion and shoreline advance of 22.11 m; a value very similar to the amount eroded during the storm. The shoreline therefore was not strongly affected by the storm event as full recovery was made.*

Storm three: *During the storm peak the shoreline cutback a total of 31.87 m over a four day period. This is the largest shoreline retreat experienced over the entire study period. This generated a considerably large erosion rate of 0.33 m/h, the largest of all storms. The following accretion period lasted a total of 27*

days, almost an entire month. Wave heights were reduced considerably during this period allowing the shoreline to advance by 34. 4 m. This was the largest accretion distance experienced throughout the time period as well. Overall, the beach gained sediment during this storm event despite the large cutback as more sediment was returned to the beach during the extensive accretion period.

Storm four: *This particular storm had the longest storm erosion phase of all storms. The total erosion period lasted almost 11 days and a total of 245 hours. The significant wave height was the second largest throughout the three year period above the 4 m storm wave height classification. Wave approach direction was approximately from the east. Despite the elongated erosion period, the shoreline retreated 21.33 m at a rate of 0.09 m/hr. This erosion rate was closely matched to the following accretion rate of 0.08 m/hr. Sediment accretion was enabled for 135 hours, however the shoreline accretion advanced seaward only 11.17 m. This meant the shoreline did not recover fully and resulted in a net sediment loss during this storm.*

Storm five: *This storm subsequently followed storm four almost immediately, interrupting the post storm accretionary phase. Storm conditions allowed for another large erosion phase, the second largest for the entire study period. The significant wave height maximum was 4.4 m and the waves approached from a more north-east direction. For 202 hours (8 days, 10 hours) the beach profile eroded at 0.04 m/hr, the slowest erosion rate for the entire period. Shoreline movement landward was totalled at 8.68 m, the smallest retreat distance of all storms. Considering the accretion rate was quite large at 0.21 m/hr, a total shoreline advance of 14.78 m occurred as a result. Due to the large quantity of sediment stored offshore in the bar, a large low energy period encourages the onshore movement of sediment. Previous storms reduced sediment available during the storm so erosion distances are limited, and larger accretion distances are created as a result.*

Storm six: *Waves approached directly from the east with a significant wave height of 4.4 m during this event. The total erosion period as a result of the storm was 98 hours. Beach profiles were eroded at a rate of 0.23 m/hr, allowing*

Table 3-2: Maximum shoreline position prior to peak storm erosion, minimum shoreline position during the storm, maximum post storm shoreline position. Erosion/accretion rate marked with a * indicates where the accretion period was smaller than the erosion period.

	Prior storm max shore position (m)	Storm min shore position (m)	Post storm max shore position (m)	Total Erosion (m)	Total Accretion (m)	Erosion period (hr)	Accretion period (hr)	Erosion/Accretion rate (m/hr)
Storm one	652.18	661.63	649.15	9.45	12.48	150	49	0.06 / 0.25 *
Storm two	650.29	672.76	650.65	22.47	22.11	108	149	0.21 / 0.15
Storm three	644.78	676.65	642.25	31.87	34.4	99	646	0.32 / 0.05
Storm four	652.68	674.01	662.89	21.33	11.12	245	135	0.09 / 0.08 *
Storm five	662.89	671.57	656.79	8.68	14.78	202	71	0.04 / 0.21 *
Storm six	653.78	676.58	665.45	22.8	11.13	98	161	0.23 / 0.07
Storm seven	665.39	677.23	665.73	11.84	11.5	69	145	0.17 / 0.12
Storm eight	642.59	658.37	650.6	15.78	7.77	53	97	0.30 / 0.08
Storm nine	655.59	667.46	654.51	11.87	12.95	64	149	0.19 / 0.09

the shoreline retreat of 22.8 m. Recovery accretion extended over 161 hours, larger than the erosion period. The shoreline displayed accretion of 11.13 m, a lower amount than what was eroded, and the accretion rate was considerably lower than the erosion rate erosion at 0.07 m/hr. Overall the shoreline did not accrete to previous levels despite a larger accretion period than erosion, therefore the beach lost more sediment and became eroded.

Storm seven: *The total erosion period during storm seven lasted 69 hours. Waves approached from an eastern direction with a significant wave height maximum of 4.7 m. Shoreline draw back equated to 11.84 m with an erosion rate of 0.17 m/hr. The accretion period that followed lasted 145 hours, longer than the erosion. Sediment accretion at rate of 0.12 m/hr led to the landward repositioning of the shoreline by 11.5 m. This was a very similar amount of sediment accreted than what was originally eroded, due to the similar erosion and accretion rates. Therefore the shore did not experience large re-positioning as a result of the storm.*

Storm eight: *Prior to the wave event the profile was in a very accreted position. The shoreline was 14.3 m above the three year average position. Waves approached from a more northerly direction, and the maximum significant wave height was 4.3 m. A 53 hour erosion period with an erosion rate of 0.30 m/hr resulted in a landward movement of the shoreline by 7.7 m. This is the smallest accretion movement over the entire sample period. As a result the beach remained in an eroded state following this storm and throughout the adjoining accretion period. This was because quantities of sediment that were eroded remained offshore as it was not transported back onshore.*

Storm nine: *The total shoreline retreat over 64 hours was 11.87 m for this event. Waves were approaching from the north-east and the maximum significant wave height was the same as storm eight. During this time the erosion rate was 0.19 m/hr. In comparison, the following accretion period was 9 hours in duration with an accretion rate of 0.09 m/hr, to get a total shoreline movement of 12.95 m. Accretion exceeded erosion during this event, so the beach gained an increase in sediment than what was originally lost, allowing the beach to head into an accreted state.*

3.4.1.2 Uniform alongshore variability

Pauanui Beach tends to erode in response to storm events. It is of interest to determine whether this erosion is uniform in the alongshore or whether erosion is causing rotation. Rotation is when one end of the beach is eroded while the other accretes generating a 'twisted' or 'angled' effect. Three locations alongshore have been selected at even distances. The northern location was taken at 550 m alongshore, middle location at 1550 m alongshore, and the southern location at 2550 m. Figures 3.3 a, b and c display the shoreline positions prior to the storm, during the peak of the storm, and after the storm (post). Appendix II displays the full alongshore shoreline profile for these three time steps for reference. The cross shore location is displayed where offshore is 600 m (ocean) and onshore (land) is 700 m. The gap in storm four data displayed on

Figure 3.3 (a) represents a lack of shoreline data as a result of poor visibility alongshore when extracting shorelines.

During storms one and nine, at the peak of the storm the northern end accreted and moved seaward. Middle and southern positions of the beach during the same time eroded. All other storms experienced increased erosion at the peak of the storm over all transects. Post storm one, the northern transect eroded following the accreted storm peak. Post storm nine, the northern transect continued the accretion pattern. Storm three had the largest cutback of shoreline position over all three transects during the storm peak, indicating uniform behaviour alongshore. During the same event, the post storm accretion total was larger at both the northern and southern ends compared to the midpoint. Therefore, either end responded more than mid beach areas. The southernmost transect during storm six gradually eroded over the three time periods. During the post storm period, the shoreline continued to erode further than the peak storm erosion position. Both the northern and middle transects accreted during this period. Post storm period accretion occurred during the remaining storms and their respective transects.

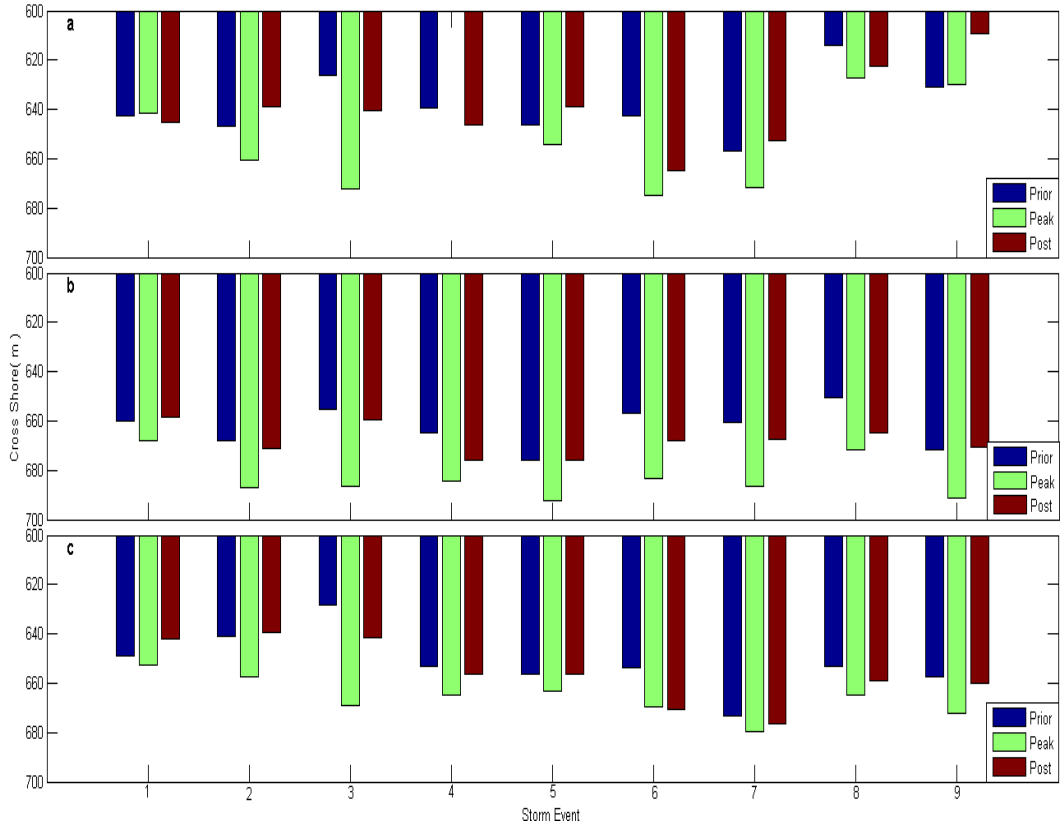

Figure 3.3: a) 550 m alongshore location to the north of the beach (by harbour entrance). b) 1550 m alongshore location at the middle of the beach. c) 2550 m alongshore location to the south of the beach (by Pauanui Mountain). Shoreline position prior to the storm is blue, shoreline position during the storm peak is green, shoreline position post storm is burgundy. The cross shore location is displayed where offshore is 600 m (ocean) and onshore (land) is 700 m. Note the gap in data during storm four in graph (a) was a result of visibility constraints during shoreline extraction from video images.

3.4.2 Medium term shoreline variation

3.4.2.1 Seasonal change

Five of the nine storms identified in Table 3-1 were observed during the winter months between June and August. 2003 in particular, experienced increased storminess during the summer months (storms three, four and five) along with one large summer event in 2004. Shoreline data was separated into monthly time periods to determine the monthly averages as presented in Figure 3.4. Months were then grouped according to season; summer (January, February, December), autumn (March, April, May), winter (June, July, August) and spring (September, October, November) for comparison.

The beginning of 2002 saw a decrease in shoreline position from January to the end of March (summer and first month of spring). The entire retreat of the shoreline totalled a loss of 8 m throughout these three months. Following a slight shoreline increase of 4 m and decrease of 3 m during April and May respectively, the shoreline accreted considerably during the start of winter (June). The shoreline moved seaward by 12 m in total even though the largest wave event over the entire study period occurred on the 20th of the month. This event caused a larger amount of sediment to move back onshore during the successive accretion period than what was eroded away throughout the storm. During July the shoreline experienced an overall 6.4 m cutback. The month featured a large storm event, although a larger amount of sediment than what was initially lost during the storm was regained in the following accretion period. Consecutive storms less than 4 m in height were experienced throughout the rest of July as shown on Figure 3.2 (b). August displayed a monthly shoreline average advance of 3.4 m. This accretion pattern continued until the rest of the year throughout the spring season until a strong cutback was experienced during the start of summer in December. Therefore overall patterns indicate summer cutback and winter advance.

January 2003 had an exceptionally small average shoreline movement and remained in a similar position to December. Total landward movement during this month was only 0.0034 m. The largest erosion and accretion values were

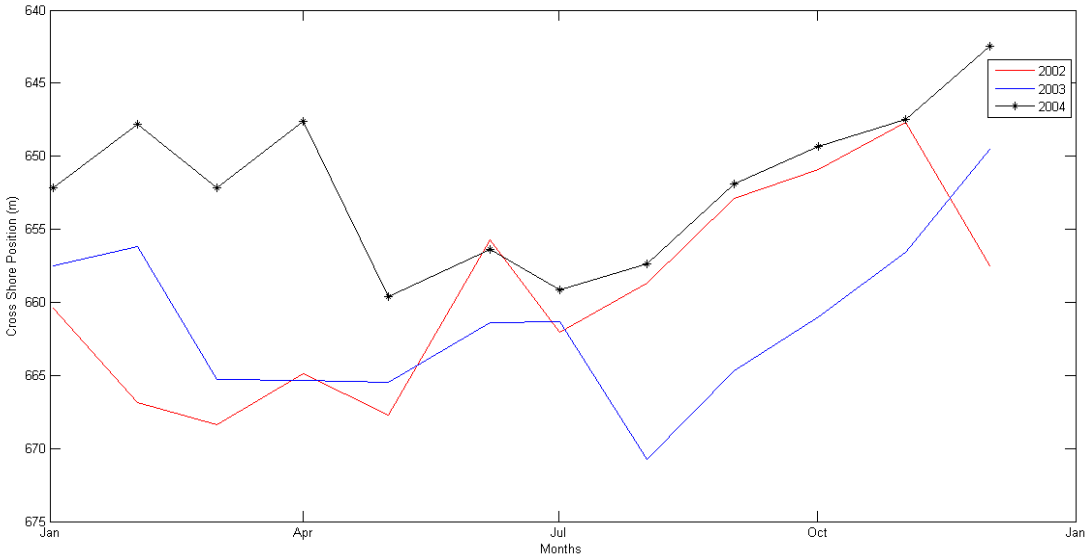

Figure 3.4: Monthly mean shoreline position at Pauanui Beach. Red line is 2002, blue line is 2003 and black dotted line is 2004. Cross shore position seaward is towards the top of the graph, cross shore position landward is bottom of the graph.

experienced during this month as a result of a 4.4 m wave event. The rest of the month experienced considerably lower wave heights with no other storm events occurring. Increases in monthly shoreline position from 657.5 m to 656.2 m occurred as a result. This was a total shoreline accretion of 1.3 m (noting that the smaller (larger) cross shore position represents seaward (landward) movement). February consisted of a decline in average shoreline position by 9 m until March. February also featured a very large wave event where the amount eroded exceeded the amount returned during the accretion period. Over the spring season, considerably little movement occurred. The shoreline increased seaward at a total of 0.18 m over the whole season, despite a large wave event occurring in March. The start of winter (June) featured shoreline advance and accretion which plateaued during July. August displayed shoreline cutback and was the lowest average monthly position for the entire study period. A large storm event was also present during this month where the total erosion almost equalled total accretion. Rapid accretion occurred for the rest of the year

throughout the spring season and start of summer where the shoreline reached the maximum seaward point for 2003 during December; a total shoreline position increase of 21.2 m. Seasonal patterns overall display summer accretion, autumn cutback, winter accretion with a large cutback during August, and spring accretion.

January 2004 prevented the accretionary pattern from August 2003 to continue as shoreline retreat of 2.6 m occurred. There were no wave events during this month that exceeded 2 m in significant height. February showed seaward movement, although there was a large storm event during this month retreating the shoreline a greater distance that what it advanced during the accretion period. This monthly erosion/accretion pattern continued throughout autumn and winter consecutively. May displayed the largest cut back during one of the erosion/accretion patterns. No wave events exceeding 3m in wave height were present during this month. July was the only winter month to present shoreline decline and retreat. Despite a 4.3 m wave event occurring during July which returned more sediment during the accretionary phase than what was eroded. Similarly to August 2002, the shoreline during August 2004 accreted and moved seaward. Accretion continued throughout the rest of the year (five months) until the dataset stopped. December had the most seaward shoreline position out of the entire dataset. 2004 shows strong seasonal patterns (visible on Figure 3.4) where summer experiences accretion and winter experiences erosion and cutback.

3.4.3 Long term shoreline variation

It has been previously determined that alongshore uniformity does not occur at Pauanui Beach during storm events. Three transects at 550 m, 1550 m and 2550 m were analysed to determine whether the beach behaves similarly alongshore over time, as opposed to during high frequency fluctuation events such as storms. Figure 3.5 displays movement constancy between all three transects. As one increases, the other two will also increase, as one decreases, the other two will also decrease. During the beginning of 2002, the northern area

of Pauanui had a strong seaward extending shoreline, prior to eroding rapidly during the end of February. All three transects gradually accreted together, although the middle transect (two) experienced stronger short term variation particularly during July, than transects one and three. Towards the end of 2003 the northern area displayed a considerably larger amount of accretion than the middle and southern areas (transects two and three), although transects two and three too experienced accretion to some level. Overall, transect two (middle Pauanui) was in a more cutback cross shore position, while northern Pauanui consistently displayed a position further seaward than any other area. The long term beach response trend showed a relatively uniform erosion and accretion behaviour alongshore, although at differing cross shore positions. Therefore no inverse relationship between the northern and southern ends of the beach exists where the northern accretes and the southern erodes leaving the middle to act as a fulcrum point for shoreline rotation. However as a result of the varying cross shore positions of each transect where the north is more accreted than the south, a rotation co-efficient may exist.

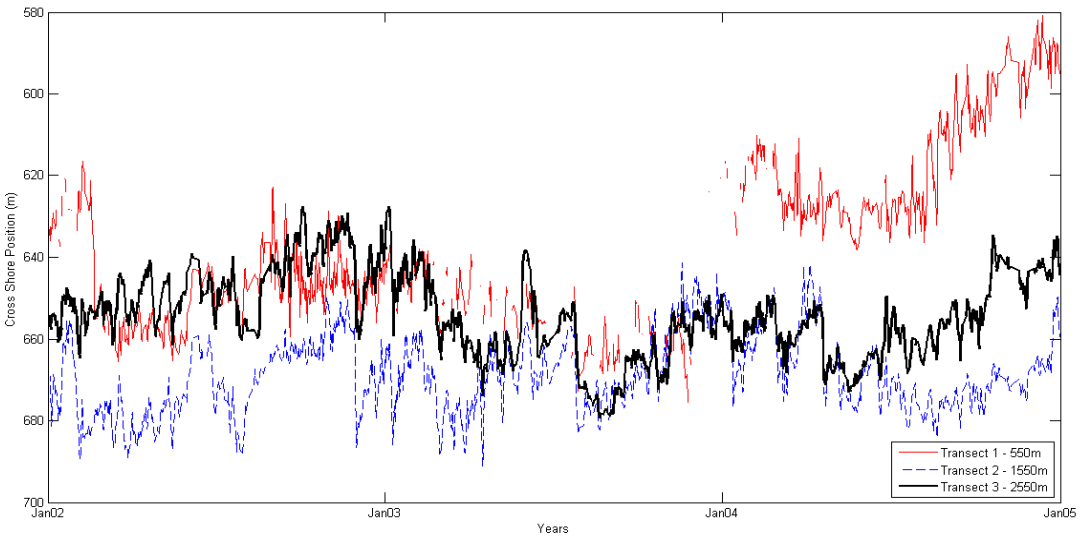

Figure 3.5: Mean shoreline positions at three transect points along Pauanui Beach. Data has been fitted with a 3 point moving mean. Gaps in transect one represent missing data. Cross shore position towards 600 m is seaward and 700 m is landward.

Climatic shifts affect the shoreline over longer time scales than storms or seasons. Oscillations vary meteorological conditions including wind, waves and precipitation; all of which influence sediment transport in specific ways. La Niña conditions are favoured when ENSO indexes are positive. Onshore winds cause erosion to north-east facing beaches in New Zealand (de Lange, 2000), including Pauanui. The opposite occurs when the ENSO index is negative and El Niño conditions are favoured. Figure 3.6 displays the ENSO index between 2002 and 2004 against the mean monthly shoreline position. When the ENSO is positive the shoreline cuts back, confirming behaviour associated to La Niña conditions. When the ENSO is negative, El Niño conditions are favoured and the shoreline accretes. The long term trend evident in the ENSO index data indicates strong El Niño conditions. As mentioned, El Niño influences the shoreline over time by encouraging sedimentation. Over all, Pauanui Beach during this time period accreted a total of 11 m, agreeing with negative ENSO theory.

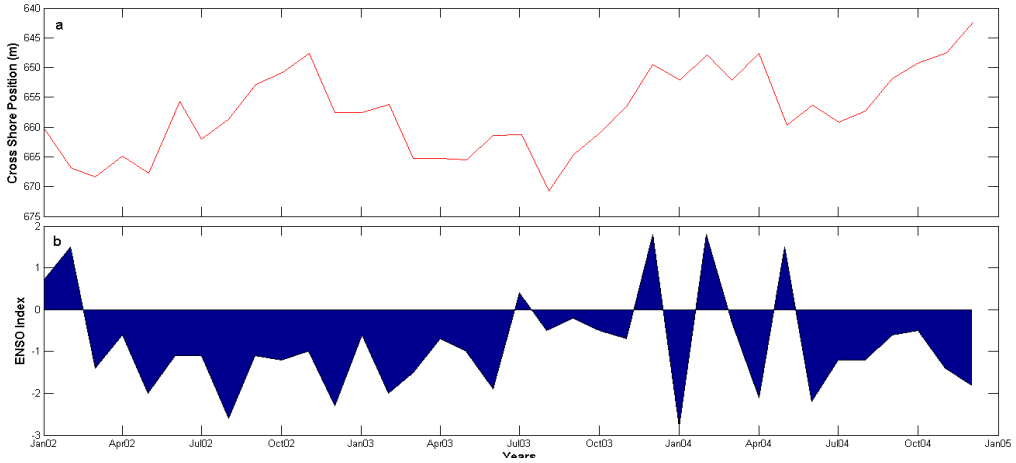

Figure 3.6: a) monthly shoreline position, seaward is towards top of the graph and landward is towards the bottom of the graph. b) ENSO index where positive values show La-Niña conditions. Negative values show El-Niño conditions.

3.5 BEACH ROTATION RESULTS

Pauanui Beach does not display uniform alongshore shoreline placement. During storm events the northern end often experiences a more varying behaviour than the middle and southern areas of the beach. It is hypothesised that this alongshore variability is caused by the interactions of offshore island shadowing generating alongshore currents. Evidence of rotation was observed during short term shoreline analysis, however the shoreline did not display a theoretical rotation pattern and therefore was elaborated. Shoreline data was fitted with a polynomial curve (using the function 'polyfit' in matlab) where the slope of the curve was taken as the rotation co-efficient. A positive co-efficient relates to the southern end rotating, generating what is known as anti-clockwise rotation, while the opposite (negative co-efficient) relates to northern rotation, or clockwise rotation.

Figure 3.7 displays the extracted shorelines for the entire sample period (2002-2004). Northern Pauanui is located towards the top of the graph (0 m) while southern Pauanui is located towards the bottom (2900 m). Despite quite a parabolic shape to what is generally referred to as a long straight beach, hot spot erosion and long term rotation is evident throughout the timeseries. Blue colours represent a seaward movement while red colours represent a landward movement. Pauanui does not exemplify considerable short term or seasonal variation, instead long term patterns are particularly strong from mid 2003 through until the end of the timeseries. Here the northern end of the beach steadily rotates seaward due to increases in sediment. Sediment continues to accumulate over time and the beach width increases southwards alongshore. This response is often found on headland embayed beaches as a barrier exists for sediment to pile against. Northern Pauanui features an ebb tidal delta in the lee of Paku Hill however so this sediment build up is unusual. Middle areas of the beach experience hotspot erosion caused by rip current location, while the southern areas remain in a parabolic shape throughout this period.

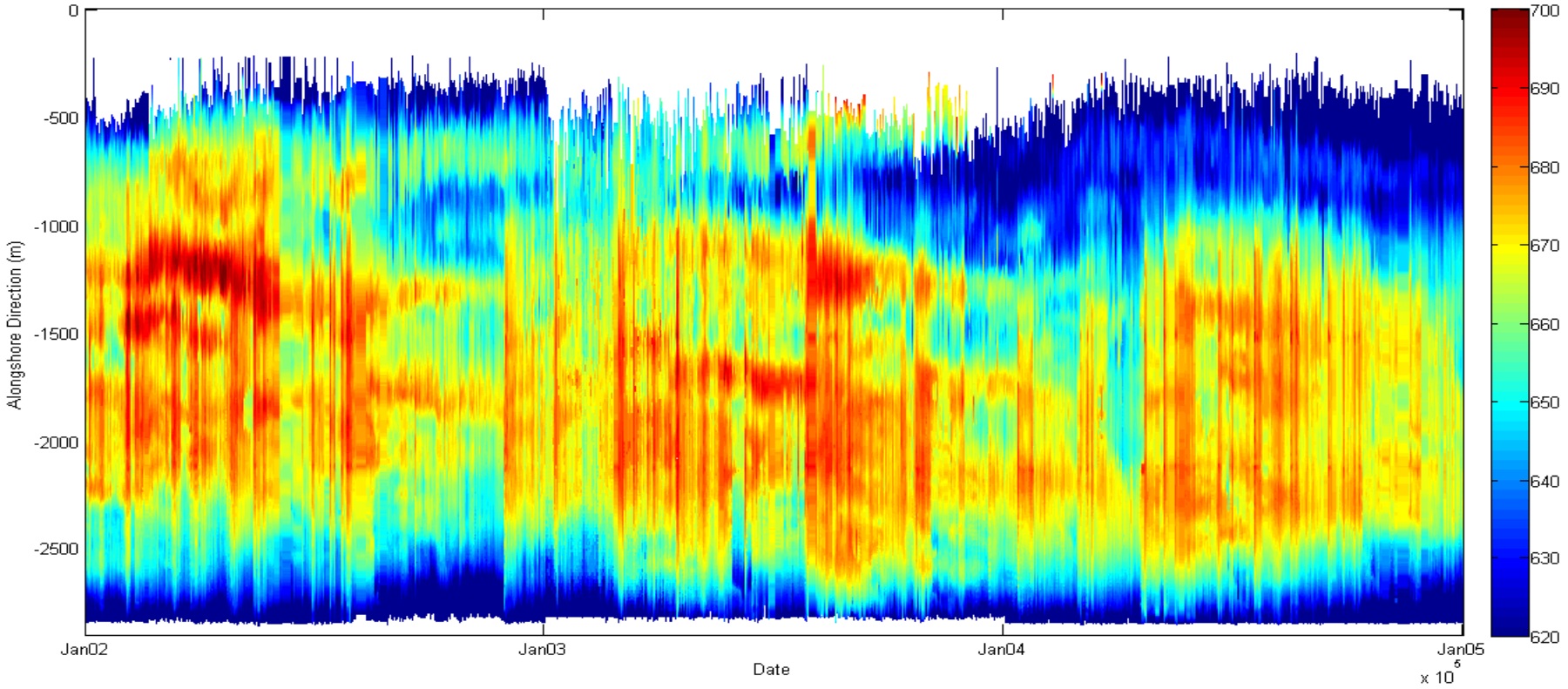

Figure 3.7: Merged shoreline dataset of Pauanui Beach. Y axis shows the alongshore direction with 0 m being northern most point of the beach where the Tairua harbour entrance terminates. Colour bar represents the cross shore direction where red is landward movement and blue is seaward movement in metres. Data has been interpolated to bridge any gaps caused by missing data.

3.5.1 Beach rotation and alongshore wave energy flux

Beach rotation co-efficients were compared to the alongshore wave energy flux to determine a relationship between the two. The wave energy flux is given by:

$$Ey = \frac{1}{8}.\rho.g.Hs^2.\sin\theta \qquad (1)$$

Where ρ is the density of seawater (1025 kgm^{-3}, g is acceleration due to gravity (9.81 ms^{-1}), Hs is significant wave height in metres, and θ is the shore normal wave approach angle where 0^o is directly onshore. Figure 3.8 displays the rotation and energy flux timeseries fitted with a 3 point moving mean. Ongoing small fluctuations in rotation occurred throughout; however any significant energy event did not cause a large change in beach rotation. Linear analysis (Figure 3.8 (c)) produced an extremely weak correlation co-efficient between rotation and wave energy flux at 0.05. Neither positive nor negative energy fluxes influence the shoreline rotation more than the other. Thus proving other factors need to be taken into consideration that is potentially interfering with the wave climate projected onto Pauanui, such as island shadowing.

The beach displayed considerable rotation change four times over the three year period. These were during January/February of 2002 and December/January of 2003. Rotation during 2002 decreased from a positive co-efficient (southern end rotated) to zero (0), meaning the northern end began to rotate to the same extent as the southern, producing a parabolic shoreline. This pattern continued until February where the southern end then rotated above the 0.01 co-efficient, and the northern end cutback. The same pattern was experienced during the 2003 rotation event. Wave energy flux for the 2002 January/February event displayed no large flux events that could have potentially triggered the rotation event. The energy flux remained between 2000 and -2000 J/m^2. For the 2003 December/January event however slightly increased energy flux was associated

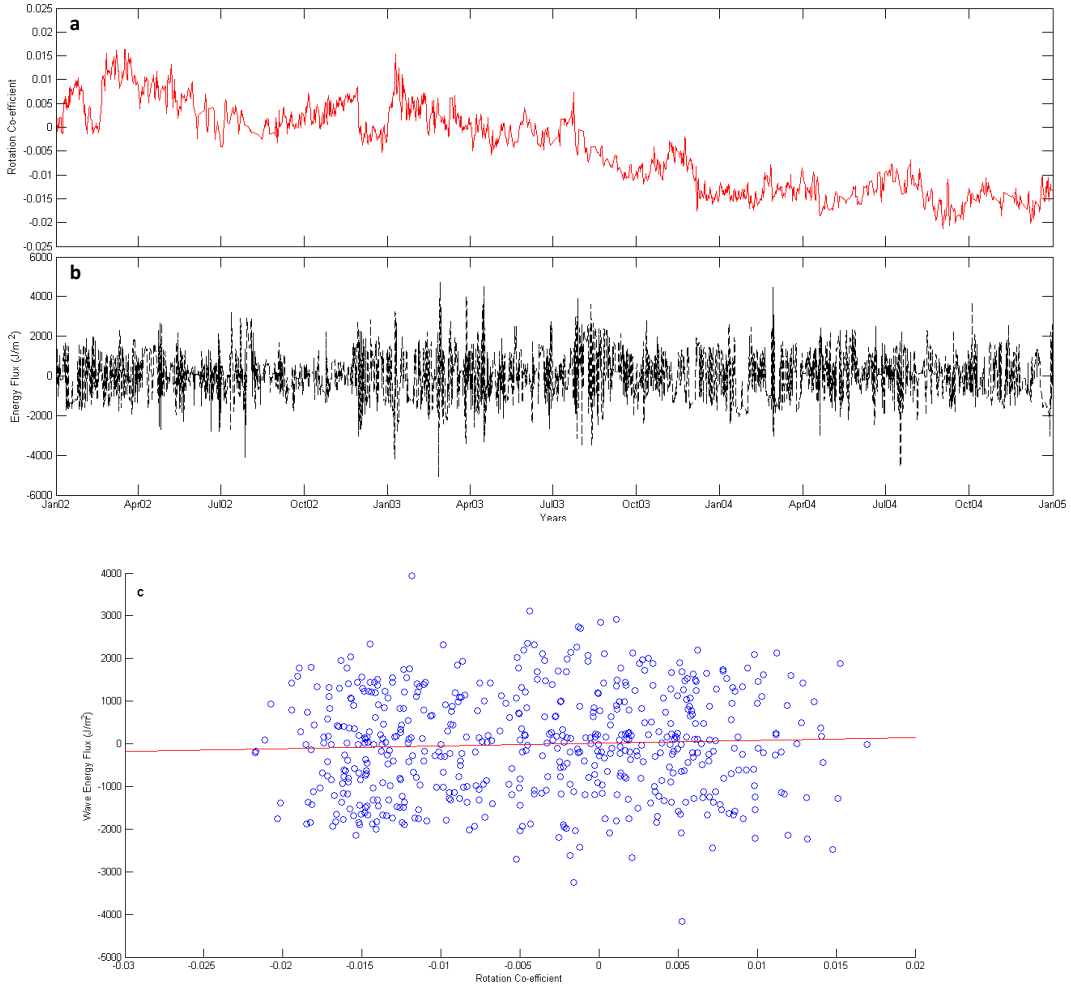

Figure 3.8: a) Rotation co-efficient for Pauanui Beach. Positive co-efficient relates to southern rotation, negative co-efficient relates to northern rotation. b) Alongshore wave energy flux where 0^{o} is shore normal. c) Correlation statistics between rotation co-efficient and the wave energy flux. A weak correlation exists with an R^2 value of 0.05. The red line is the line of best fit (least squares sense).

to the rotation variation. A considerable large wave energy event reaching over 4000 J/m^2 caused a shift in positive rotation (southern rotation).These were the only times where the shoreline rotated significantly for considerable periods. Figure 3.8 displays a long term negative rotation trend towards the northern end of the beach. A phenomenon that agrees with the initial assumptions determined through merging the shorelines in Figure 3.7.

3.5.2 Beach rotation and ENSO oscillations

Long term rotation was present at Pauanui towards the northern end. Previous studies (Ranasinghe *et al.,* 2004; Short & Trembanis, 2004) have linked long term rotation to SOI and IPO indexes. Negative correlations of the northern and southern transects (550 m and 2550 m) identified an out of phase relationship between the two beach ends. Further correlations of transect one (northern) with the ENSO index found that with increasing ENSO, the northern end would erode, although at a 13 month lag. Transect three (southern) correlations with the ENSO index found the opposite. With increasing ENSO, the southern end will accrete, although at a nine month lag. As mentioned, the northern and southern areas display uniformity by experiencing erosion and accretion at the same time during the long term. It is hypothesised that these correlations of shoreline position and ENSO index, and the said rotation determine the extent of erosion or accretion experienced at either end during a specific climatic vent. As increasing ENSO enables accretion at the southern end, the northern end may also experience accretion to some degree. Accretion levels in the north would not be as considerable as at the southern end, but rotation would be caused as a result.

3.6 BEACH PROFILE COMPARISON

3.6.1 Beach profiling dataset

Traditionally beach monitoring has been completed through the manual collection of beach profile surveys. Cross shore measurement of beach elevation

provides a detailed cross-sectional look into the beach volume and its features (Short & Trembanis, 2004). Continual collection of profiling data can help visualise long term variation including beach morphodynamics and seasonal and long term phenomenon (Short & Trembanis, 2004). In order to analyse long term variation, long term profile collection with appropriately spaced sampling periods is required (Short & Trembanis, 2004). Highly erosive storm events can impact the beach within hours, while large scale cutback can occur gradually over decades. This highlights the importance for consistent profile monitoring, in order to generate a dataset that can cover the majority of beach response as a result of these events.

Waikato Regional Council initially established beach profile collection at Paunaui Beach during the 1970s. Sample times were quite sporadic and there was no consistent sampling period prior to 1995. Profiles were collected using level and staff six-monthly during this time (Wood, 2010). Only recently has this changed where profiles are now collected six-weekly by Keith Smith (Private Consultant; Wood, 2010). Note that this thesis utilises profiles owned by Waikato Regional Council and are therefore sampled at quarterly intervals, not 6 weekly. Profile sites are named using CCS (Coromandel Coastal Survey) followed by their benchmark location number associated to the sampled beach in 2004 (Wood, 2010). Not all profile transects were initiated at the same time. The northern most profile at Pauanui for example was added to increase the spatial monitoring extent along the beach (Wood, 2010). The locations of each profile are displayed in Appendix II followed by the beach volume timeseries at each location.

3.6.2 Long term shoreline variability and beach rotation

Due to the sampling period of the profile dataset, constraints were placed on determining short and medium term shoreline variation. Profiles are collected quarterly (three-monthly) and do not provide any evidence of shoreline response associated to storm events, nor are they a representative outlook of seasonal change. As a result, short and medium term variation analyses on the profile

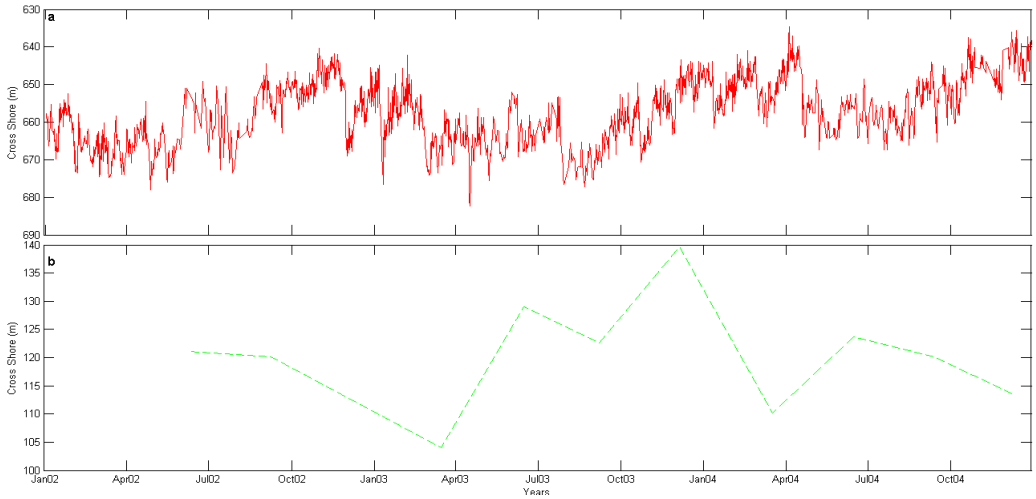

Figure 3.9: a) long term mean shoreline position taken from video data. b) Long term mean shoreline position taken from profile data. Seaward movement is towards the top of the graph, landward movement is towards the bottom of the graph.

dataset were not completed during this study. Long term analysis over the three year study period was completed in order to determine the shoreline variation and rotation, and to then compare with the video dataset. Initially the mean shoreline position was compared for long term analysis with the mean video data shoreline position in Figure 3.9. As a result of the sample period there are large jumps between the mean shoreline positions from the profile data as opposed to the shoreline positions from video data. Cross shore positions also vary due to the sampling techniques used when collecting the data, however seaward movement is towards the top of the graph while landward movement is towards the bottom. Ignoring the high frequency events that are present in graph (a), the two datasets agree. Therefore events identified by profiling are also identified in the video data.

All four profiles were compared with each other in Figure 3.10 to determine alongshore uniformity. Similar to the video dataset, the northern most profile is located further seaward than profiles to the south. This is represented in video data, specifically Figure 3.5. The parabolic shape is attained in this dataset with the southernmost profile being located further seaward than the middle (profile

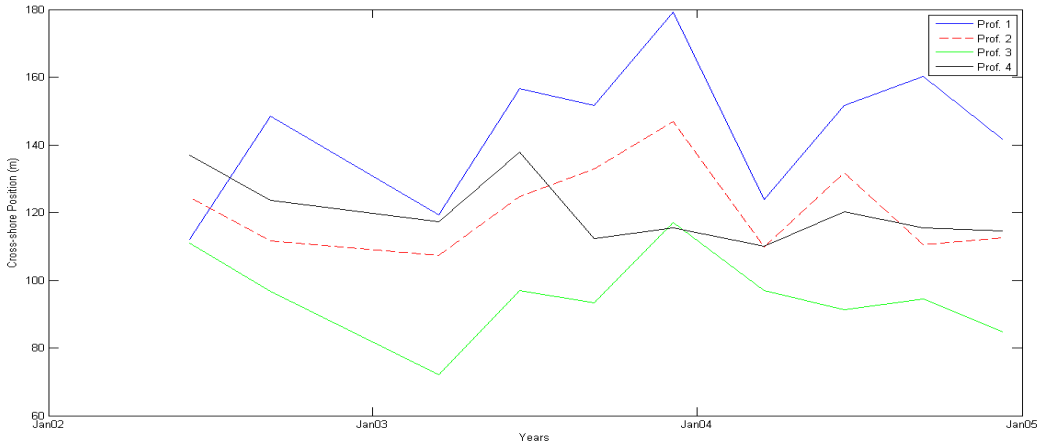

Figure 3.10: Shoreline location (0 m contour) of the four profile sites located from north to south (Profile 1 to 4) at Pauanui Beach. Cross shore position is from land (0 m) extending seaward (180 m).

three). Uniformity is displayed between the first three profiles, however profile four to the south is not as consistent during the end of 2003. Over time, gradual accretion and seaward movement of the northern most profile was shown in video data. However profile data presents a strong cutback during the beginning of 2004, following the highest accretion rate over the time period. Therefore alongshore findings are similar but not completely consistent with the video data, potentially caused by the variation in sampling period. A negative correlation co-efficient between profile one and four indicates an out of phase behaviour between each end of the beach. This result agrees with video data.

Rotation co-efficients were created on video data by fitting a polynomial curve to the shoreline data. Shoreline data was extracted from profiles at the 0 m contour line. Despite a parabolic nature of the northern and southern ends of Pauanui, rotation was evident due to the variation in cross shore position of the shoreline. Polynomial curves were fitted to profile data to determine the rotation of the shoreline and is shown in Figure 3.11. An increasing negative rotation indicates gradual accretion towards the northern end of the beach. This agrees with video shoreline data that also displayed northern end accretion. Due to the sampling period of the profiles once every three months, there is not a considerable short term rotation pattern evident in profile data. Therefore video data is a good

monitoring technique that can be used to determine beach rotation at Pauanui Beach, especially over a range of time scales as opposed to profiling.

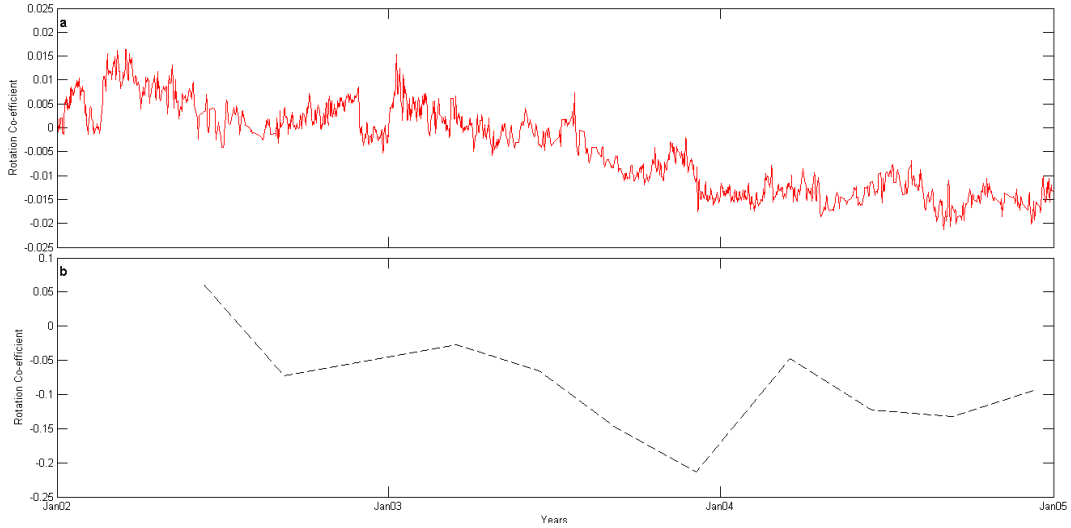

Figure 3.11: Rotation co-efficient comparison between the profile dataset (b) and video dataset (a) both collected at Pauanui Beach. Positive co-efficient relates to southern rotation, negative co-efficient relates to northern rotation.

3.7 DISCUSSION

3.7.1 Shoreline variation

3.7.1.1 Short term

Storm events present an increased and varied short term wave climate than what is experienced on average. As a result, the beach tends to favour erosive conditions where sediment is lost to the offshore bar. The shoreline in response retreats landward reducing the beach width. During periods of reduced energy, sediment is regained and the berm accretes, allowing the shoreline to advance shoreward and increase the beach width. Pauanui was subject to nine large wave events throughout the three year study period. These wave events were selected as their significant wave heights exceeded 4 m. The dominant pattern experienced during and after these storm events matched the erosion/accretion process described above. However the beach did not respond instantaneously to

the change in wave height in any storm event. An average delayed reaction or 'lag' of 2 days over all nine storms was evident between the maximum significant wave height and the minimum shoreline retreat. Yates (*et al.,* 2009) explain that there is a weak correlation between wave height, wave energy flux and beach shoreline position. This is caused by the rapid variation in wave height and climate over a space of a few hours, in comparison to the time and consistent conditions needed for morphology evolution (Yates *et al.*, 2009). Correlation statistics completed on the Pauanui dataset prove this theory with the mean shoreline position and the significant wave height (Figure 3.12) due to an R^2 value of 0.40. Although this is classified as a weak correlation, this is a larger value than what was returned between the mean shoreline position and wave energy flux correlation R^2 of 0.17 (Figure 3.13).

Damage to beach width and shoreline position is dependent upon the pre-existing beach state. Similar storm conditions may present extremely different results on beach morphology as a consequence (Bryan *et al.*, 2009). This is particularly true for four storm events where wave heights were the same; storm three and six (4.4 m) and storms eight and nine (4.3 m). Large quantities of sediment were removed during storms three and eight, with a reduced amount being removed during storms six and nine regardless of having the same significant wave height respectively. Pre-existing conditions also affect the degree of erosion a storm may generate. Morphological changes are not a factor of storm persistence, but whether the beach is in an accreted or eroded state prior to the wave event. Storm five for example displayed the smallest retreat during a storm (8.78 m), despite a large erosion period (the second largest time during the study). Pre-existing storm conditions placed on the beach meant the sediment reserve in the berm was depleted due to erosion. With the onset of large wave events, little sediment was available for cross shore transport processes between the berm and bar, thus providing a small erosion rate and retreat distance during this event. Reduced wave heights and energy that followed due to a lull period meant there were considerable volumes of sediment obtainable for cross shore transport from the bar to the berm. The berm accreted rapidly, advancing the shoreline seaward. Regardless of the fact

this event was marked as an exception where the accretion period was smaller than the erosion. An equilibrium shoreline change model developed by Yates (*et al.,* 2009, 2011) elaborates on this erosion/accretion and wave climate phenomenon. Non-linear relationships between the wave climate and beach itself mean morphology alteration varies according to changes in forcing. This alteration is ultimately determined by the shoreline position prior to the wave event, equilibrium wave height and wave energy (Yates *et al.,* 2009). Therefore the positioning of the shoreline (in an eroded or accreted state) prior to the storm determines the shoreline modification during the event. If a beach is in an accreted state, a smaller wave height can erode the beach. The same smaller wave height if projected onto an eroded beach however, may have a small enough energy to promote accretion.

Alongshore uniformity does not occur throughout every storm. Variations in shoreline position between the three locations are evident with the northern transect being the most variable. Alongshore uniform behaviour is important to detail in order to understand unusual erosion or accretionary processes. Three shoreline position transect graphs (Figure 3.3) display the alongshore variability in shoreline position before, during and after all nine storm events. Storm three was the only event to display alongshore uniformity during the storm peak with large shoreline cutback. It is hypothesised that this uniform behaviour is a result of the wave approach direction. At the peak of the storm the waves were approaching onshore at an angle of 82^0. This direction is free of island interference from offshore Shoe Island that can cause shadowing according to wave angle. Shadowing presents a zone of reduced wave energy and height alongshore. Longshore currents can be created allowing for sediment accretion at one particular end of the beach, while the other end erodes. Storms one and nine display this alongshore discrepancy where the northern shoreline position accreted and middle and southern shoreline position eroded. Waves approached from a 79^0 angle during storm one, where waves had to impact Shoe Island before propagating onshore. Storm nine wave approach angle was from 44^0 where waves too had to experience diffraction as a result of Shoe Island.

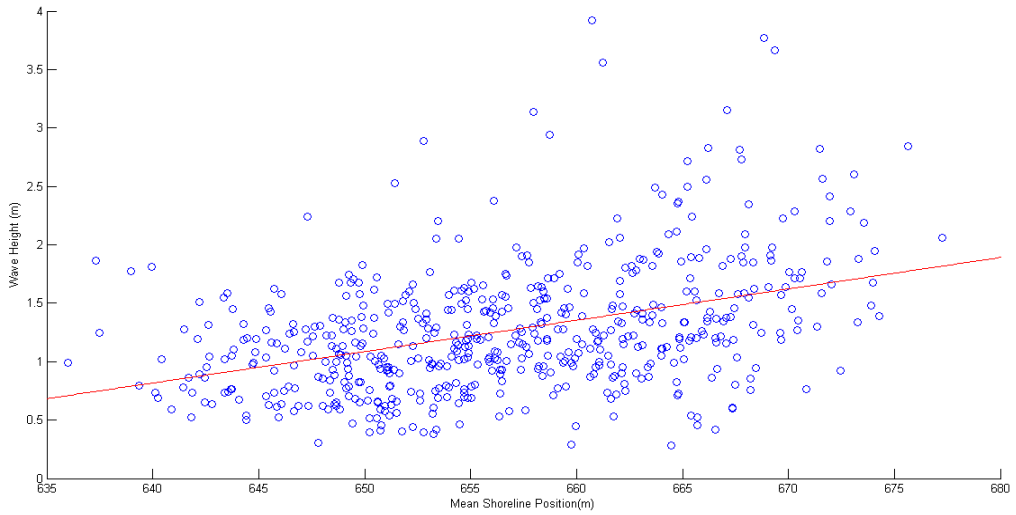

Figure 3.12: Correlation statistics of the significant wave height and mean shoreline position. A weak R^2 value exists between the two of 0.40. The red line indicates the line of best fit (least squares sense).

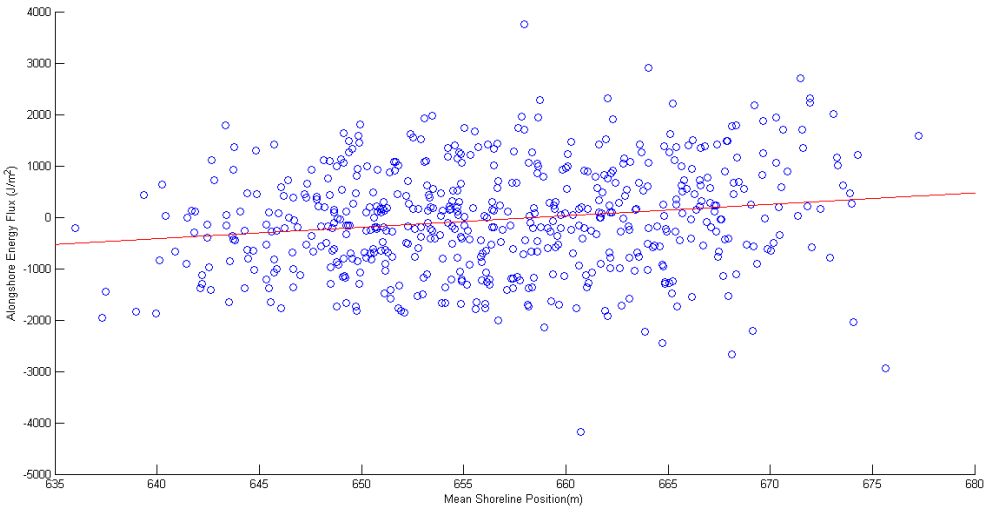

Figure 3.13: Correlation statistics of the wave energy flux and mean shoreline position. A weak R^2 value exists between the two of 0.17. The red line indicates the line of best fit (least squares sense).

It is premised that shadowing is causing this alongshore variability and will be analysed through wave modelling in Chapter Four.

3.7.1.2 Medium term

Most beaches experience cyclical variability in relation to the change in season. Winter brings higher levels of storm activity and wave energy in comparison to summer (Munoz-Perez & Medina, 2010; Yates *et al.,* 2009). Literature notes that beach morphology tends to experience erosive profiles during the winter period, while reduced wave energy during summer promotes sediment accretion (Dubois, 1988; Komar, 1998). Pauanui in theory should experience shoreline retreat during winter months (June, July and August) and shoreline advance during summer (January, February and December). However Pauanui Beach does not follow uniform seasonal patterns that are described in literature. Winter cutback and summer accretion are not consistent throughout the entire season and large wave events during specific months - more often than not - do not impact the beach negatively. Six out of nine storms returned either the same or larger quantities of sediment onshore following the onset of reduced wave energy.

The timeseries began in 2002 with an erosive phase extending over the two summer months and the first month of autumn (March). This is an opposing phenomenon to literature that suggests accretion should occur. Two out of three winter months experienced accretion rather than erosion. Winter patterns for the month of July and August agree with winter profile theories, however June does not. The month of June therefore responded with an accreted profile during this winter period. June and July featured wave events larger than 4 m significant wave height, and had pursuant accretionary phases which returned more sediment onshore than what was eroded. Overall patterns indicate summer cutback and winter advance. 2003 shoreline data similarly did not display strong seasonality. Summer experienced accretion, autumn cutback, winter accretion with a large cutback during August, and spring accretion. Visible seasonal shoreline patterns were evident during 2004 only. Accretion was

experienced throughout summer, where the shoreline mean position was cut back considerably during autumn and into winter. The shoreline accreted considerably during spring and the start of summer to its most outer seaward position.

Summer months bring decreases in wave energy and storminess. Declines in energy trigger accretion phases to dominate due to the reduced sediment transport mechanisms associated to large energy fluxes. On occasion, cyclone tracks shift westward during summer and bring tropical storms to the Coromandel Peninsula (Bryan *et al.,* 2009). Increased wave energy is created and this influences the decrease in shoreline position due to erosion. Tropical cyclones were experienced during the summer of 2003 cutting back the shoreline. Reduced wave energies between the final summer storm (March) and the largest winter storm during July, meant sediment stored in the offshore bar was transported back to the berm allowing accretion during winter. It is also hypothesised that large sediment fluxes ejected from the estuary mouth into the Pauanui Beach system throughout the winter season influenced the shoreline position. As a result of the large surrounding catchment, sediment retained within the estuary from runoff is potentially flushed from the estuarine environment and transported onto the adjacent beach. This was not elaborated further throughout this study due to time constraints and research restrictions.

3.7.1.3 Long term

Alongshore uniformity at Pauanui Beach was lacking during storm events, however over long term scales, uniform behaviour was quite strong. This is potentially due to the interaction of offshore island with wave approach direction. All three transects analysed over the length of Pauanui Beach (north, mid, south) experienced erosion and accretion cycles together. The extent of the erosion and accretion to the cross shore position however was not uniform. Northern aspects of Pauanui tended to be located further seaward than the other transects, particularly from the end of 2003 through 2004. Increasing rates of sedimentation at this end resulted in the larger sediment accretion. The ebb

tidal delta is located at this end of Pauanui Beach and does not provide a barrier for sediment to accumulate against, unlike headland bay beaches. The increasing shoreline position seaward is therefore estimated to be a result of the alongshore sediment transport to the north, and the accumulation of sediment at the ebb delta from estuarine flushing. The shoreline had a total movement range of 47 m over a three year period, with net accretion of 11 m. The mean shoreline position (averaged over the entire alongshore distance) moved between a maximum onshore position of 682.3 m and maximum offshore position of 634.7 m in the cross shore (where offshore and onshore movement is towards 600 m and 700 m respectively). The gradual increase in beach width and seaward shoreline position of Pauanui Beach matches theories of beach width movement caused by the ENSO index. Long term negative ENSO values relate to El Niño Conditions which influence beach accretion due to the onshore directed wind and reduced storminess (as opposed to positive ENSO values and eroding La Niña conditions). Therefore the shoreline positions not only vary in response to short term storm events or seasons, but they also respond to climatic oscillations at the inter-annual time scale.

3.7.2 Beach rotation

Research suggests that beach rotation is a phenomenon confined to embayed beaches (Klein *et al.,* 2002; Ranasinghe *et al.,* 2004; Short & Masselink, 1999; Wood, 2010). Wood (2010) noticed however that Pauanui Beach, a harbour adjacent intermediate beach experienced rotation during the analysis of beach profile surveys. It was noted that this defies current literature and would require further research to distinguish the processes governing this rotation. Pauanui Beach shoreline data created in this study display long term rotation from mid 2003 as opposed to regular short term variation. Correlation statistics of rotation co-efficient with wave energy flux returned poor results with an r-squared value of 0.05. This correlation agrees with findings by Wood (2010). It was noted in his research that r-squared values of rotation and energy flux were very poor across the entire peninsula. During two sudden rotation changes on Pauanui between

2002 and 2003 (December/January) rotation was linked to increases in energy flux. The large January flux is related to an extreme wave event, identified previously as storm event three. The shoreline responded during this event with the largest erosion cutback throughout the entire period. Rotation experienced throughout this event was therefore generated by a large wave event and a large energy flux, of which had a strong alongshore component (when a negative energy flux is created, the southern end rotates). This phenomenon is not representative of the entire timeseries as not all negative fluxes during large wave events created a strong rotation. It is hypothesised that the offshore islands cause a shadow effect on the incident wave approach angle and project a varied wave height alongshore. Longshore currents are created as a result of the pressure gradient and sediment is transported, causing rotation.

During the long term shoreline analysis of three transects at 550 m, 1550 m, and 2550 m their alongshore uniformity, it was identified that rotation was occurring. Theory suggests however that rotation occurs between two ends of a beach accreting and eroding that are in an out of phase relationship (as one end accretes the other erodes), while the middle areas act as a fulcrum point (Short & Trembanis, 2004). Pauanui does not display this phenomenon, and it is hypothesised that a rotation co-efficient is created in response to the variation in cross shore position of the shoreline, despite the uniform erosion or accretion phenomenon at either end. The parabolic nature of Pauanui also defies theory as rotation has been limited to embayed beaches. Comparisons of the transect positions with long term ENSO index data were made to determine the existence of rotation. Negative correlations of the northern and southern transects (550 m and 2550 m) identified an out of phase relationship between the two beach ends. Further correlations of transect one (northern) with the ENSO index found that with increasing ENSO, the northern end would erode, although at a 13 month lag. Transect three (southern) correlations with ENSO index found the opposite, with increasing ENSO, the southern end will accrete, although at a nine month lag. Ranasinghe (*et al.,* 2004) researched the relationship between rotation and SOI index at Narrabeen Beach, Australia. Rotation was identified using cross-correlation statistics between individual profile surveys. Negative correlation

between the first and last profile related to a negative phase relationship between the erosion and accretion cycles at either beach end (Ranasinghe *et al.,* 2004). In order to determine effects of SOI, beach widths were used as an indicator. Negative correlations of SOI with northern beach width showed erosion at the north (width decrease) conversely positive correlations of southern beach width and SOI showed accretion (width increase). Lags existed between SOI and beach response by 3 months at the northern end and 1.5 years at the southern. Techniques used during the Ranasinghe (*et al.,* 2004) study were very similar to those used in this study. Variations to those methods used by Ranasinghe (*et al,.* 2004*)* during profile analysis were however using a beach profile shoreline dataset (instead of beach width) that had been collected at three monthly intervals (instead of monthly).

3.7.3 Beach profiling

Video shoreline data were compared to a long term beach profiling dataset gathered at a three monthly period. Both datasets were sampled at considerably different timeseries, however overall shoreline variation results were quite similar. Correlation statistics between the alongshore uniformity of shoreline placement showed that the northern and southern ends were out of phase. However this out of phase relationship is due to the variation in cross shore positioning of the shoreline, rather than erosion and accretion relationships. The northern end of Pauanui gradually accretes seaward, while the southern end does the same at a considerably lower rate and cross shore distance. Rotation co-efficients determined by this alongshore shoreline position also displayed similar results to video data results. A gradual accretion to the northern end was associated to a negative rotation co-efficient. Sample times were identified as the problematic cause to this lack of short term and seasonal rotation patterns. High resolution data collection by cameras allows for highly quantitative results to be generated that are representative over long time periods. Therefore video technology provides an accurate monitoring technique to determine rotation

events at Pauanui. Smaller sampling times of profile collection would be needed at monthly time scales instead to determine smaller scale patterns.

3.8 SUMMARY

Analysis of the short, medium and longterm term behaviour at Pauanui Beach showed results that are not typical of non-embayed beaches.

- Short term wave events larger than 4 m significant wave height were separated and analysed against shoreline position. Pauanui shoreline was found to respond by eroding during large wave events.

- Accretion was triggered when wave heights decreased and storm conditions subsided allowing the shoreline to recover. Exemptions to this pattern did occur however.

- Despite the mean shoreline positions presenting a uniform erosion/accretion pattern (not rates or durations of erosion/accretion), analysis into alongshore uniformity was developed.

- The northern end showed increased variability, specifically during two events where accretion was experienced at the peak of the storm. This incident did not agree with behaviour displayed at the middle and southern ends of the beach, where shorelines were eroded.

- Seasonal changes in shoreline were highly irregular at Pauanui and there was no definitive seasonal structure. 2004 was the only year that displayed some regularity in seasonal change where summer brought shoreline accretion and winter shoreline erosion.

- Variations of the shoreline in winter are potentially caused by the sediment flux entering the beach system during winter from the estuary.

Allowing more sediment to be transported alongshore prevents the shoreline to deplete in sediment during storm events.

- Long term accretion trends were evident at Pauanui associated to the long term negative ENSO index trend. When El Niño conditions are present, beaches tend to accrete, conversely during La Niña conditions beaches tend to erode.

- Long term alongshore uniformity was present at Pauanui, an opposite phenomenon than what occurs during short term events. However the cross shore positioning of the shoreline alongshore was not uniform. The northern areas extended further seaward than both the mid and southern areas, while the southern area extended further seaward than the mid, thus creating a significant parabolic shape to the beach.

- Beach profiling data had similar results to these and therefore agrees with the video shoreline data.

- Beach rotation was indicated through the lack of alongshore uniform behaviour during short term events. Once compared to wave approach directions, it was hypothesised that rotation was being caused by the alongshore variation in wave height generated by island shadowing.

- Correlation statistics completed during this thesis found a distinctly poor relationship between the rotation co-efficient and wave energy flux. However during one instance where the shoreline rotated suddenly, rotation was strongly associated with a distinct increase in energy flux for the same time.

- Throughout the rest of the timeseries, flux changes did not interfere with the beach rotation found at Pauanui.

- Long term rotation was also present at Pauanui where the northern end accreted considerably more than the southern. As opposed to energy flux events, this rotation is linked to the ENSO index where El Niño conditions enable the long term rotation and accretion of the northern end.

Chapter Four -

Wave Climate Modelling

4.1 INTRODUCTION

The wave climate experienced at Pauanui and Tairua Beaches is described in this chapter. Both beaches are located on the eastern coast of the Coromandel Peninsula and are subject to similar wave conditions due to their geographic proximity. This chapter describes the modelling techniques used to determine the near shore hydrodynamics offshore Pauanui and Tairua Beaches. These results are then used to understand shoreline variation and beach rotation results identified by video imaging.

4.2 EASTERN COROMANDEL WAVE CLIMATE

Pauanui and Tairua Beaches are located on the eastern Coromandel Peninsula, exposed to waves generated in the Pacific Ocean. Storm and swell waves dominate from the north and east directions with mean significant wave height and peak period of 1.3 m and 10 s respectively. Although the wave climate is of medium energy (Bogle *et al.,* 2000) large energetic winter storms can present a significant wave height of 4-6 m in 50 m water depth (Bryan *et al.,* 2009). The mean spring tidal range at Pauanui and Tairua is 2 m (Bryan *et al.,* 2009). Both beaches are flanked by headlands to the north and south which reduces wave focussing from these directions. Wave approach angles are therefore from the north-east through to the south-east. Located offshore to the south-east and north-east of Tairua and Pauanui respectively is Shoe Island, while to the south-east of Pauanui lies Slipper Island. Waves from the appropriate direction interact with these offshore islands, prior to breaking onshore. Interaction of waves with islands can reduce incident wave energies projected onto beaches by creating a shadowing effect (Thomas *et al., 2011)*. Energy becomes dissipated and it is

hypothesised that an alongshore gradient is created allowing sediment transport to one end of the beach, causing rotation.

4.3 WAVE DATA

Wave data was collected by Wave Watch III (WWIII) wave hindcast from 1979 through until 2009. No long term wave dataset exists for the eastern Coromandel or the Pauanui-Tairua embayment. Only sporadic short term datasets collected by various research projects (de Lange, 2000). The WWIII dataset was extracted offshore in 50m water depth and represents deep water wave conditions. Waves collected in this water depth are different to those experienced on the beach. Further away from the generating conditions wave period increases and wave shoaling adjusts the wave height according to wave energy and water depth. For this purpose, wave modelling was undertaken to understand the relationship shallow water waves and currents have with the beach morphology variation. Figure 4.1 displays the combinations of significant wave heights and wave directions for the entire three year period. The most common wave height was 1.3 m experienced at 30^0 relative to due north. .

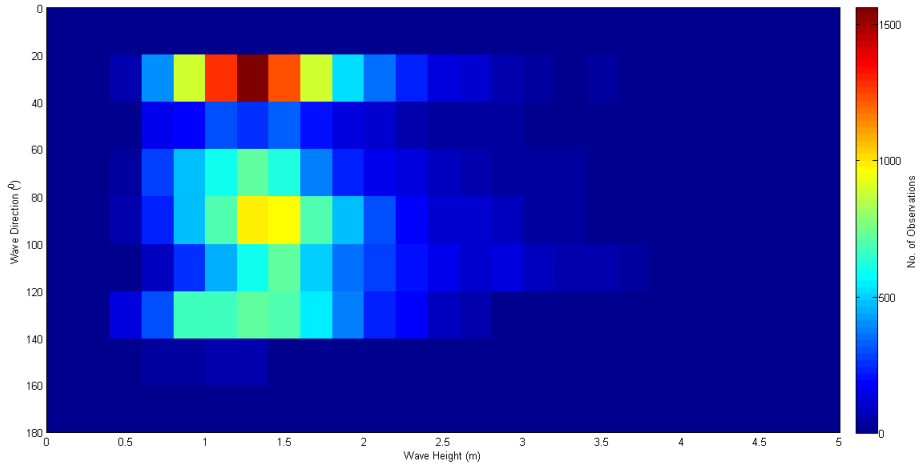

Figure 4.1: Wave height and direction combination. Most common wave height was 1.3 m experienced at 30^0 relative to due north. Colour bar represents the number of observations throughout the three year period.

4.4 BATHYMETRY

Wave climate modelling requires an accurate bathymetry (bathy) that extends to a depth that matches the depth where the wave data was collected. For this instance, a depth greater than 50 m offshore was used as the WWIII data was extracted from this depth. The required bathy was created through the digitising of a hydrodynamic marine chart, multibeam surveys, and LIDAR surveys from Waikato Regional Council. Features displayed (Figure 4.2) include bottom contours (colour bar), offshore islands and land barriers (white areas). The Tairua estuary is also included on this bathy map indicating the location of Pauanui and Tairua Beaches. Pauanui Beach is the long straight beach to the south of the entrance, and Tairua Beach is to the north of the entrance past Paku Hill. In order to get truthful wave data, the bathy needed to cover a significant distance further south and north of Pauanui and Tairua respectively. This ensures waves entering from the model boundary have enough distance to 'warm up' before propagating onto the coast. Otherwise waves reaching Tairua Beach were not being generated in deep water caused by the northern boundary being too shallow; and waves impacting Slipper Island directly at the southern boundary prior to reaching Pauanui Beach.

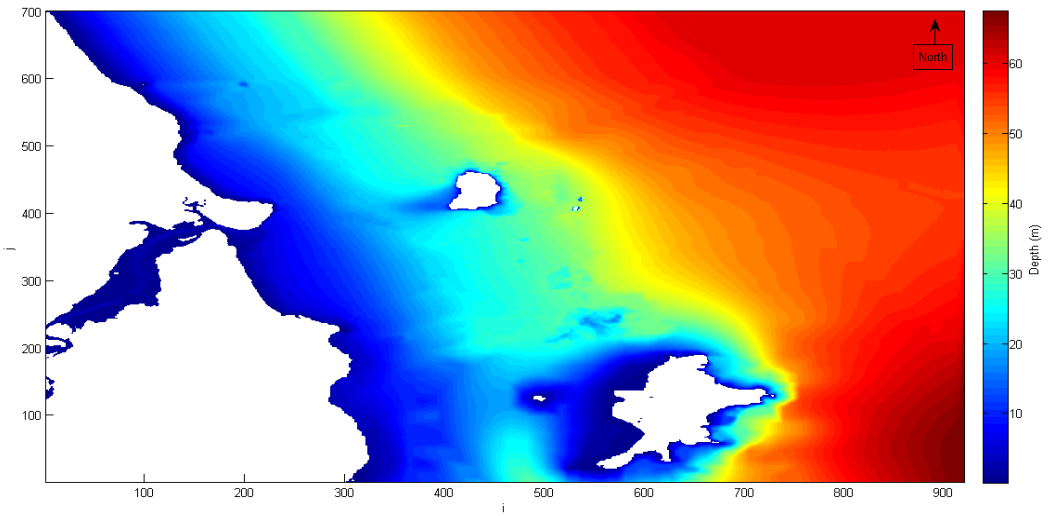

Figure 4.2: Model bathymetry covering Pauanui and Tairua Beaches. White areas represent land boundaries and depth contours are marked by the colour bar. X and Y axis marked by i and j respectively represent the number of grid cells in either direction (one grid is 20 m).

4.5 DHI Mike21

Wave climate modelling was initially conducted using the DHI Mike 21 Nearshore Spectral Model software. Set ups incorporated the bathy and wave climate dataset mentioned. The model set up required the use of significant wave height, wave period, wave direction and the directional spread throughout the modelled time period. Calculated runs were then automatically extracted every 24 hours throughout that 1 year period. However the wave directional spread parameters in the dataset exceeded those limitations set by the DHI program itself. The range of conditions used to force the model exceeded the range of conditions allowed. Therefore the wave data used in this project was not compatible with the software and model runs produced false results. Modelling using this software was abandoned from this point forward.

4.6 SWAN

SWAN modelling software was selected as the next best modelling programme to be used. SWAN is a third generation model developed to simulate waves in coastal zones (Violante-Carvalho *et al.,* 2009). No limitations were placed on the wave directional spread, and the same bathy and wave data used in DHI were compatible with SWAN. However initial model runs were unstable and crashed after a certain amount of time steps. The performance of SWAN was tested during research undertaken by Violante-Carvalho (*et al.,* 2009) on spectral models and the diffraction and reflection parameters. Detailed were the limitations to the SWAN model and the use of the two mentioned parameters simultaneously. When both parameters were used, the model crashed after a short number of time steps. Further test runs were initiated using reflection or diffraction parameter, but not both. All these runs were successfully concluded without the model crashing. Analysis of these results found that the model estimated significant wave heights better with diffraction enabled than without. However the importance of reflection on future wave propagation is greater than diffraction. Therefore the model is more successfully run without the diffraction parameter than without refraction (Violante-Carvalho *et al.,* 2009).

Their study concluded that with the effect of directional spreading, the importance of diffraction parameter is reduced as more energy will naturally be diffracted around the lee of a barrier anyway (Violante-Carbalho *et al.*, 2009).

Due to the poor stability SWAN runs had with diffraction enabled initially, stationary runs without diffraction were prepared. Model runs completed with the new settings used the nine storm event characteristics identified in Table 3-1. Each storm was modelled individually to determine the nearshore wave climate associated to these deep water wave conditions. Tairua Estuary was blocked during these runs to prevent further instability. During the model runs, significant wave height and radiation stress data were extracted along the 8 m contour line offshore of both Pauanui and Tairua Beaches. This data was compared to shoreline position at the same time to determine alongshore variability. These results are presented in Appendix III. Further model output parameters included the significant wave height, wave period, wave direction and radiation stress and these outputs are presented below.

4.7 MODELLING RESULTS

During shoreline variation and beach rotation analysis short term rotation was present at high frequencies. Once shorelines were fit with a polynomial curve, a rotation co-efficient was created due to the rapid variability in shoreline position between northern and southern ends. For long term analysis, these high frequency events or 'noise' were ignored in order to determine the overall trend of northern rotation. Modelling initiatives focused on the large wave events that exceeded 4 m in wave height, whose characteristics are displayed in Table 3-1. Snapshots of these nine peak storm conditions are presented as frames below, created during each model run (north is towards the top of the graph). Each individual storm was modelled to understand the near shore wave climate, particularly in the alongshore. Relationships between the alongshore variation in wave climate and alongshore variation in shoreline position was completed using this data, and the graphs in Appendix III.

4.7.1 Alongshore wave climate

Storm one: Waves approached from 79^0, almost directly onshore. The southern end of Pauanui Beach was located further seaward than the northern area, although during shoreline analysis, the northern area accreted more than the southern area during this time. Alongshore distribution of wave height is displayed on Figure 4.3. Visible is a zone of reduced wave height in the lee of Shoe Island that extends to the coast line to the northern areas of Pauanui Beach. Radiation stress alongshore remained constant throughout the mid beach area. Peaks at the northern and southern ends correspond to changes in wave height at the northern and southern areas also. As radiation stress increases, wave height decreases. Tairua Beach experienced a considerable reduction in wave height to the south by approximately 1 m. The mentioned zone of reduced height in the lee of Shoe Island extends to the southern areas of Tairua Beach also. Due to gaps in the dataset there is no shoreline profile available to visualise the alongshore shoreline profile. Therefore this comparison was ignored and hypothesis made in the discussion. Radiation stress along Tairua was highly variable in comparison to Pauanui Beach. Similarly, at either end of the beach, wave heights were decreased which corresponded to peaks in radiation stress gradients .

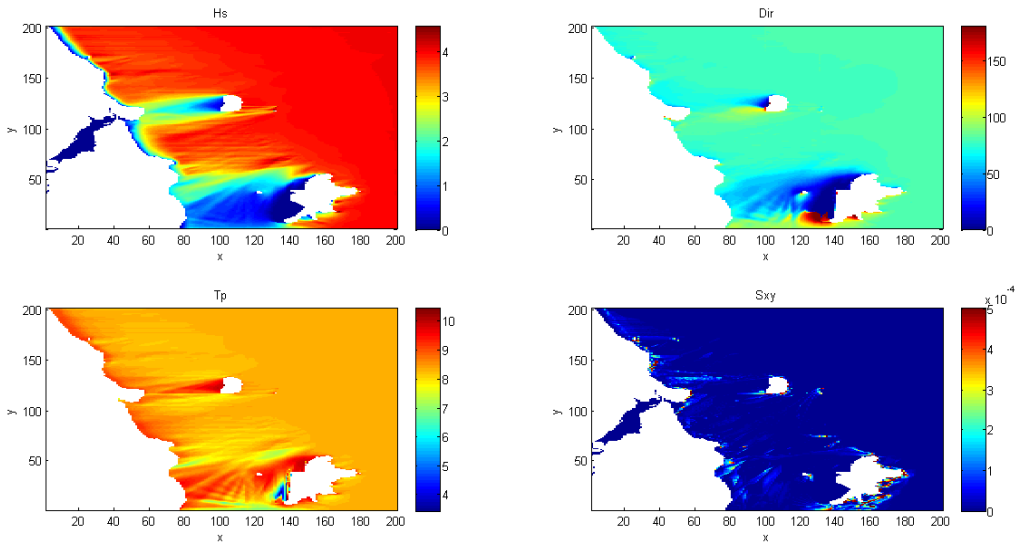

Figure 4.3: Storm one model results. Hs is significant wave height in metres, Dir is in degrees relative to due north, Tp is peak wave period in seconds, and Sxy is the radiation stress. X and Y axis represent the number of grid cells in either direction (one grid is 20 m).

Storm two: Waves approached from a more north easterly position of 65^0. Pauanui had reduced wave heights to the north with larger heights to the south. Zones of reduced wave climate to the north were created as a result of offshore island interference, allowing non-interfered wave conditions to propagate towards and impact the southern Pauanui beach. A noticeable decline in wave height was shown at the middle of the beach. This decline is in conjunction to a spike in radiation stress. Alongshore the radiation stress gradually increased with decreasing wave height at the northern end. Low variation in stress occurred at the south with a high wave height. Tairua Beach experienced a strong decline in wave height at the northern and southern beach end, this continuing the wave height/radiation stress trend that was experienced at Pauanui Beach as these zones were marked with high radiation stress gradients. Similar to storm one, gaps in the shoreline dataset prevented any alongshore shoreline profile to be used. Wave heights displayed a gradual decrease in height with increasing southward movement, although this was only to a magnitude of 0.3 m (Figure 4.4).

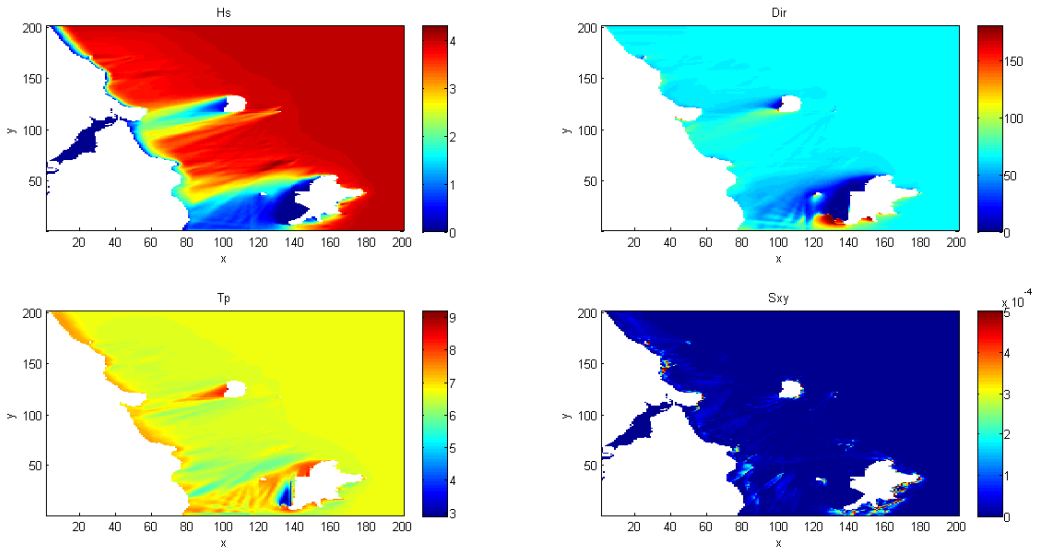

Figure 4.4: Storm two model results. Hs is significant wave height in metres, Dir is in degrees relative to due north, Tp is peak wave period in seconds, and Sxy is the radiation stress. X and Y axis represent the number of grid cells in either direction (one grid is 20 m).

Storm three: Pauanui Beach experienced the largest level of shoreline erosion during this time period. Waves approached from 82^0, a more easterly direction. Created was a shadow zone at the northern and southern ends of Pauanui and Tairua Beaches respectively (Figure 4.5). Distribution of wave height in 8 m depth offshore of Pauanui is reduced in to the north and larger in the south. Significant wave height increases and maintains a level of 3.5 m height further south where shadowing is not present. Radiation stress and the inverse relationship with wave height meant an increase in stress to the north which decreased southwards. Tairua Beach shoreline position for the same time experienced hot spot erosion due to rip currents. Alongshore shoreline trends point to southern accretion due to the seaward extent of the shoreline. Wave heights alongshore gradually taper in height further southwards towards Paku Hill. As mentioned the shadowing from Shoe Island reduces wave heights in this area. Unlike the noted trend of radiation stress and wave height at Pauanui, variations were not linked for Tairua. Radiation stress was highly variable alongshore, and this is not represented by changes in wave height.

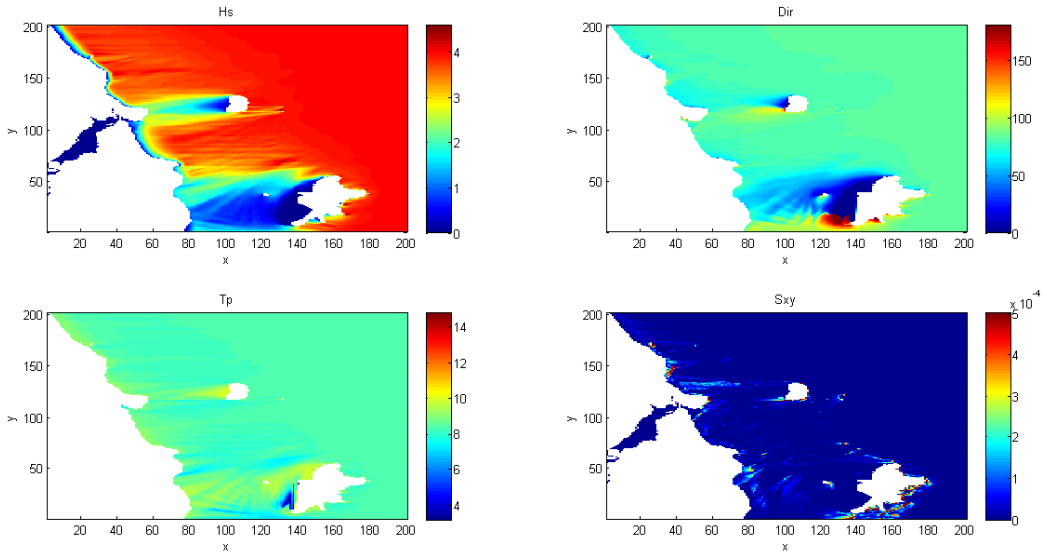

Figure 4.5: Storm three model results. Hs is significant wave height in metres, Dir is in degrees relative to due north, Tp is peak wave period in seconds, and Sxy is the radiation stress. X and Y axis represent the number of grid cells in either direction (one grid is 20 m).

Storm four: Pauanui Beach is not shadowed during storm four as much as other storms due to waves approaching from an 87^0 angle. An almost easterly direction created a larger shadow zone on Tairua instead. Northern areas of Pauanui Beach display slightly reduced wave heights, caused by the southernmost point of this shadow zone. Wave heights alongshore are within 0.5 m of this value therefore shadowing does not alter alongshore distribution greatly. The inverse relationship between wave height and radiation stress is experienced throughout the alongshore length of Pauanui. Tairua Beach again experiences a variable radiation stress alongshore that is not visible in wave height data. Gradual decline in wave height to the south from 4 m to 3 m is associated to this shadow zone displayed in Figure 4.6. The wave height is constant and does not vary. The northern areas of Tairua display a further seaward extending shoreline during this time.

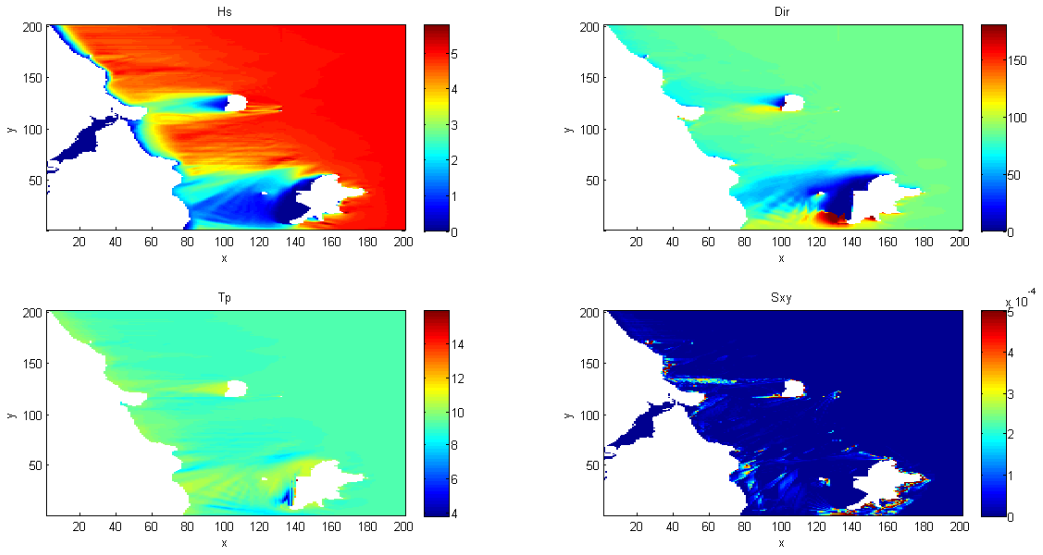

Figure 4.6: Storm four model results. Hs is significant wave height in metres, Dir is in degrees relative to due north, Tp is peak wave period in seconds, and Sxy is the radiation stress. X and Y axis represent the number of grid cells in either direction (one grid is 20 m).

Storm five: Alongshore distribution in wave height is varied at Pauanui Beach. Waves approach from a 63^0 direction and cause a shadow zone to the northern aspects of Pauanui. Wave heights in this area are reduced from 4 m experienced in the south, to 2.2 m. High radiation stress values are also experienced in this area for a considerable distance alongshore. Areas of decreased wave height and increased stress agree with the ongoing inverse relationship trend found at Pauanui Beach. The shoreline continues to display a parabolic nature but the northern end is accreting gradually at higher levels than the southern. Tairua Beach is also experiencing a northern accretion trend. Wave heights are decreased at this area and radiation stress gradients are high. Wave heights at the middle of the beach show zones of reduced height (Figure 4.7). These areas correspond to accretion zones either side of hot spot erosion caused by rip currents. Radiation stress spikes are experienced at the northern and southern extremities although gradients are reduced considerably in middle beach areas. No shadowing is experienced from Shoe Island during this period.

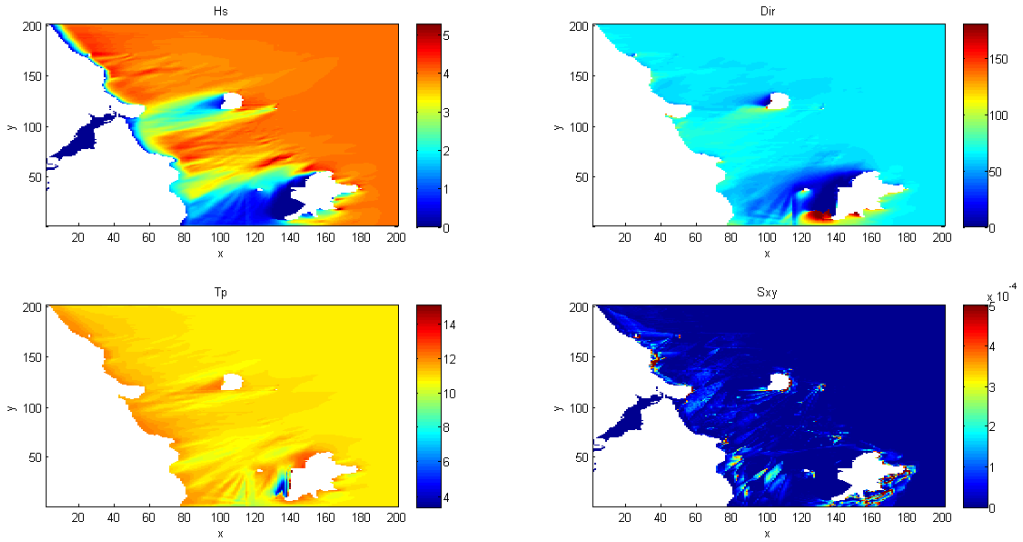

Figure 4.7: Storm five model results. Hs is significant wave height in metres, Dir is in degrees relative to due north, Tp is peak wave period in seconds, and Sxy is the radiation stress. X and Y axis represent the number of grid cells in either direction (one grid is 20 m).

Storm six: A direct easterly wave direction caused a strong shadow zone onto Tairua Beach. Pauanui Beach does not display any considerable zones of reduced wave height as a result of this shadowing (Figure 4.8). The northern end experiences a slight decline in wave height by approximately 0.5 m due to the southernmost extend of the shadow zone and its location. Southern areas of Pauanui Beach experienced a reduced wave height also. Uncommon shadowing from south-easterly located Slipper Island was projected onto Pauanui Beach. Increased radiation stress in the south is not experienced although in the north it is. Southern areas of Tairua Beach are considerably shadowed due to the lee of Shoe Island. Wave heights decrease from over a metre; however southern shorelines are displaying landward movement. Shoreline analysis will determine whether this area did erode during this period or whether accretion did occur moving an already eroded shoreline location seaward.

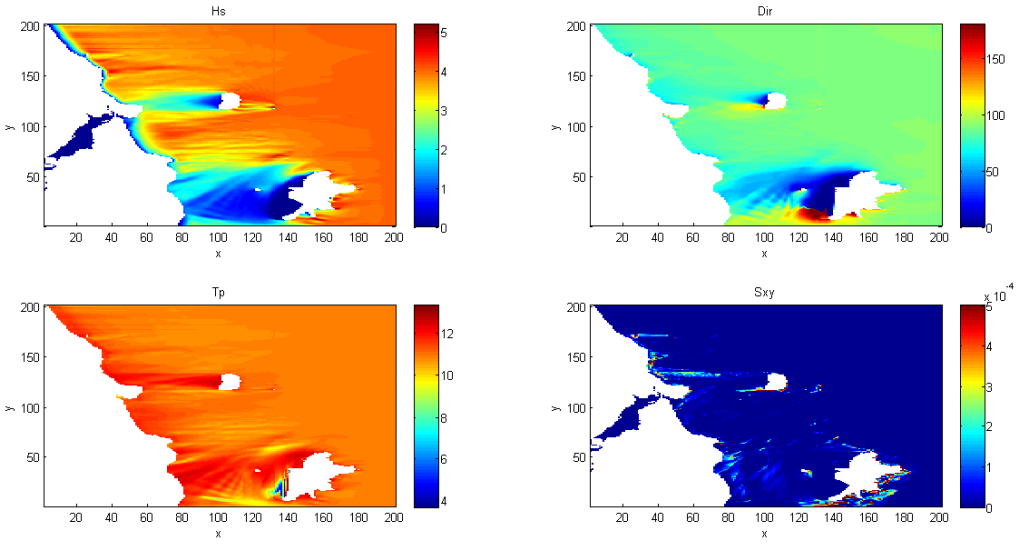

Figure 4.8: Storm six model results. Hs is significant wave height in metres, Dir is in degrees relative to due north, Tp is peak wave period in seconds, and Sxy is the radiation stress. X and Y axis represent the number of grid cells in either direction (one grid is 20 m).

Storm seven: Wave approach angles were considerably eastern in direction (87^0) projecting shadow zones onto the southern end of Tairua Beach and the northern most areas of Pauanui Beach. Wave heights did not vary largely and a total variation of 0.2 m occurred alongshore. The northern area of Pauanui displayed the zone of reduced wave height but not over a considerable longshore distance. Radiation stress at this northern end displayed higher values which gradually decreased with increasing southern movement. Tairua Beach instead experienced the shadow zone created by Shoe Island as a result of this wave approach direction. Southern ends are reduced in wave height and the shoreline is further landward than seaward. Northern areas featured higher wave heights, more than 1 m higher than the southern areas (Figure 4.9). Radiation stress spiked towards the middle of the beach but remains consistently low over the rest of the beach (nearly non-existent).

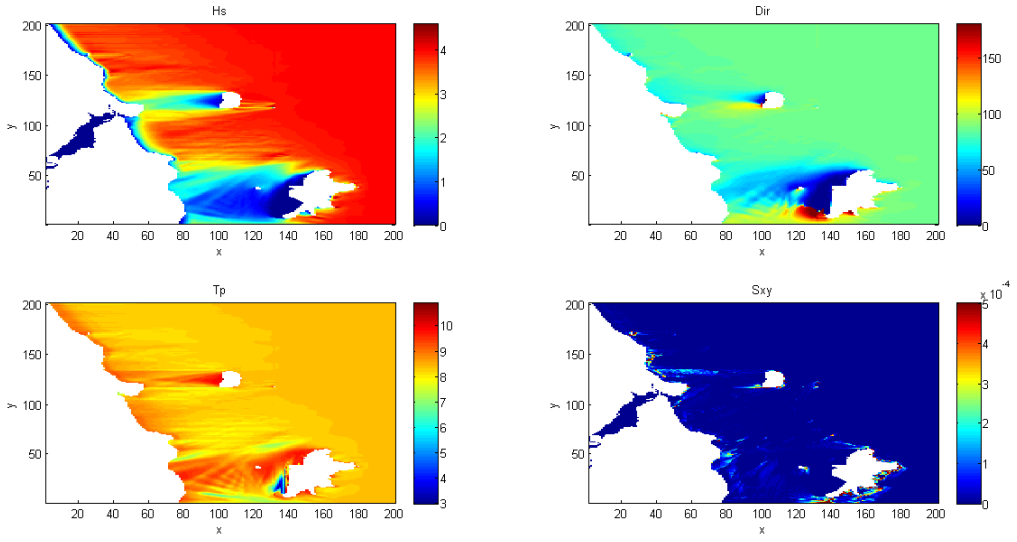

Figure 4.9: Storm seven model results. Hs is significant wave height in metres, Dir is in degrees relative to due north, Tp is peak wave period in seconds, and Sxy is the radiation stress. X and Y axis represent the number of grid cells in either direction (one grid is 20 m).

Storm eight: The northern most directed wave angle occurred during storm eight from an angle of 23^0. Shadow zones extended further south along Pauanui rather than at the north like previous storm events. Wave height distribution therefore was larger at the north and gradually decreased by 1 m towards the south. Radiation stress remained rather consistent at the north but increased slightly to the south as a result of the inverse relationship between wave height and radiation stress. Tairua did not experience any shadowing from Shoe Island at this time (Figure 4.10). Due to the 23^0 wave angle, shadowing was generated at the northern area due to Pumpkin Mountain headland instead. Wave heights to the north were decreased as a result but remained at higher levels towards the south. Radiation stress was still variable like other storms but spikes did not correspond to a change in significant wave height.

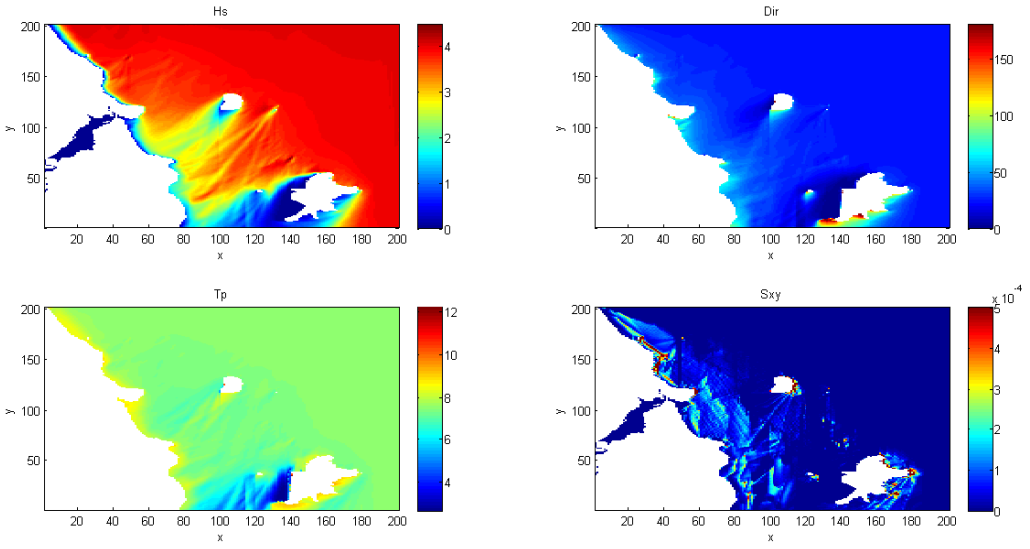

Figure 4.10: Storm eight model results. Hs is significant wave height in metres, Dir is in degrees relative to due north, Tp is peak wave period in seconds, and Sxy is the radiation stress. X and Y axis represent the number of grid cells in either direction (one grid is 20 m).

Storm nine: Shadow onto Pauanui Beach was projected directly towards the middle of the beach (Figure 4.11). A north-easterly wave angle resulted in a higher wave height at the north and south which decreased towards the middle of the beach. The northern area accreted during this time, and was potentially caused by longshore currents. Radiation stress was large at the north and constantly low for the rest of the alongshore direction. Tairua was not shadowed during this wave event by Shoe Island, although some sheltering occurred due to the northern headland. Reduced wave heights were evident at the northern end than at the southern end. Radiation stress too followed this pattern which was large at the north and reduced at the south. The alongshore shoreline position for this period was rather level and did not display strong rotation towards the north or south. Pauanui in comparison, displayed strong northern rotation with greater than 50 m difference in cross shore position between the northern end and middle area of the beach.

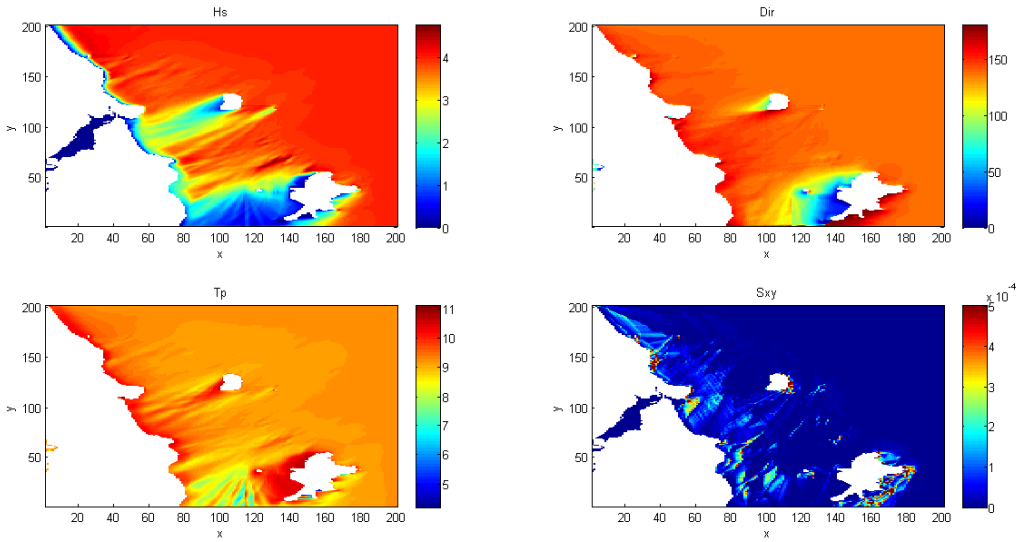

Figure 4.11: Storm nine model results. Hs is significant wave height in metres, Dir is in degrees relative to due north, Tp is peak wave period in seconds, and Sxy is the radiation stress. X and Y axis represent the number of grid cells in either direction (one grid is 20 m).

4.7.2 Radiation stress and longshore currents

Radiation stress is termed "the excess flow of momentum due to the presence of the waves" (Komar, 1998 pp. 168). Two components of radiation stress exist, the momentum flux in the x-direction (Sxx) and momentum flux in the y-direction (Syy) (Dean & Dalrymple, 2002; Komar, 1998; Sorensen, 1993). Combined, these two fluxes determine the onshore flux of longshore momentum due to waves and breaking (Sxy) (Dean & Dalrymple, 2002). Radiation stress gradients are associated to the generation of wave phenomenon including longshore currents and wave setup or down (Sorensen, 1993). Longshore currents occur in the nearshore zone and are generated by two factors, the oblique wave approach angles to the shoreline, and cell circulation from rip currents (Komar, 1998). Longshore currents are generated between breaker zones and the shorelines and are responsible for the longshore movement in sediment (Mei *et al.,* 2005; Dean & Dalrymple, 2002). Wave breaking turbulence dislodges and releases sediment from the bed, and longshore currents transport sediment alongshore (Mei *et al.,* 2005). Nearshore currents are not generated when waves are not breaking (Masselink & Hughes, 2003), and without breaking, sediment would not be entrained.

Currents generated by oblique waves are less complicated than cell systems and involve the y-component of radiation stress. As waves propagate from deep water the Sxy component is unaltered until breaking. Reductions in water level cause an increase in radiation stress gradients and vice versa. When these waves break, the Sxy is exhausted and causes a longshore current. The intensity of currents is determined by the amount of wave incidence and breaking, therefore strong currents are generated during storms (Masselink & Hughes, 2003). The magnitude of longshore currents can be determined through the wave incidence and breaker height using:

$$V_l = 2.7.Umax\,.\sin\alpha_{br}\,.\cos\alpha_{br} \qquad (2)$$

where $Umax$ is the maximum horizontal orbital velocity and α_{br} is the breaking wave angle. The maximum horizontal orbital velocity ($Umax$) is given by:

$$Umax = \frac{\Upsilon_b}{2} . C \quad (3)$$

Where Υ_b is the breaker ratio, C is the speed of the wave shape, known as the celerity. Longshore currents were found for three out of nine storms where wave angles approached from a more northerly (23^0), north easterly (63^0) and easterly direction (90^0) (storms eight, storm five and storm six respectively).

Storm five had a north-easterly wave incidence (63^0) creating a shadow zone to the northern aspects of Pauanui Beach. This wave direction is almost directly onshore to Pauanui Beach (65^0). Radiation stress gradients are high at this northern end compared to Tairua which had a strong peak at the far northern point. Southern areas of Tairua were slightly shadowed but wave heights were not reduced enough to affect the mean water height and radiation stress. Due to the oblique angle of Tairua facing more north than Pauanui (53^0), this wave angle is not directly onshore. The oblique wave incidence created a longshore current towards the south of Pauanui and Tairua at 0.94 m/s. Storm six had the most eastern wave incidence throughout all identified storms. Waves approached from 90^0 extending the shadow zone from Shoe Island to the southern areas of Tairua Beach. Pauanui Beach as a result did not experience a large proportion of the shadow zone to the north. Longshore currents created at both beaches were directed northwards at 2.29 m/s. Storm eight had the most northern angled wave approach direction at 23^0. Pauanui features a large shadow zone in the southern areas of the beach that extends northwards to the middle of the beach. Longshore currents generated at Pauanui and Tairua were towards the south at 2.58 m/s.

4.8 DISCUSSION

4.8.1 Offshore islands

Both Tairua and Pauanui experience the same deep water wave climate. Modelling results show however that the nearshore wave climate varies between the two beaches according to wave incidence. Wave approach directions are predominately from the north-east to east and oncoming waves are forced to interact with offshore Shoe Island. Waves from any other direction do not occur throughout this dataset, and thus means Pauanui is affected by shadowing from Shoe Island rather than Slipper Island to the south-east. Tairua Beach also experiences zones of shadowing from Shoe Island when oblique wave incidence is greater than 70^0. Shoe Island generates a barrier for waves to obstruct prior to propagating onshore of Pauanui and Tairua. Wave heights decrease and waves are refracted causing a reduced zone of wave height in the lee of the island. A decline in the mean water level occurs in these zones as a result of the reduced wave height and causes an increase in the Sxy component of radiation stress. This affects the alongshore wave driven currents in surf zones that are created by oblique wave incidence.

Shoreline erosion and accretion cycles identified in Chapter Three were found to be related to the alongshore variation in wave height. Areas that featured higher wave heights were associated to shoreline retreat due to erosion, compared to areas that featured lower wave heights and their association to shoreline advance. Selecting three transect locations alongshore of Pauanui Beach provided a reference dataset for long term sectional movement. Northern, middle and southern areas of Pauanui Beach were sampled from the original shoreline dataset. Shoreline positions over these three transects during major storm events provided evidence to the initial assumptions of wave height and shoreline positioning. However unusual features during storm eight where there was large erosion at one end of the beach and little accretion at the other, led to the suggestion that there is possibly other processes interacting to allow this phenomenon to occur. Gaps in the Tairua shoreline dataset meant the alongshore shoreline positioning for comparison to significant wave height distribution could not be completed. It is hypothesised based on other storm

observations however, that areas of decreased wave height are associated with zones of accretion. Storm one demonstrated a gradual wave height decrease towards the south by approximately 1 m. This zone is estimated therefore to be a zone of accretion, while the northern areas erode.

4.8.2 Radiation stress and longshore currents

Parabathic currents are confined to both the swash and surf zones as littoral drift and alongshore currents. Longshore currents are generated by two factors, although they can also be used in conjunction with each other (Klemas, 2009). Longshore variations in wave heights cause a longshore pressure gradient due to the variation in water level alongshore. Currents are forced to flow from areas of high pressure or elevated water level, to areas of low pressure or decreased water level. Longshore currents are also created by the oblique wave angle of wave trains to the beach. Dissipation of momentum associated with wave orbital motions generate an alongshore current parallel to the shore. Longshore currents were created at both Pauanui and Tairua Beaches throughout all storm events. Waves approaching from a direction less than 90^0 created a southward moving current while a northward moving current was experienced at 90^0 or larger. Storm five (63^0) experienced erosion over all three transects sampled alongshore of Pauanui Beach, although the beach gradually accreted to the north. Longshore currents created during this storm were directed southwards, transporting sediment entrained from breaking to the southern areas. Wave approach angle therefore generated the longshore current during this event. The accretion to the north is assumed to be in response to the flushing of estuarine sediment.

Modelling of the Pauanui and Tairua Beaches wave climate and extracting radiation stress from the 8 m depth contour gave an alongshore distribution of Sxy radiation stress component. These can be seen in Appendix II where comparisons are made with the alongshore wave height extracted at the same time, and the shoreline positions found using video data also for the same time. Pauanui often displayed higher radiation stress gradients at the northern and

southern areas compared to Tairua which displayed strong variation alongshore. Positive radiation stress gradients are caused by shoaling and a decline in water level, known as 'wave set down'. The opposite situation occurs when radiation stress gradients are negative and 'wave set up' raises water levels for breaking. The inverse relationship between water level (increased wave height increases water level and vice versa) and radiation stress gradient is related to sheltered zones created by Shoe Island or headlands. When water levels decreased to the north of Pauanui for example, radiation stress was high, producing wave set down. This is caused by areas of breaking within close proximity to the Paku Hill headland, and the reduced water level caused by shadowing. Although at considerable cross shore distance from Pauanui Beach itself, breaking occurs along the land boundary close to the rapid 8 m drop off. Once waves break, wave heights and the mean water level decrease, causing a rise in radiation stress. When waves propagate onshore, the mean water level must change in order to allow the radiation stress gradient to remain balanced (Lin *&* Zhang, 2005*)*. Shadow zones created by Shoe Island similarly generate increased radiation stress gradients due to the variation in wave height and mean water level within these zones. Water levels are decreased from the sheltering of the offshore island, creating higher radiation stresses in the lee due to the longshore flow.

4.9 SUMMARY

Nearshore environments are highly dynamic systems due to the complex feedback mechanisms between offshore hydrodynamics and beach morphology (Klemas, 2009). Interactions between wave orbits and currents with the bottom bathymetry effectively move sediment and causes large morphological variability. Wave climates present diverse ranges of wave heights, periods and approach directions to any one location. This provides opportunities for beach erosion, accretion and several other small to large scale phenomenon to occur.

- Approaching waves are reflected and refracted around offshore islands and bordering headlands of either beach. Islands are causing a shadowing effect on beaches, although this is dependent on wave approach angles.

- Alongshore distribution of wave height is therefore varied due to the sheltering from Shoe Island. An inverse relationship between wave height with the shoreline position is created as a result.

- Oblique wave angles generate an alongshore variation in radiation stress gradient on both Pauanui and Tairua Beaches. The Sxy component of radiation stress determines wave set up or down and is an important component of longshore currents or 'littoral drift'. Sediment is transported alongshore in these currents once being entrained in the water column through wave breaking.

- When the radiation stress gradient is strong, the water level at Pauanui is low and wave set down is occurring. When radiation stress is weak, the water level at Pauanui is high and wave set up is occurring.

- Shoreline variability and beach rotation at Pauanui and Tairua Beaches are therefore not subject to one hydrodynamic phenomenon. Interactions of the alongshore distribution in wave height and oblique wave incidence cause the morphological variability in shoreline seen throughout the three year period.

- Rotation in particular, is strongly linked to the longshore current produced during storm events, through the deposition of transported sediment.

Chapter Five -

Tairua Beach Comparison

5.1 INTRODUCTION

This chapter compares the shoreline variability and beach rotation found at Pauanui Beach between 2002 and 2004 with the same phenomenon occurring at Tairua Beach. Shoreline data had already been extracted during previous research initiatives on rip current dynamics (Gallop *et al.,* 2009). Standard video image processing techniques were used in the development of these two datasets, and shoreline extraction for the Pauanui dataset was based on processes undertaken on the Tairua dataset. Therefore dataset analysis between Pauanui Beach and Tairua Beach was made consistent to ensure the two datasets could be compared.

5.2 TAIRUA BACKGROUND

Tairua, located within close proximity to Pauanui Beach, has been well studied in the past. Unlike Pauanui, rip current formation, swash runup, and beach rotation have all been the focus of research initiatives on Tairua Beach. Tairua is an embayed beach surrounded at the northern and southern terminus respectively by Pumpkin Mountain and Paku Hill. International research suggests that beach rotation occurs on these types of beaches, and Tairua is no exception. Bryan *(et al.,* 2009) identified the regular short term transformation of beach morphology as a result of beach rotation. Shoreline rotation tends to be in unison with the barline rotation and is strongly controlled by the alongshore energy flux (Bryan *et al.,* 2009). Northward and southward alongshore energy flux events that were over 3500 J/m^2 were related to this beach rotation (Bryan *et al.,* 2009). Observations were made that three persistent rip currents were present at the end of the beach which was rotated seaward (Bryan *et al.,* 2009). These results were taken into consideration during the comparative analysis in this chapter.

5.3 SHORELINE VARIATION RESULTS

5.3.1 Short term shoreline variation

5.3.1.1 Storm events

Waves identified in Table 3-1 were used for comparison in this chapter. Similarly with results found on Pauanui Beach, an inverse relationship between large wave events and shoreline position exists. This is represented in Figure 5.1 which presents a strong mutual relationship between mean shoreline positions at Pauanui and Tairua Beaches. Ultimately events that affect the Pauanui shoreline will also affect the Tairua shoreline in a similar manner. This includes the response of large shoreline cutbacks to large wave events (Figure 5.2). High energy events will cause shoreline retreat landward and will gradually recover seaward during periods of low energy. Shoreline position values governed by the nine storm events are presented in Table 5-1.

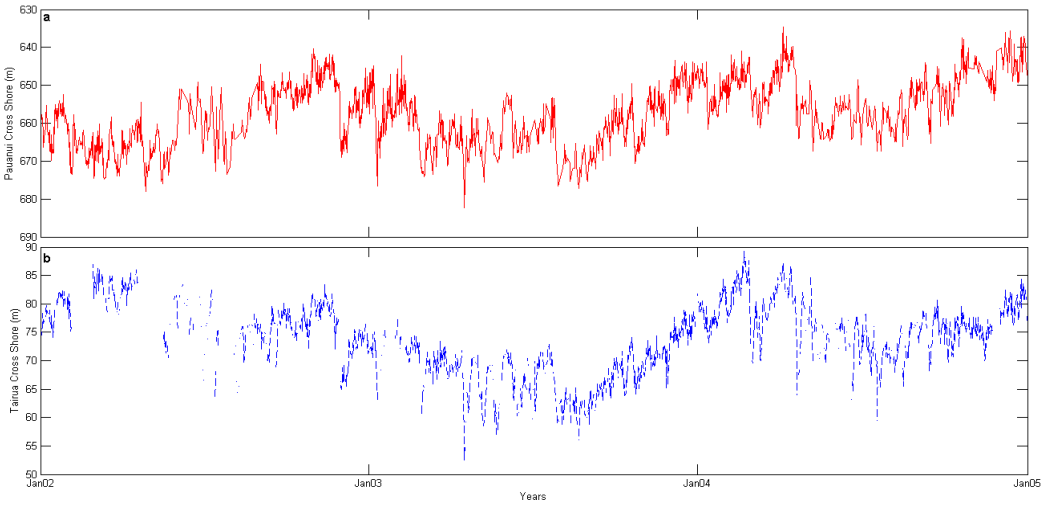

Figure 5.1: Mean shoreline position for a) Pauanui Beach and b) Tairua Beach. Seaward movement is towards the top of each graph and landward is towards the bottom.

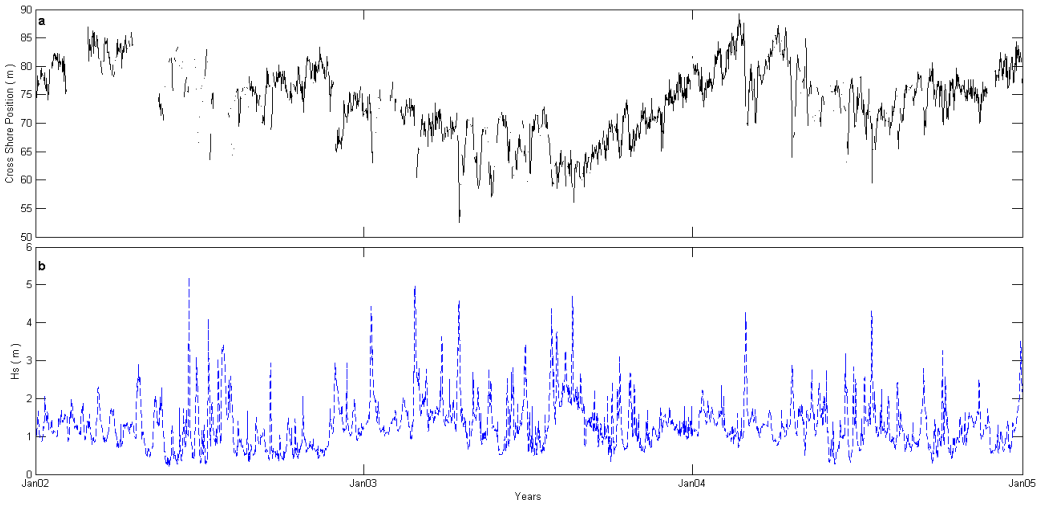

Figure 5.2: a) Mean shoreline position over the dataset period 2002-2004 at Tairua Beach. Seaward (landward) movement is towards the top (bottom) of the graph indicating accretion (erosion). b) Deep water significant wave height against time over the same time period.

Storm one: *This storm is not discussed as a result of missing data during the shoreline extraction process.*

Storm two: *This storm is not discussed as a result of missing data during the shoreline extraction process.*

Storm three: *Waves approached from 82^0 which created a shadow zone to the south of Tairua and the north of Pauanui. Deep water wave heights decreased in these shadow zones from 4.4 m to 3.4 m. Erosion periods during this storm was for 98 hours resulting in a 12.1 m shoreline cutback (0.12 m/hr erosion rate). Accretion periods that followed lasted 137 hours although there was an extremely small accretion rate (0.01 m/hr) with a total shoreline recovery of 1.45 m. Therefore the shoreline was put in an erosive state following this storm as a result of the poor quantities of sediment returned by cross shore transport.*

Storm four: *An easterly directed wave climate shadowed the southern aspects of Tairua as shown in Figure 4.5. Like storm three, wave heights decreased in this zone. Total erosion was 12.57 m at a rate of 0.17 m/hr and was succeeded by an accretion period lasting 133 hours. This was the largest accretion period of all storms. The shoreline accreted 10.98 m, leaving a deficit in*

Table 5-1: Maximum shoreline position prior to peak storm erosion, minimum shoreline position during the storm, maximum post storm shoreline position at Tairua Beach. Erosion/accretion rate marked with a * indicates where the accretion period was smaller than the erosion period. Gaps in the dataset resulted in no statistics for storms one and two.

	Prior storm max shore position (m)	Storm min shore position (m)	Post storm max shore position (m)	Total Erosion (m)	Total Accretion (m)	Erosion period (hr)	Accretion period (hr)	Erosion/Accretion rate (m/hr)
Storm one	-	-	-	-	-	-	-	-
Storm two	-	-	-	-	-	-	-	-
Storm three	75.11	63	64.45	12.11	1.45	98	137	0.12 / 0.01
Storm four	73.08	60.51	71.49	12.57	10.98	74	133	0.17 / 0.08
Storm five	71.75	52.53	70.73	19.22	18.2	74	212	0.26 / 0.08
Storm six	71.46	59.61	63.17	11.85	3.56	159	72	0.07 / 0.05 *
Storm seven	65.25	56.01	63.24	9.24	7.23	71	99	0.13 / 0.07
Storm eight	89.23	69.98	80.34	19.25	10.36	171	99	0.11/ 0.10 *
Storm nine	75.96	59.49	72.82	16.47	13.33	87	220	0.19 / 0.06

total amount returned in comparison to what was eroded. The shoreline remained in an eroded state after the accretion period which did not allow for large shoreline advance seaward.

Storm five: *one of the largest shoreline cut backs occurred during this storm. 19.22 m of shoreline was eroded at a rate of 0.26 m/hr. The fastest erosion rate over all storms was experienced at Tairua. A considerably large accretion period followed lasting 212 hours. Total amount of shoreline recovered did not match what was initially eroded during the peak (18.2 m) and the accretion rate was the same as storm four, 0.08 m/hr. Again, the shoreline did not fully recover keeping the shoreline in a post storm eroded state.*

Storm six: *Accretionary periods following the storm peak lasted for a reduced time period than the erosion period. This was the only storm to exhibit this behaviour at Tairua. In comparison to Pauanui, this event did not coincide as*

two instances where this phenomenon occurred was during storms four and five. Total amount of shoreline retreat was 11.85 m over 159 hours (0.07 m/hr erosion rate) while total amount of shoreline recovery was 3.56 m over 72 hours (0.05 m/hr accretion rate). Considerably short shoreline accretion distances were attained following this storm due to the length of the accretion period. Strong shoreline cutback remained as a result of the sediment being held in the offshore bar system.

Storm seven: *Shoreline erosion lasted a total of 71 hours as opposed to the accretion period lasting 99 hours. Waves approached from a similar direction to storms three and four which created shadow zones to the southern areas of Tairua. The total shoreline erosion resulted in a 9.24 m retreat. The total shoreline accretion resulted in a 7.23 m advance. These were the smallest erosion and accretion distances at Tairua Beach out of all nine storms. The erosion rate was 0.13 m/hr while the accretion rate was 0.07 m/hr. Storm seven continued the ongoing trend of net erosion following storm events that features waves greater than 4 m significant wave height. Sediment remained in the offshore bar instead of being transported onshore to the berm.*

Storm eight: *The furthermost extended shoreline position occurred during this event. Despite the shoreline eroding at the storm peak, the overall location was more seaward than any other transect prior to the storm. The erosion period lasted 171 hours where the shoreline retreated by 19.25 m, the largest cutback experienced over all storms. At a rate of 0.10 m/hr for a period of 99 hours, the shoreline advanced 10.36 m. The accretion period for this storm was much smaller than the initial erosion period also. The beach was highly accreted prior to the peak of this event, where erosion resulted in a large shoreline cutback. Not all sediment lost was regained, which left the shoreline in an eroded state post storm.*

Storm nine: *The ongoing trend of a longer shoreline erosion period than shoreline accretion period continued throughout this storm. The shoreline eroded for a period of 87 hours at a rate of 0.19 m/hr. This moved the shoreline landward by 16.47 m. Accretion of the shore position lasted for 220 hours at a*

rate of 0.06 m/hr. This is the largest accretionary period for all storms. Seaward movement of the shoreline occurred by 13.33 m. Waves approached from 44^0 during this period, almost directly onshore of Pauanui. This means that no shadowing to Tairua from Shoe Island occurred. The shoreline therefore was put in an eroded state following the net erosion of sediment caused by the storm.

5.3.1.2 Uniform alongshore variability

Pauanui Beach experienced little alongshore uniformity during alongshore analysis. A highly variable northern end resulted in accretionary phenomenon during two storm peaks (one and nine) while the southern two transects displayed erosion. Analysis was completed on the Tairua dataset utilising three transects, one to the north, one in the middle and on to the south of the beach. Distances selected at Tairua were 350 m, 800 m, and 1250 m respectively. Figure 5.3 a, b and c displays the mean shoreline positions prior to the storm, during the peak of the storm and after the storm (post) at each transect. The cross shore position is displayed where offshore is 120 m (ocean) and onshore (land) is 0 m. Only seven storms were analysed due to missing data for storms one and two, assumed to be caused by visibility constraints during shoreline extraction. Similar cutback patterns were present at Pauanui Beach although two exceptions during storms one and nine were observed. Instead of erosion dominating during the storm peak, the northern areas of Pauanui accreted. Tairua did not display any unusual shoreline displacement during the storm peak, but instead displayed consistent erosion.

One of the largest shoreline retreat measurements occurred during storm five. The shoreline cut back a total of 19.22 m which was the second largest mean cut back total of all storms. This shoreline retreat coincides with the largest transect cutback level experienced over all transects. Northern areas of the beach were in an accreted state prior to the storm, however a cutback of 27.3 m retreated the shoreline landward at the storm peak. Middle and southern areas of Tairua too featured erosion during storm five, but not to this extreme extent.

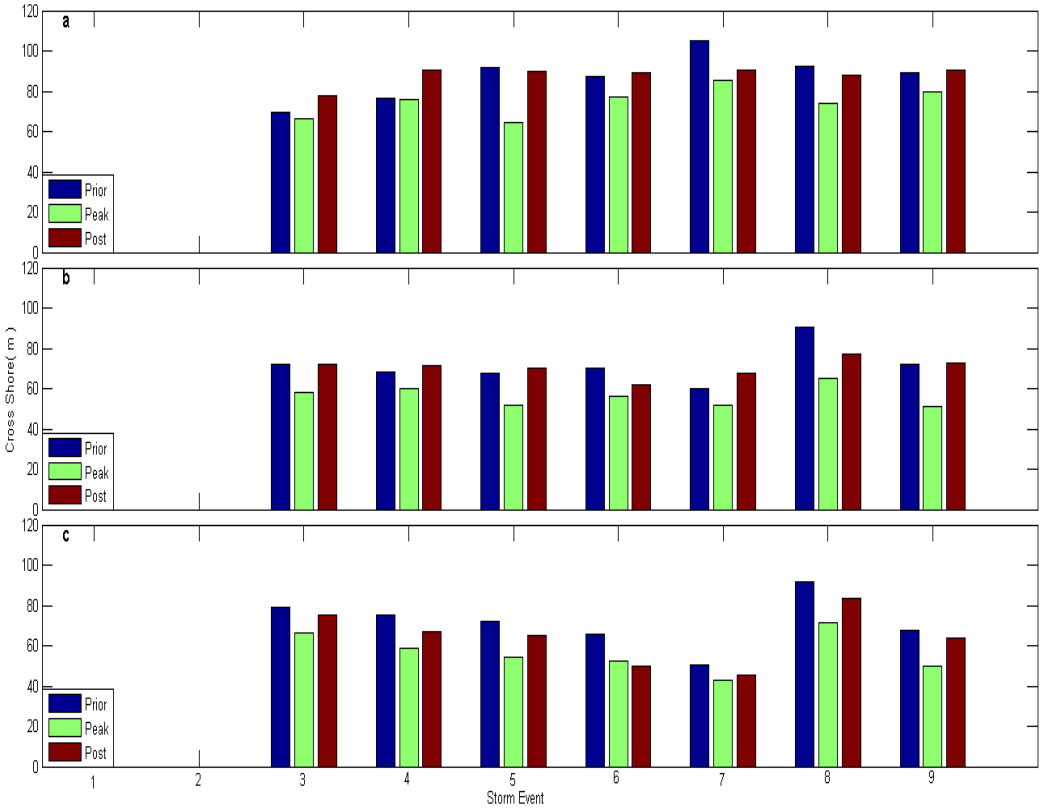

Figure 5.3: a) 350 m alongshore location to the north of the beach (by Pumpkin Mountain). b) 800 m alongshore location at the middle of the beach. c) 1250 m alongshore location to the south of the beach (by Paku Hill). Shoreline position prior to the storm is blue, shoreline position during the storm peak is green, and shoreline position post storm is burgundy. The cross shore location is displayed where offshore is 120 m (ocean) and onshore (land) is 0 m. Note the gap for storms one and two is a result of missing data presumably caused by visibility constraints during shoreline extraction from video images.

Therefore an alongshore distribution of decreasing erosion from north to south existed. Shadows projected to the south of Tairua Beach during storms three, four, six and seven caused variation in shoreline position alongshore. Small levels of shoreline change were experienced at the northern areas for storms three and four. Southern and middle transects exhibited larger erosion distances during these storms than the northern transect. Erosion to the south corresponds to zones of reduced wave height due to the projection of island shadowing. This suggests sediment was being transported by longshore currents created by oblique wave incidence, rather than a pressure gradient caused by the alongshore variation in wave height. Relatively uniform erosion alongshore Tairua was experienced during storm six. Storm seven caused less erosion to the south as opposed to storms three and four, and instead had larger quantities eroded in the north and in the middle of the beach. Both storms eight and nine were not affected by shadowing from Shoe Island.

5.3.2 Medium term shoreline variation

5.3.2.1 Seasonal change

Medium term analysis completed on the Tairua dataset was the same as that done on the Pauanui dataset. Five of the nine storms identified in Table 3-1 were observed during the winter months between June and August. Increased storminess was experienced during the summer of 2003 and 2004 however, as shown by storms three, four and five (2003), and storm eight (2004). Shoreline data was separated into monthly time periods to determine the monthly averages presented in Figure 5.4. Seasons were compared by separating data into three monthly periods; summer (January, February, December), autumn (March, April, May), winter (June, July, August) and spring (September, October, November).

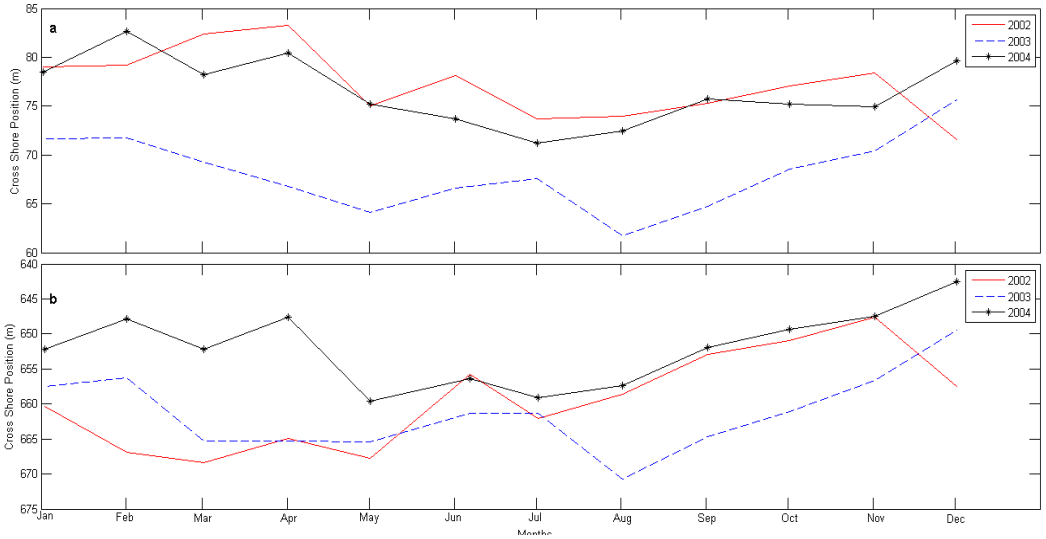

Figure 5.4: a) Monthly mean shoreline position at Tairua Beach. b) Monthly mean shoreline position at Pauanui Beach. Red line is 2002, blue line is 2003 and black dotted line is 2004. Cross shore position seaward is towards the top of the graph, cross shore position landward is towards the bottom of the graph.

Shoreline position during 2002 was further seaward than the shoreline in the progressive years. Throughout the year this accreted state declined and the shoreline moved further landward instead. The beginning of 2002 brought a slight movement increase in shoreline position seaward from January to February. Accretion continued throughout March and April where the maximum monthly average shoreward position over the entire period was displayed. Considerable shoreline cutback occurred during May but did not continue through the start of winter into June. Accretion of the shoreline instead occurred which defies the analogy of winter profiles. Similar patterns were experienced at Pauanui despite the largest wave event over the entire study period happening on the 20th of the month. July experienced increased storminess and shoreline cutback of 4.4 m, while August displayed opposing trends by accreting slightly (less than a metre). Shoreline movement seaward dominated the spring season until the start of summer where the shoreline eroded to the minimum position of the entire year. Overall, seasonal features do not present strong summer advance and winter cutback. Throughout the three

month seasonal periods there were instances where the shoreline accreted in winter, and eroded in summer.

Monthly shoreline positions during 2003 were the lowest experienced over the entire period. The shoreline position during summer periods were in a more seaward location than those experienced during the winter periods, however strong accretion was not evident during this time. Winter periods also did not bring strong erosive conditions to the shoreline, instead gradual accretion moved the previously eroded shoreline seaward. January and February mean shoreline positions remained rather constant and only accreted a total of 0.2 m from December 2002. Erosion occurred throughout the autumn months until the start of winter where June and July shoreline positions accreted seaward. This is unusual during a winter period as increased storminess tends to erode profiles and retreat the shoreline landward. August was the only month during winter to display strong erosion and this was the most landward point over the entire three year period. From this point through until the start of summer, the shoreline strongly accreted. Advance of 13.8 m pushed the shoreline position seaward significantly. Overall the shoreline position did display some seasonality as mentioned. However there were months where trends did not continue where accretion occurred instead of predicted erosion (June and July).

Shoreline positions at Tairua Beach through the year of 2004 displayed strong seasonality like Pauanui Beach. Summer months at the beginning of the year were in an accreted position where shorelines moved seaward during both January and February. Spring brought a varied shoreline position throughout the three months where an overall decreasing pattern was experienced. The shoreline varied throughout the spring season with a range of 5.3 m. Overall shoreline cutback during this season however totalled 3.1 m. During winter, the shoreline was in an eroded position with the most landward cross shore location throughout the entire year. June and July monthly locations displayed gradual erosion until August where the shoreline then accreted by 1.2 m. Despite a slight decline in shoreline position landward (0.2 m) during October and November, the shoreline recovered to an accreted position through until the end of 2004.

The shoreline location in December 2004 was further seaward than either December 2002 or 2003. Therefore strong seasonality was experienced at Tairua during 2004. These results match those detailed on Pauanui Beach in Chapter Three which also state a strong seasonal trend during this period.

5.3.3 Long term shoreline variation

Isolated transects at three locations alongshore were analysed to determine alongshore variation in the short term. Storm events and their various wave approach directions impacted Pauanui and Tairua Beaches through the shadowing of certain transects and reducing the wave climate. Variations in the alongshore distribution of shoreline position were created as a result, generating at times strong beach rotation. Long term analysis of this transect data was completed on Pauanui Beach and it was found that all three transects moved in conjunction with each other, however at different cross shore locations. Due to this cross shore disparity, a rotation co-efficient was created. Figure 5.5 displays

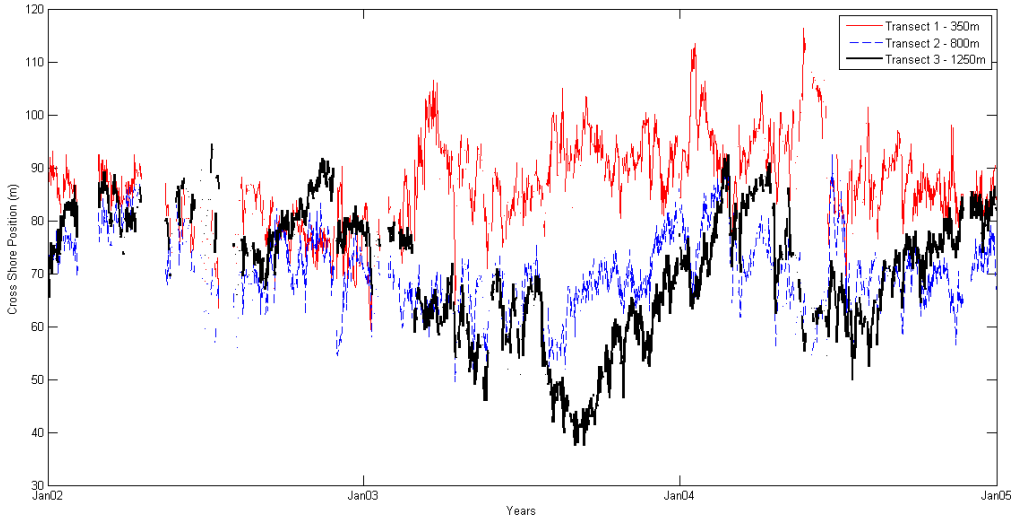

Figure 5.5: Mean shoreline positions at three transect points along Tairua Beach. Data has been fitted with a 3 point moving mean. Gaps in transect one represent missing data. Cross shore position towards 120 m is seaward and 0 m is landward.

the long term transect dataset at Tairua Beach at 350 m, 800 m and 1250 m. Cross shore position seaward is towards 120 m and landward is towards 0 m. During the beginning of 2002 all three transects were relatively uniform and similar in cross shore position. Throughout time this pattern deteriorated and an inverse relationship between the northern and southern areas developed while the middle profile acted as a fulcrum point. This was particularly evident during the winter of 2003 where the southern profile eroded considerably as the northern accreted. The middle profile remained relatively constant. Over the entire period the southern end is highly variable than the middle or northern. Strong cut back and accretion is experienced at the south but magnitudes of opposing behaviour caused by the inverse relationship are not matched to the north. This phenomenon agrees with rotation descriptions that state as one end of a beach accretes, the other erodes while the middle acts as a fulcrum point. Towards the end of 2004 the cross shore range of shoreline positions between the three transects decreases. This demonstrates a similar shoreline position to those experienced at the start of 2002.

Climatic shifts and oscillations affect the shoreline over long time periods by varying the meteorological conditions and wave climate experienced on the beach. La Niña conditions are favoured when ENSO indexes are positive, while El Niño conditions are favoured when ENSO indexes are negative. Onshore winds during La Niña cause erosion to north-east facing beaches in New Zealand while the opposite occurs during El Niño (de Lange, 2000). Figure 5.6 displays the ENSO index between 2002 and 2004 against the mean monthly shoreline position at Tairua Beach. When ENSO is positive (negative) La Niña (El Niño) conditions are represented. Pauanui results confirmed the behaviour shown by the negative ENSO index as the beach gradually accreted by 11 m throughout the timeseries. Tairua in comparison also gradually accreted in overall position throughout the entire period, a total of 1.13 m. This indicates that the shoreline accreted in response to the El Niño conditions favoured. However due to the lack of terrigenous sediment input into the beach system, Tairua could not accrete

considerably. Pauanui instead could accrete a large distance due to the estuary flushing and providing an additional sediment supply to the flanking beach. This sediment was allowed to accrete due to the wave climate presented, as opposed to La Niña conditions which would encourage the erosion of this sediment.

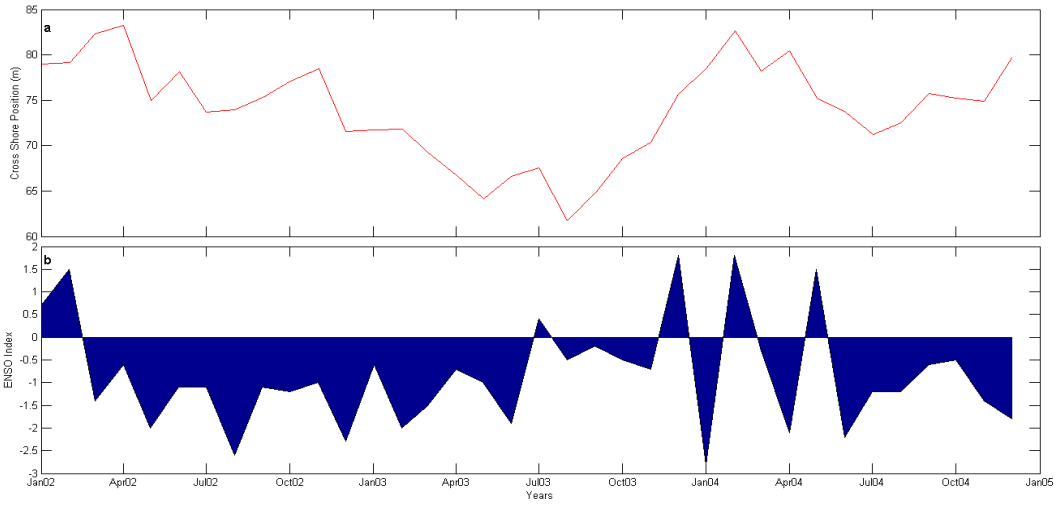

Figure 5.6: a) monthly shoreline positions, seaward is towards top of the graph and landward is towards the bottom of the graph. b) ENSO index where positive values show La Nina conditions. Negative values show El Niño conditions.

5.4 BEACH ROTATION

Rotation along Tairua Beach is strongly a result of wave climate variations alongshore. Transect analysis indicated the presence of shoreline rotation due to an inverse relationship between the north and south existing throughout the entire dataset. When compared to wave climate modelling results, it is clear to see that interactions of offshore island shadowing onto the beach causes alongshore variation in wave height. Alongshore currents are generated as a result transporting sediment entrained by wave breaking (Chapter Four). Shoreline data were fitted with a polynomial curve where the slope of the curve was taken as the rotation co-efficient. The same process was undertaken on the Pauanui dataset. A positive co-efficient relates to the southern end rotating and

an anti-clockwise rotation, while a negative co-efficient relates to the northern end rotating and a clockwise rotation.

Figure 5.7 displays the merged shorelines for the entire sample period. Northern Tairua is towards the top of the graph (0 m) while southern Tairua is towards the bottom (1400 m). Blue areas represent a seaward movement of shoreline position in comparison to red areas which represent a landward movement of shoreline. Any gaps are caused by missing data generated during the shoreline extraction technique. At the beginning of 2002 a parabolic beach shape existed at Tairua Beach where the terminal ends were seaward in location. Periodic shoreline cutback was also present in the alongshore at this point due to the persistence of four rip currents. At no other point in the timeseries did this pattern occur. Shoreline retreat landward was evident towards the end of 2002 at the northern end of Tairua. Southern areas for the same time period displayed a seaward movement, indicating anti-clockwise rotation. Particularly strong shoreline cutback was experienced to the south of Tairua during the middle of 2003. This has been identified during long term timeseries analysis. The northern areas for the same period accrete which indicate a strong clock wise rotation event lasting for approximately nine months. Therefore the alongshore extent of shoreline rotation is evident in this graph.

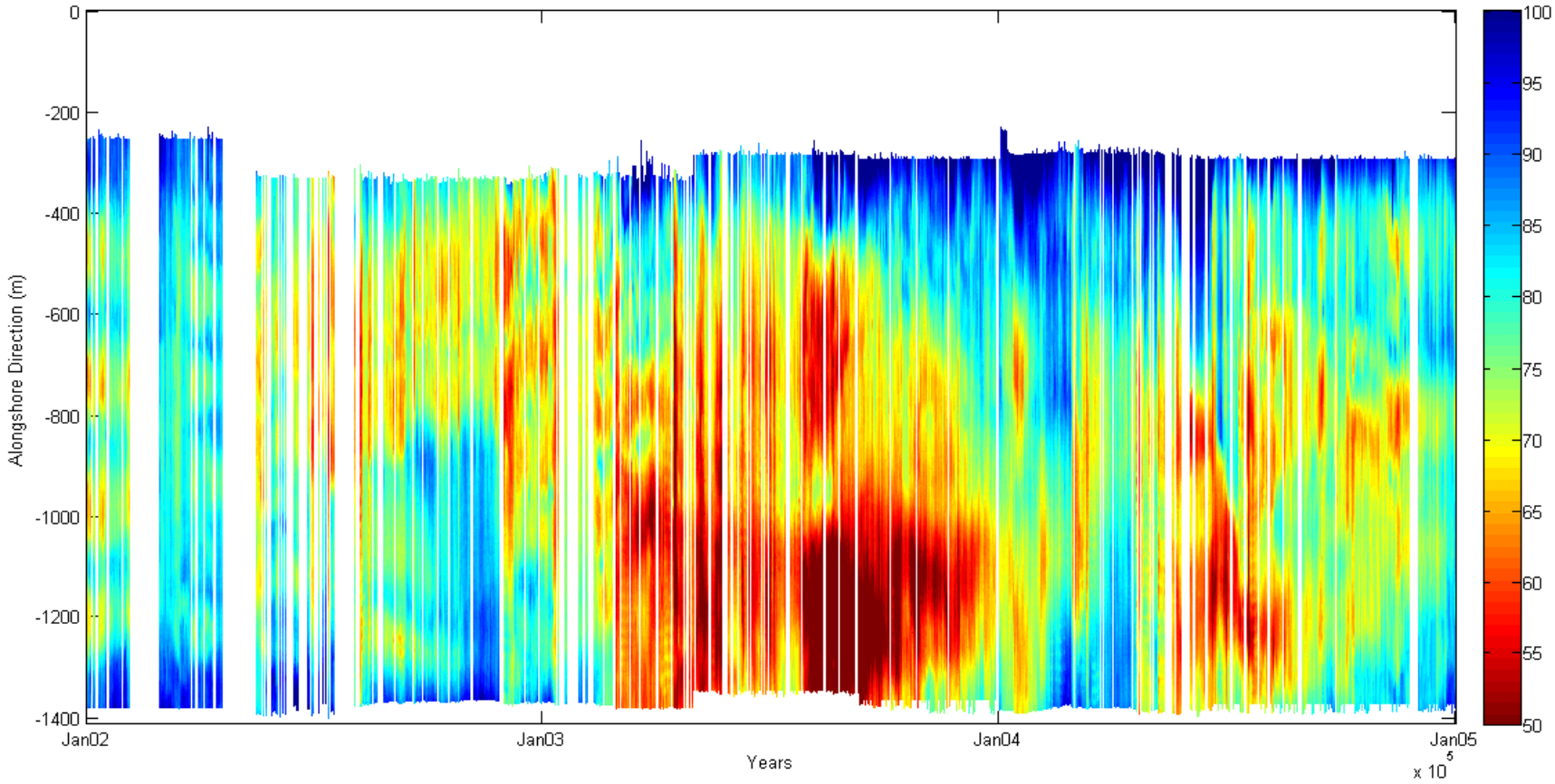

Figure 5.7: Merged shoreline dataset of Tairua Beach. Y axis shows the alongshore direction with 0 being northern most point of the beach. Colour bar represents the cross shore direction where red is landward movement and blue is seaward movement in metres. Gaps in the dataset are represented by white areas in the timeseries.

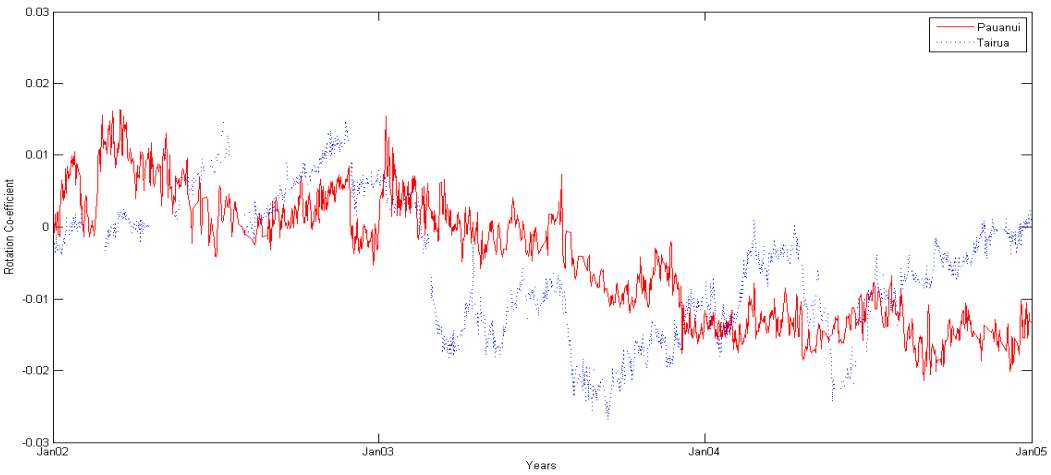

Figure 5.8: Combined Pauanui and Tairua rotation co-efficients over time. Pauanui is the red line while the dashed blue like is Tairua. Positive rotation co-efficients mean southern rotation while northern rotation is during negative rotation co-efficients.

Comparisons of the Pauanui rotation dataset to the Tairua rotation dataset are presented in Figure 5.8. Tairua tends to show a more variable beach rotation co-efficient in the short term, while Pauanui in comparison displays a long term rotation trend and has little short term variance. There were only two events were strong rapid rotation occurred at the same time at the two beaches. During the end of 2002 both datasets display a strong negative decline in rotation co-efficient, followed by a plateau period, and then an abrupt positive increase in co-efficient. Therefore both shorelines rotated in response to the same forcing mechanism. Other abrupt changes in rotation experienced at Tairua were not matched by phenomenon at Pauanui. Potentially this is caused by the wave direction and influence of offshore islands, as well as rip currents on the specific beach.

Comparison of the rotation co-efficients with alongshore wave energy flux provides insight into the cause of short term rotation variation at Tairua (Figure 5.9). Sharp changes in the alongshore energy flux did not influence the rotation of Pauanui Beach consistently due to the lack of inverse relationship between the opposite ends of the beach. Instead a long term rotation trend was evident towards the north which allowed for long term rotation comparison to climatic

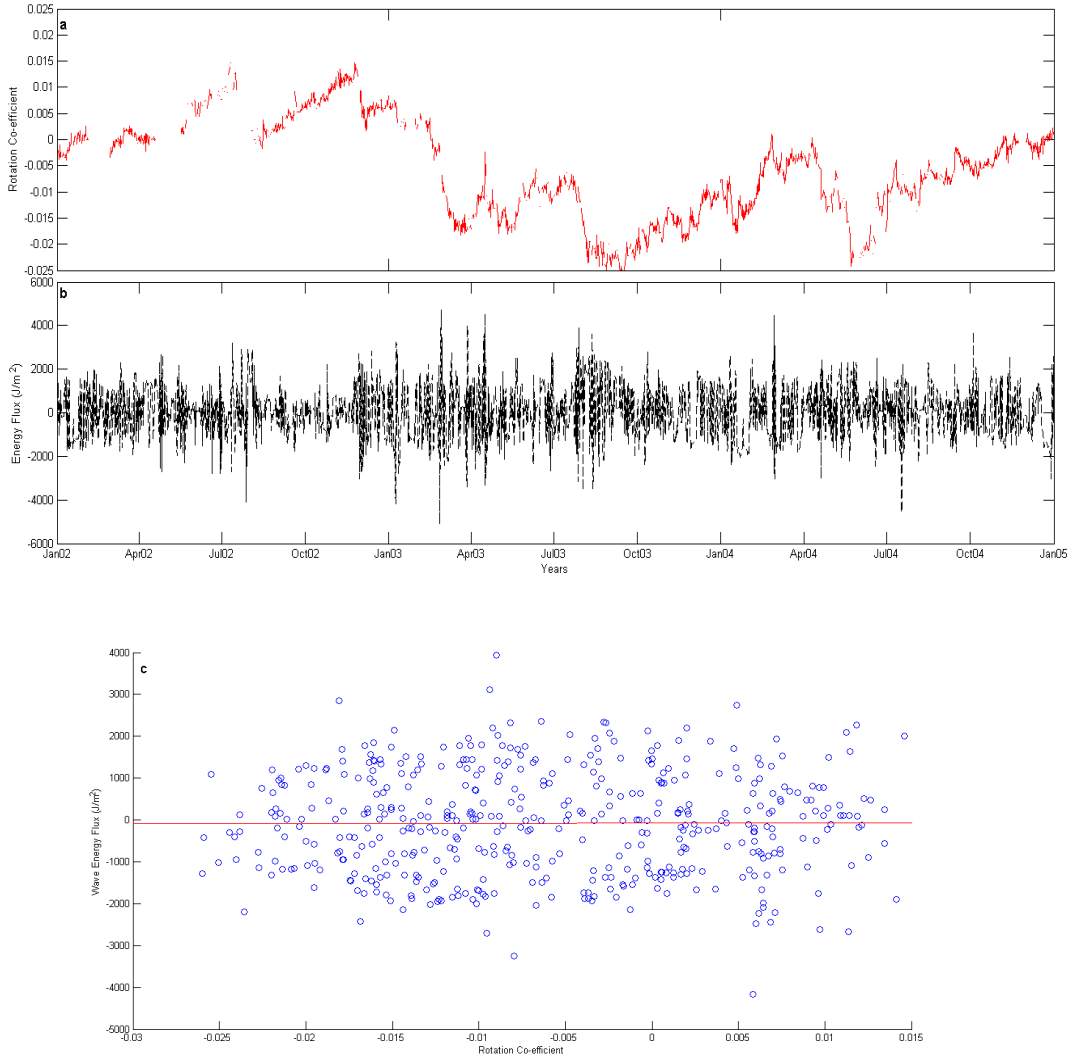

Figure 5.9: a) Rotation co-efficient for Tairua Beach. Positive co-efficient relates to southern rotation, negative co-efficient relates to northern rotation. b) Alongshore wave energy flux where 0^{o} is shore normal. c) Correlation statistics between rotation co-efficient and the wave energy flux. A weak correlation exists with an R^2 value of 0.004. The red line is the line of best fit (least squares sense).

oscillations. This was not undertaken on Tairua due to the persistent short term variation in rotation being more dominant than any long term trend. The only short term exception to Pauanui was during the sudden rotation transition from December/January of 2003/2004 where movement was associated to a flux event over 4000 J/m^2. Previous research indicates that rotation on Tairua Beach is generated as a result of flux events over 3500 J/m^2. However it is indicated by this research that beach rotation can occur with lower flux events as long as they are maintained for a considerable amount of time. This is despite a poor correlation co-efficient of 0.004 as indicated by Figure 5.9. Rotation changes during the December/January of 2002/2003 event (also shown by Pauanui) do not associate to flux events over 3500 J/m^2. Instead, a persistent energy flux around 2000 J/m^2 and -2000 J/m^2 was linked to the sudden shoreline rotation of the south (anti-clock wise). This phenomenon was experienced throughout the timeseries however agreement is also made to previous research suggestions (Bryan *et al.,* 2009) where short term large flux events greater than 3500 J/m^2 also trigger rotation at Pauanui.

5.5 DISCUSSION

5.5.1 Shoreline Variation

5.5.1.1 Short term

Short term variation in shoreline position was generated by large wave events. When wave heights increased, sediment was transported away from the beach, and when wave heights decreased, sediment was transported back. Pauanui Beach also experienced this erosion/accretion pattern during storm events although at a 2 day lag. Tairua too experienced a lag, smaller however than Pauanui at 1 day 18 hours. This was only determined over seven storms due to the lack of data for storms one and two as opposed to the Pauanui lag determined over all nine storms. Correlation statistics between the mean

shoreline position with significant wave height and energy flux returned r-squared values of -0.15 and -0.04 respectively. These are both considered poor correlations as a result of the lag and are consistent with results described by Yates *et al.* (2009) with regards to morphology evolution and time.

Shoreline response of Tairua over all storms was net erosion. Shorelines retreated landward leaving the beach in an eroded state. During successive accretionary periods, sediment was moved back onshore by cross shore transport processes. However rates of accretion tended to be lower than the erosion so the shoreline instead needed longer periods to recover to previous positions, which did not occur. Pauanui beach in comparison experienced both net erosion and net accretion throughout the nine storms. Storms one, three, five and nine all experienced net accretion where the shoreline in successive accretionary phases, advanced seaward to a position beyond the original profile before the storm. Tairua did not experience this phenomenon at any point throughout the seven storms (note storms one and two were ignored). The shoreline never fully recovered in the low energy accretion periods and always had a sediment deficit as a result of the events. This is a result of fluid dynamics and the forces needed to suspend sediment from the bar at Tairua and Pauanui. Sediment size at Pauanui is much smaller than at Tairua, which allows sediment to be more easily entrained and moved once in suspension, prior to falling out onshore during cross shore transport. Coarser sediment requires increased energy levels to initiate transport and during low energy events, sediment is not encouraged to move onshore due to the lack of force. Rip currents at Tairua also add to the net erosion of the shoreline during storm events. Sediment that has been entrained ready for cross shore transport may be transported back offshore via undertow rather than being deposited onshore. Reduced wave heights and energy in these accretionary phases encourage rip current formation, as small rip channels tend to disappear during large wave events (Gallop *et al.,* 2009).

Also compatible with Pauanui results, is the lack of uniformity pattern at Tairua in the alongshore direction. Consistent erosion did occur during storm peaks however the extent of erosion was not homogeneous in the alongshore direction.

Pauanui Beach featured uniform trends of alongshore erosion during the majority of storm events. Yet during storms one and nine accretion was experienced at the northern aspects of the beach, while erosion was experienced at the southern aspects. This was not repeated at Tairua Beach during the same time period due to the lack of additional sediment input from the Tairua Harbour of which Pauanui instead gained. Due to the wave climate, the two shorelines respond in the same way and to the same events, however the degree of response depends on the wave climate experienced in shallow water. Variations are created to the alongshore processes when the wave climate is adjusted by island shadowing. Depending on wave approach angle and the shadow projection onto which ever beach, the alongshore uniformity will disagree as there is a variation alongshore. During storm five for example, Pauanui had a shadow zone projected towards the northern end, creating a longshore current southwards due to the oblique wave approach angle. Sediment was transported from the north towards the south as a result of the current. Accretion occurred to the northern ends and it is hypothesised that increased sediment loads being flushed from the estuary are causing this sedimentation. This causes an alongshore variation and non-uniform behaviour of the shoreline between the north and south. Wave climate modelling results for the same storm show there was no strong shadowing onto Tairua from Shoe Island, although wave heights at the south were reduced slightly. A strong cutback was experienced at the northern end of Tairua, relating to a longshore current created by the oblique wave angle travelling south. This confirms that there are alongshore variations being experienced at the two beaches. However the overall patterns experienced are not consistent between Pauanui and Tairua due to the presence of Shoe Island the interference it has with wave climate.

5.5.1.2 Medium term

Tairua beach on a medium term scale behaved relatively similar to Pauanui Beach. Poor seasonality was evident during 2002 and 2003 at Pauanui where monthly mean shoreline positions were highly variable. Summer accretion and

winter erosion profiles were experienced during 2004 marking the only year out of the whole period to display strong seasonality at Pauanui Beach. Results found at Tairua also depicted the seasonal trends throughout 2004. Summer shorelines were in a far more accreted position than the more landward location of the shoreline during winter. Previous years did not display to the same extent these theoretical shoreline locations in response to the season, although 2003 did so more than 2002. Monthly mean shoreline position during 2002 was highly variable and little seasonal consistency was evident. In comparison, 2003 illustrated a stronger seasonal trend where shorelines during the summer were located further seaward than the shoreline location during winter. Variation did occur and the seasons did not show a consistent profile as a result. Overall the shoreline throughout this year was further landward than the previous and following year. The considerably lower shoreline position on average was caused by the large number of storms experienced throughout this year compared to any other. A total of five storms were projected onto the shore whereas only two were generated during 2002 and 2004.

5.5.1.3 Long term

Tairua Beach displayed a strong inverse relationship alongshore in the long term. Transect analysis detailed the different behaviours of the northern end to the southern end throughout the entire period. As the northern end accreted for example, the southern end eroded. Middle areas of the beach seemed to act as a fulcrum point as minimal movement occurred during the same instance. During mid 2003 the inverse nature of either beach end was magnified as magnitudes of cross shore position were enhanced. Strong accretion was matched by strong erosion until the start of 2004 where the cross shore extent began to diminish. Beach rotation was exampled as a result, although in a differing situation to that experienced at Pauanui. The shoreline at Tairua had a total movement range of 36.7 m over a three year period, with an overall accretion of 1.13 m. The mean shoreline position (averaged over the entire alongshore distance) moved between a maximum onshore position (landward) of 52.53 m and maximum

offshore position (seaward) of 89.23 m in the cross shore. The gradual increase in beach width matches ideologies of beach width and ENSO index, as well as results found at Pauanui Beach. Although long term accretion rates did not coincide to the same scale, differing sediment inputs at Pauanui from the estuary, encouraged by El Niño conditions, allowed the shoreline to accrete considerably. Therefore, like Pauanui Beach, the shoreline positions not only vary in response to short term storm events and seasons, but they also vary at the inter-annual time scale in response to climatic conditions.

5.5.2 Beach rotation

Beach rotation co-efficients were created at Pauanui Beach from the variation in cross shore position of the shoreline. Rotation co-efficients were also created using the Tairua shoreline dataset but were generated by a different rotation process than Pauanui Beach. Tairua Beach displays strong rotation due to the out of phase behaviour of either end of the beach. As the northern end accretes and moves seaward, the southern erodes and moves landward. Middle areas of the beach act as a fulcrum point for this rotation to occur. Pauanui in comparison does not experience an out of phase erosion/accretion relationship between the northern and southern areas. Instead as the northern areas accrete, the southern also accrete but not to the same extent. Variations in cross shore positioning of the northern and southern areas caused by this alongshore non-uniformity, creates a rotation co-efficient. During mid 2003 the shoreline experienced considerable rotation towards the north as the southern ends eroded and moved landward. Two storm events during this period approached from an easterly direction and shadows formed onto the southern areas of Tairua Beach. Shorelines continued to erode in the south despite the reduced wave heights that were created in these lee zones. Wave energy flux events associated to this time period does not present strong one off events that could trigger rotation. Instead consistently raised flux levels around 3000 J/m^2 were experienced allowing the negative rotation co-efficient to dominate. Previous research by Bryan *et al.* (2009) detailed rotation events on Tairua Beach to be in

response to wave energy flux events greater than 3500 J/m^2. However this research details how rotation can also occur via a persistent flux event of less than 3500 J/m^2, not just through individual events.

5.6 SUMMARY

Similar analysis to that completed on the Pauanui dataset in Chapter Three was undertaken on the Tairua shoreline dataset. Separation of data analysis into four main categories (short term, medium term, long term and rotation) allowed for direct comparison to Pauanui results. Aims for this chapter were to determine the response behaviour of the two beaches considering they experience the same deep water wave climate and are within close proximity to each other.

- Pauanui and Tairua Beaches mean shoreline position were harmonious during short term analysis. When one experienced sharp short term erosion due to a storm event, the other too presented the same behaviour.

- Magnitudes of change were not consistent between the two datasets however the overall pattern displayed some uniformity between the beaches.

- Seasonal analysis (medium term) found poor seasonality during 2002 at Tairua which gradually increased through until the end of 2004. Pauanui Beach also experienced poor seasonality during 2003 and 2003; however this also was rectified during 2004 where strong summer and winter profiles were instead evident.

- Separating the shoreline into three alongshore transects diagnosed the alongshore behaviour of the beach. Uniformity in shoreline position was not apparent at Tairua particularly with the inverse relationship between

the northern and southern areas. This lack of uniformity is caused by the variation in wave climate alongshore caused by island shadowing.

- Strong rotation was indicated at Tairua Beach as the northern end accreted and the southern eroded, leaving the middle areas to act as a fulcrum point and not move considerably.

- Pauanui Beach instead displayed a level of uniformity in the alongshore during transect analysis. Both the northern, middle and southern areas accreted together however not to the same cross shore position. This variation in position generated a rotation co-efficient used in rotation analysis.

- Tairua and Pauanui rotate similarly in the long term, particularly during the middle of 2003 where northern rotation occurred. Only two events coincide between the two beaches where there was rapid rotation change (towards the end of 2002).

- Tairua experiences several short term rotation events throughout the timeseries, compared to Pauanui which displays a long term rotation trend towards the north.

- Large flux events were detailed in previous research as being the generating conditions for these rotation events. However this research identified slightly smaller flux events that lasted longer also causing rotation at Tairua.

Chapter Six -

Conclusions

6.1 INTRODUCTION

Harbour adjacent beaches present complex physical morphodynamic processes that are poorly researched. Harbour adjacent beach systems can potentially display severe erosion or accretion cycles as they are subject to sediment pulses ejected from the harbour. This thesis tries to isolate shoreline phenomenon occurring at Pauanui Beach over three years. In order to achieve this, shoreline detecting algorithms were created that extract shoreline data from a series of video images. Shoreline variation analysis was completed analysing the short, medium and long term time scales. Physical processes governing the shoreline change were detailed and some modelled using SWAN software. All of the results found at Pauanui Beach were then compared to previously well studied Tairua Beach to determine if the two neighbouring beaches respond similarly. Below is a summarised collation of findings presented in this thesis.

6.2 VIDEO IMAGING AND SHORELINE DETECTION ALGORITHMS

Image collection at Pauanui has been successful for over 10 years. Two cameras capture the Pauanui coastline in the north and south every daylight hour, providing a less demanding technique for data collection than traditional methods. The southern located camera produced the most useful images for this study and the northern images were disregarded. Due to the physical location of the camera, climatic conditions at times degraded the image resolution and clarity. Fog and cloud restricted the coastline visibility, and raindrops distorted the image. The cameras tilt angle also shifted due to strong winds which required manual adjustment of the cameras xyz co-ordinates prior to rectification. Shoreline detection algorithms were created to identify the water/land intercept

based on RGB colour variations. Algorithms were highly accurate in finding the shore location within close proximity to the camera. With distance, colour intensities varied and algorithms were not so exact. Manual correction was required to ensure precise shorelines were selected. Algorithms were created from techniques developed by Salmon (2008) and Gallop (2009) whose research focus was located at both Tairua and Pauanui Beaches. The algorithm, accurate to some degree on Pauanui Beach, worked considerably better on Tairua Beach. Tairua has a higher portion of shell content, raising the red colouration within the image. Algorithms distinguish the water/land intercept significantly well on Tairua images as a result of this. Pauanui however has lower proportion of shell content and therefore does not have a highly distinguished red intensity. The algorithms were used on a variety of morphology types within the three year data set and it only worked significantly well alongshore when visibility and colours were strong.

6.3 SHORELINE VARIATION

Beach morphology is influenced by processes acting at short, medium and long term time scales. The shoreline at Pauanui Beach in particular displays morphological variability over all three time periods and is associated with large wave events, seasonal variation and climatic oscillations. Short term variations in shoreline were in response to large wave events over 4 m significant wave height. During the peak of the storm the shoreline tended to display an eroded profile, although at times this was not uniform alongshore. More often than not the shoreline accreted in the period following the storm peak as a result of reduced wave energy and height. Seasonal changes brought variation in profile placement over three monthly periods. Shoreline positioning during the specific seasons however did not display theoretical seasonality in the form of erosion (winter) and accretion (summer) profiles alongshore. Winter causes increased storminess, increasing wave energy and erosion potential, while summer offers the opposite. Pauanui did not show a strong seasonal signal and instead displayed a highly variable shoreline position throughout 2002 and 2003. 2004

was the only year to display textbook seasonal variation. Long term analysis of shoreline positions found a gradual increase in sedimentation towards the northern end of the beach from mid 2003 until the end of the sample period. The beach accreted a total of 11 m over the three year time period and this was in agreement with ENSO index indications that remained negative for the majority of the period. Positive ENSO brings La Niña conditions which tend to erode beaches due to the offshore directed winds and increased storminess (de Lange, 2000). Negative ENSO instead brings El Niño conditions which bring accretionary conditions and beaches on the north-east coast of New Zealand tend to accrete. Therefore the net accretion over the three year time period was a result of the negative ENSO.

6.4 BEACH ROTATION

Previous studies indicate that beach rotation should be limited to embayed or pocket beaches. Few studies have focused on the rotation of other classified beaches, including intermediate, harbour adjacent beaches like Pauanui. Wood (2010), during his research on east coast Coromandel beaches, identified the rotation of said beach during analysis of beach profile surveys. Further research into the processes governing this rotation was not of focus and instead classified as an outlier. This research identified rotation occurring as a longer term phenomenon rather than short term or seasonal. Short term variation did occur as a result of storm activity; however during long term analysis this was disregarded as high frequency noise. Despite being a long straight beach, Pauanui displayed a parabolic shape which allowed a rotation co-efficient to be created. This was due to the non-uniform, cross shore seaward position of the northern areas compared to southern areas. Instead of the beach displaying out of phase erosion and accretion cycles between each beach end, the northern end accreted more than what the southern end was accreting. This uniform accretion was evident in alongshore uniformity analysis where the northern and southern areas were in a more accreted position than the central areas. Overall the northern end of Pauanui was gradually rotating seaward from mid 2003.

Weak correlations between rotation co-efficients and alongshore energy fluxes identified that other hydrodynamic processes were acting upon the shoreline allowing it to rotate. A stronger correlation of rotation to wave height (although still poor) associates the shoreline position responding to wave height variations better than energy flux.

6.5 WAVE MODELLING

Throughout the study period, Pauanui was found to rotate and it was hypothesised that rotation was caused by island interference generating a shadowing effect onto the beach. Three of the nine identified storms were separated for analysis following model runs. These three storms propagated from a variety of approach angles over the three time periods creating either a northern or southern directed longshore current. Data extracted from the model runs at 8 m water depth were analysed to help determine the longshore currents. It was found that currents were created by the oblique wave approach at Pauanui Beach (as opposed to rip current cell circulation occurring at Tairua Beach) and travelled north (south) if wave angles were greater (less than) 90^0. Shorelines did not move solely on the response of sediment being transported by longshore currents however. Storm six experienced large erosion to the north despite a northward directed longshore current. Complex processes between the shoreline, sediment deposition and an ebb tidal delta generated the exacerbated erosion at the northern end more than middle or southern areas.

6.6 TAIRUA COMPARISONS

Mean shoreline response of Tairua and Pauanui Beaches were rather consistent as both beaches are subject to the same deep water wave conditions. Periods of erosion or accretion at Pauanui corresponded to the same periods of erosion or accretion experienced at Tairua. Comparing individual storms and the relationship they had with changes to beach morphology, found that Tairua experiences net shoreline erosion as a result of all storms. Pauanui Beach does

not experience this net erosion pattern, as four of the nine storms experienced net accretion instead. Variations in sediment characteristics and cross shore transport flow, result in Tairua requiring longer accretion periods or larger wave energies to transport sediment from the offshore bar to the berm. Rip currents along Tairua Beach also affect sediment transport and prevent shoreline accretion due to under tow. Pauanui in comparison gains additional sediment from the Tairua Estuary and has a smaller sediment that can be easily transported in the cross shore. Depending on the wave approach direction, shadow zones are projected onto certain areas of either beach. Mean shoreline positions as a result are influenced by the alongshore variation in wave height and energy which are governed by storm events, seasonal changes and climatic oscillations. Tairua is affected by shadow zones when approach directions exceed approximately 85^0, while Pauanui is affected by approach angles less than this. Transect analysis found that Tairua and Pauanui Beaches do not experience the same uniform behaviour alongshore as a result of shadowing. Distributions of wave heights alongshore and oblique wave angles generate longshore currents which transport sediment to and from either beach end. Storm five in particular generated a longshore current at Pauanui towards the north due to a pressure gradient, accreting the northern end of Pauanui. Tairua instead experienced erosion at the northern end due to a longshore current created by a pressure gradient and the oblique wave angle. As a result, both ends of either beach are not in unison with each other, which creates beach rotaiton. Tairua features an out of phase relationship when northern ends accrete southern ends erode, while Pauanui features a cross sectional variation in shoreline position between the north and south. There were only two short term rotation events that were consistent between both beaches, where rotation shifted rapidly. Otherwise rotation events at Tairua were highly variable in the short term as opposed to Pauanui Beach that featured a stronger long term component. Long term rotation to the north was dominant from mid 2003, and was also shown in Tairua data.

6.7 RECOMMENDATIONS FOR FURTHER RESEARCH

Important information was gathered throughout this study about the shoreline movement of a harbour adjacent beach. However due to several restrictions and limitations associated to this type of study, there are a few areas that can be elaborated in future research initiatives to ensure the breadth of knowledge exists.

- Pauanui shoreline detection algorithms should be tested with other shoreline identification techniques (for example hue saturation). RGB colour intensities although effective for certain areas of Pauanui and specific times of day were not consistent throughout the entire alongshore distance. This would ensure less time is spent on correcting imperfections made by the algorithms.

- Create a sister dataset with the offshore bar(s) location and determine whether the shoreline and barline move in unison. At times there is evidence of a three bar system, with one extending to the seaward extent of Paku Hill during storm events, and two potentially merging and separating in the alongshore.

- Develop the shoreline dataset to cover a decade. This would allow the determination of whether longer term shoreline variation exists in relation to climatic conditions that operate at larger time scales. Extreme coastal change can generate over decadal scales and ensuring this change is not a threat to society is important for coastal planning.

- Run wave climate modelling for longer time periods to determine causes of seasonal and long term shoreline variation. Understand the long term wave climate and the influence this has on morphology will prove useful for any future coastal development or planning initiatives.

References

Aarninkhof, A.G.J., Turner, I.L., Thomas, D.T., Dronkers, M.C. and Nipius, L., 2003: A video based technique for mapping intertidal beach bathymetry. *Coastal Engineering,* vol. 49 pp. 275-289.

Alexander, P.S. and Holman, R.A. 2004: Quantification of nearshore morphology based on video imaging. *Marine Geology,* vol. 208 no. 1 pp 101-111.

Algeria, Arzaburu, A.R.d. and Masselink, G., 2010: Storm response and beach rotation on a gravel beach, Slapton Sands, UK. *Marine Geology,* vol.278 pp.77-99.

Bird, E., 2008: *Coastal Geomorphology: Beaches: Beach erosion.* John Wiley & Sons LTD: England.

Bittencourt, A.C.S.P., Sampaio, E.E.S., and Farias, F.F. , 1997: Beach imaging through the time evolution of topographical profiles. *Journal of Coastal Research,* vol. 13 no. 4 pp. 1141-1149.

Bogle, J.A., Bryan, K.R., Black, K.P., Hume, T.M., & Healy, T.R., 2000: Video observations of rip formation and evolution. *Journal of Coastal Research, Special Issue 34 pp* 117-127.

Bryan, K.R., Gallop, S.L., van de Lageweg, W.I., and Coco, G., 2009: Observations of rip channels, sandbar-shoreline coupling and beach rotation at Tairua Beach, New Zealand. In I. Dawe (Ed.), *Proceedings of Australasian Coasts and Ports Conference 2009.* New Zealand Coastal Society: Wellington, New Zealand.

Dean, R.G., 2002: *Beach Nourishment: Theory and Practice.* World Scientific Publishing LTD: Singapore.

Dean, R.G. and Dalrymple, R.A., 2002: *Coastal Processes with Engineering Applications*. Cambridge University Press: U.K.

de Lange, W., 2000: Interdecadal Pacific Oscillation (IPO): a Mechanism for Forcing Decadal Scale Coastal Change on the Northeast Coast of New Zealand. *Journal of Coastal Research,* ICS 2000 Proceedings, pp. 657:664.

Dubois, R.N., 1988. Seasonal changes in beach topography and beach volume in Delaware. *Marine Geology,* vol. 81, no.1-4 pp. 79-96.

Gallop, S.L., 2009: *Rip Current Dynamics on an Embayed Beach* (Un-published MSc Thesis). University of Waikato, Earth and Ocean Sciences: Hamilton, New Zealand.

Gallop, S.L., Bryan, K.R., and Coco, G., 2009: Video observations of rip currents on an embayed beach. *Journal of Coastal Research,* Special Issue 5 pp 49-53.

Hart, D. E. and Bryan K.R., 2008: New Zealand coastal system boundaries, connections and management. *New Zealand Geographer,* vol. 64 pp. 129-143.

Haslett, S.K., 2009: *Coastal Systems: Definitions, Energy and Classification (2nd Ed.).* Routledge: New York.

Holland, K.T., Holman, R.A., Lippmann, T.C., Stanley, J. and Plant, N., 1997: Practical use of video imagery in nearshore oceanographic field studies. *IEEE Journal of Oceanic Engineering,* vol. 22 no. 1 pp. 81-92.

Holman,R.A., Lippmann,T.C., O'Neil, P.V. and Hathaway, K., 1991: Video estimation of subaerial beach profiles. *Marine Geology,* vol. 97 pp. 225-231.

Klein, A.H.d.F., Filho, L.B. and Schumacher, D.H., 2002: Short term beach rotation processes in distinct headland bay beach systems. *Journal of Coastal Research,* vol.18 no. 3 pp. 442-458.

Klemas, V., 2009. The role of remote sensing in predicting and determining coastal storm impacts. *Journal of Coastal Research, vol.* 25 no.6 pp. 1264-1275.

Komar, P.D., 1998: *Beach Processes and Sedimentation.* Prentice Hall: New Jersey.

Lin, P. and Zhang, D., 2005: *Hydrodynamics VI Theory and Applications: The depth dependant radiation stressses and their effect on coastal currents.* Taylor & Francis Group: London.

Lippman, T.C. and Holman, R.A., 1989: Quantification of Sand Bar Morphology: A Video Technique Based on Wave Dissipation. *Journal of Geophysical Research,* vol. 94, no. C1 pp. 995-1011.

Lippman, T.C. and Holman, R.A., 1990: The Spatial and Temporal Variability of Sand Bar Morphology. *Journal of Geophysical Research,* vol. 95 no. C1 pp. 11,575-11590.

Masselink, G. and Hughe, M.G., 2003: *Introdiction to Coastal Processes and Geomorphology*. Hodder Arnold: Great Britain.

Mei, C.C., Staissnie, M. And Yue, D.K.P., 2005: *Theory and Applications of Ocean Surface Waters: Radiation stresses, bound longwaves and longshore currents.* World Scientific Publishing Co.: Singapore.

Munoz-Perez, J.J. and Medina, R., 2010: Comparison of long-,medium- and short-term variations of beach profiles with and without submerged geological control. *Coastal Engineering, v*ol. 57 pp. 241-251.

Plant, N.G., Aarninkhof, S.G.J., Turner, I.L. and Kingston, K.S., 2007: The performance of shoreline detection models applied to video imagery. *Journal of Coastal Research,* vol. 23 no. 3 pp. 658-670.

Plant, N.G. and Holman, R.A., 1997: Intertidal beach profile estimation using video images. *Marine Geology,* vol. 140, pp. 1-12.

Ranasinghe, R., McLoughlin, R., Short, A. and Symonds, G., 2004: The Southern Oscillation Index, wave climate, and beach rotation. *Marine Geology,* vol. 204 pp. 273-287.

Ruiz de Algeria-Arzaburu, A. and Masselink, G., 2010: Storm response and beach rotation on a gravel beach, Slapton Sands, UK. *Marine Geology,* vol 278 pp. 77-99.

Salmon, S. 2008: *A New Technique for Measuring Runup Variation using Sub-Aerial Video Imagery* (Un-published MSc Thesis). University of Waikato, Earth and Ocean Sciences: Hamilton, New Zealand.

Short, A.D. and Masselink, G., 1999: *Handbook of Beach and Shoreface Morphodynamics.* John Wiley & Sons: Chichester: England.

Short, A.D. and Trembanis, A.C., 2004: Decadal scale patterns in beach oscillation and rotation Narraben Beach, Australia – timeseries, PCA and wavelet analysis. *Journal of Coastal Research,* vol. 20 no. 2 pp. 523-532.

Smit, M.W.J., Aarninkhof, S.G.J., Wijnberg, K.M., Gonzalez, M., Kingston, K.S., Southgate, H.N., Ruessink, B.G., Holman, R.A., Siegle, E., Davidson, M. and Medina, R., 2007: The role of video imagery in predicting daily to monthly coastal evolution. *Coastal Engineering,* vol. 54, pp. 539-553.

Sorensen, R.M., 1993: *Basic Wave Mechanics for Coastal and Ocean Engineers: Small Amplitude Wave Theory and Characteristics.* Wiley & Sons: Canada.

Thomas, T., Phillips, M.R. and Williams, A.T., 2010: Mesoscale evolution of a headland bay: beach rotation processes. *Geomorphology,* vol. 135 pp. 129-141.

Thomas, T., Phillips, M.R., Williams, A.T. and Jenkins, R.E., 2011: Medium timescale beach rotation; gale climate and offshore island influences. *Geomorphology,* vol. 135 pp. 97-107.

Turner, I.L., Aarninkhof, S.G.J. and Holman, R.A. 2006: Coastal imaging applications and research in Australia. *Journal of Coastal Research,* vol. 22 no. 1 pp 37-48.

Uunk, L., Wijnberg, K.M. and Morelissen, R. 2010: Automated mapping of the intertidal beach bathymetry from video images. *Coastal Engineering,* vol. 57 no. 4 pp. 461-469

Violante-Carvalho, N., Paes-Leme, R.B., Accetta, D.A. and Ostritz, F., 2009: Diffraction and reflection of irregular waves in a harbour employing a

spectral model. *Anais da Academia Brasileira de Ciencias*, vol. 81 no. 4 pp. 837:848.

Wood, A. 2010: *Episodic, Seasonal and Long Term Morphological Changes of Coromandel Beaches* (Unpublished MSc Thesis). University of Waikato, Earth and Ocean Sciences: Hamilton, New Zealand.

Woodroffe, D.C., 2002: *Coasts: Form, Process and Evolution.* University Press: Cambridge: UK.

Wright, L.D. and Short, A.D., 1984: Morphodynamic variation of surf zones and beaches: A synthesis. *Marine Geology* , vol. 56 no. 1 pp. 93-118.

Wright, L.D., Short, A.D. and Green, M.O. 1985: Short-term changes in the morphodynamic states of beaches and surf zones: An empirical predictive model. *Marine Geology,* vol. 62 no. 3 pp. 339-364.

Yates, M.L., Guza, R.T. and O'Reilly, W.C., 2009: Equilibrium shoreline response: Observations and modeling. *Journal of Geophysical Research,* vol. 114 no. C09014 pp. 1:16.

Yates, M.L., Guza, R.T. and O'Reilly, W.C., Hansen, J.E. and Barnard, P.L., 2011: Equilibrium shoreline response of a high wave energy beach. *Journal of Geophysical Research,* vol. 116 no. C04014 pp. 1:13.

Appendix I

Storm Shoreline Profiles

A total of nine storms were identified throughout the three year dataset that exceeded the storm wave criteria of 4 m significant wave height. Wave data used was taken from a 28 year old WWIII hindcast dataset and compared to the shoreline dataset created using video images. The figures below display three time periods, prior, peak and post. These refer to the shoreline position before the storm, the maximum shoreline cutback position due to the storm, and the maximum shoreline accretion position following the storm. The alongshore position is located on the x-axis where 0m is the northern end towards the harbour entrance which then extends southwards. The y-axis shows the cross shore position where the top of the graph is offshore and extends landward towards the bottom of the graph. As a result of dataset limitations and missing data, shorelines for storms one and two at Tairua Beach could not be determined and are therefore ignored.

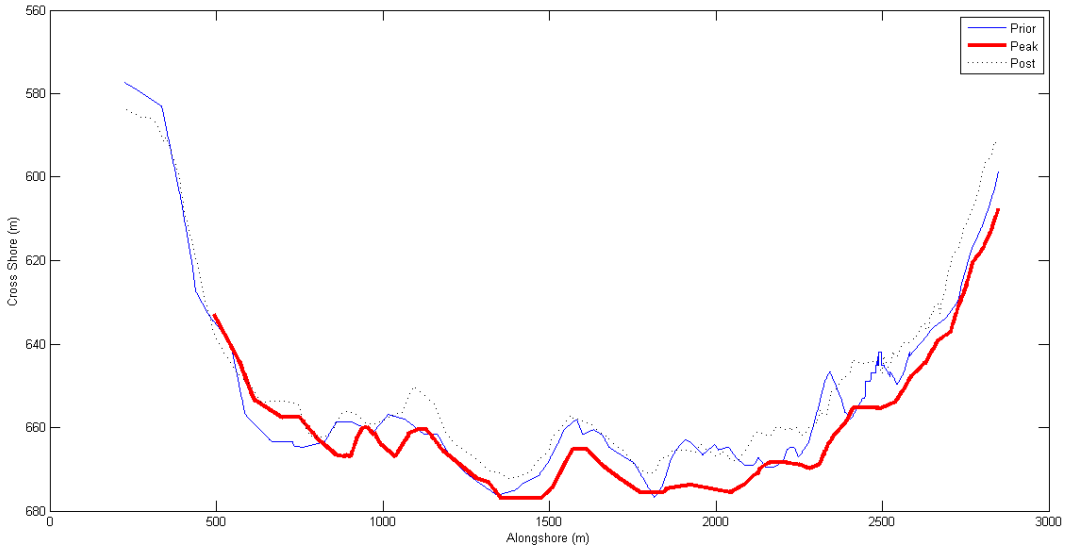

Figure I.1: Storm one alongshore shoreline positions at Pauanui Beach.

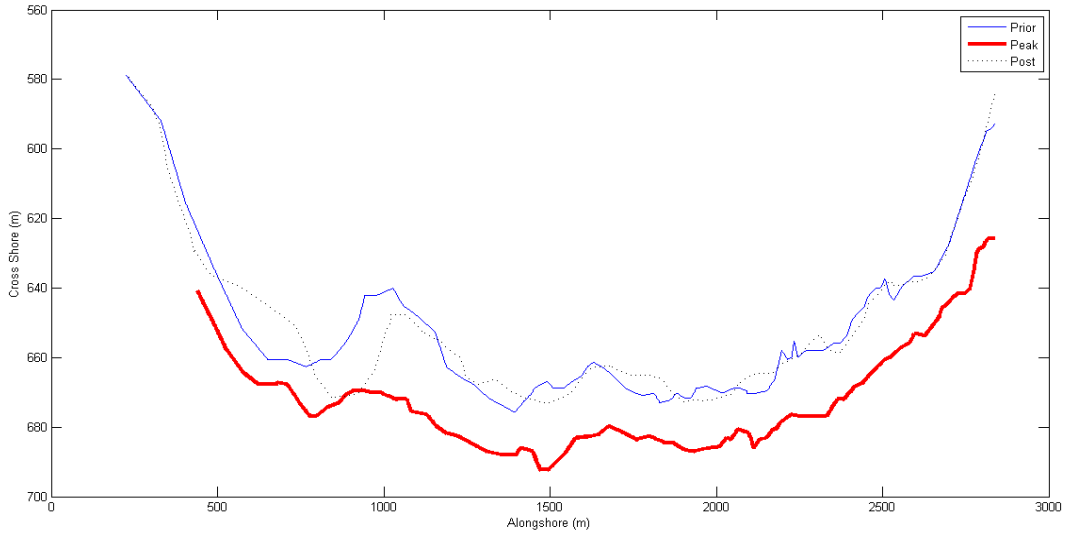

Figure I.2: Storm two alongshore shoreline positions at Pauanui Beach.

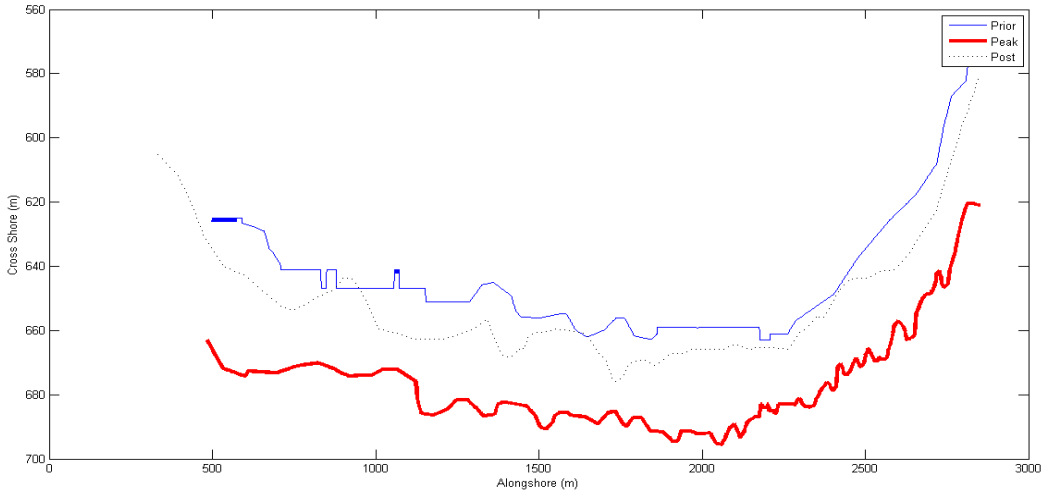

Figure I.3: Storm three alongshore shoreline positions at Pauanui Beach.

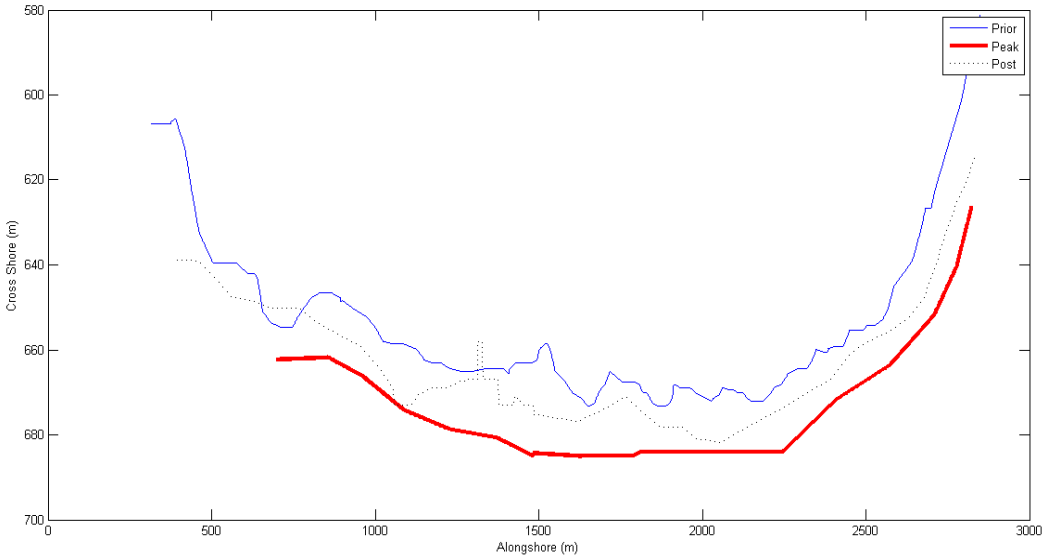

Figure I.4: Storm four alongshore shoreline positions at Pauanui Beach.

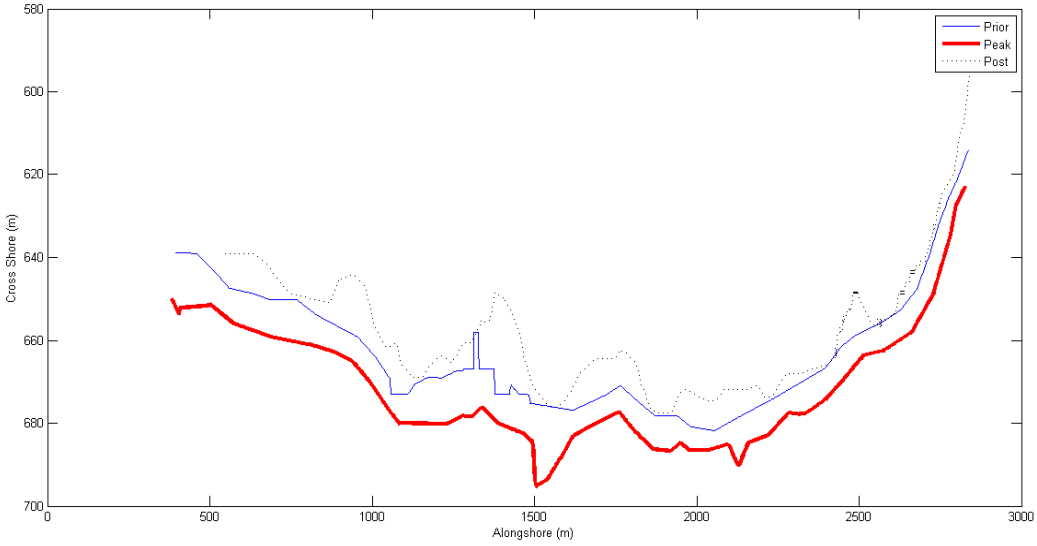

Figure I.5: Storm five alongshore shoreline positions at Pauanui Beach.

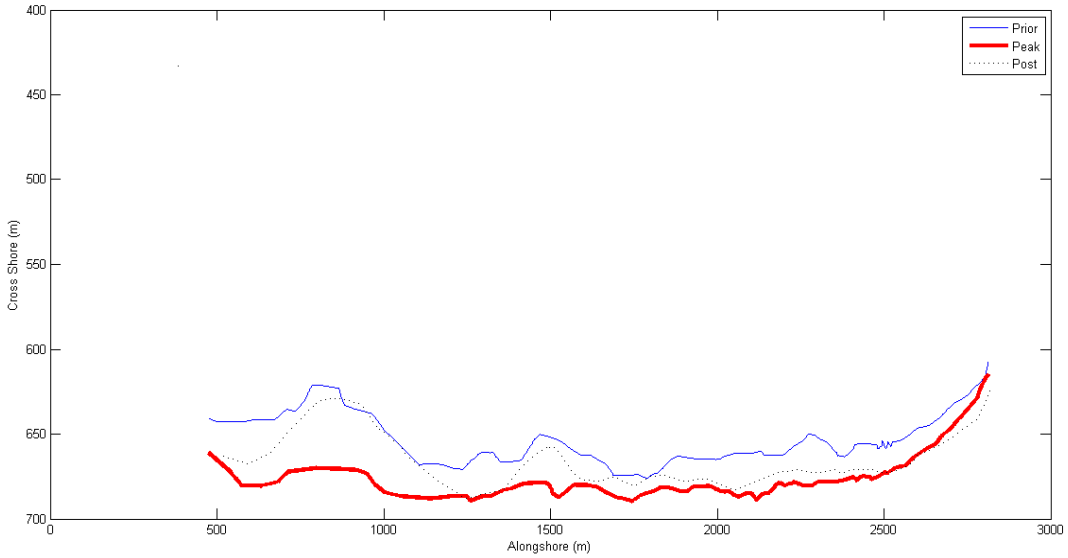

Figure I.6: Storm six alongshore shoreline positions at Pauanui Beach.

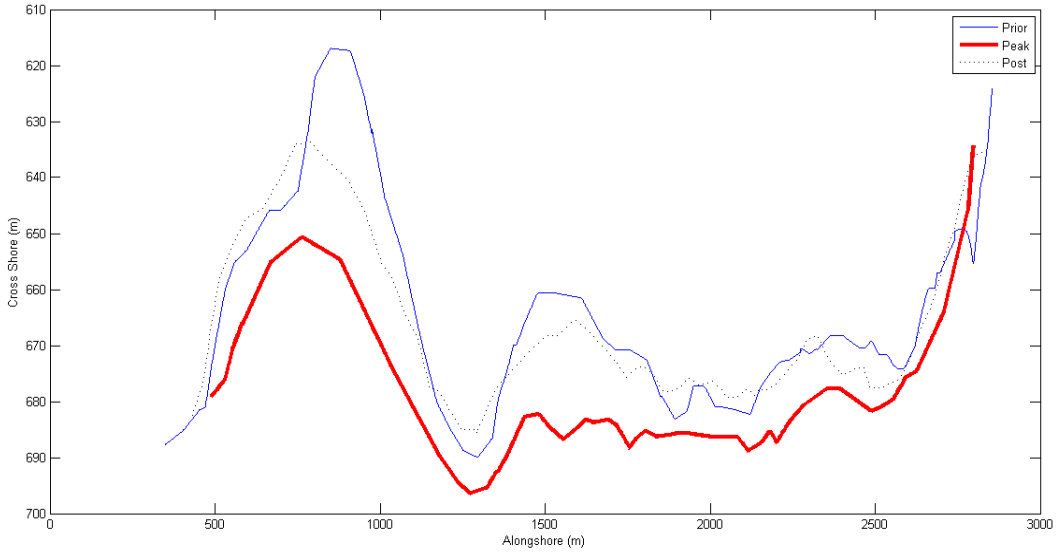

Figure I.7: Storm seven alongshore shoreline positions at Pauanui Beach.

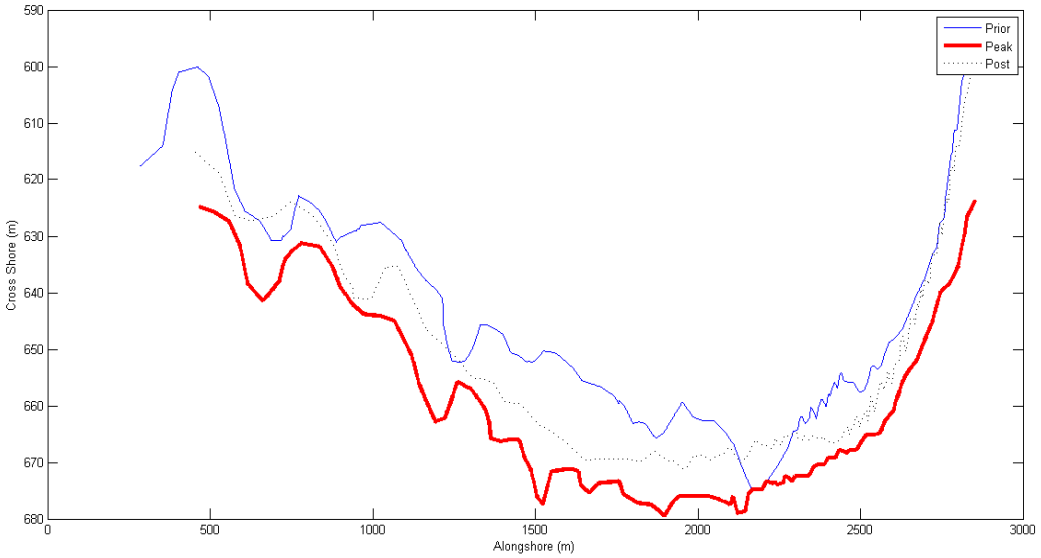

Figure I.8: Storm eight alongshore shoreline positions at Pauanui Beach.

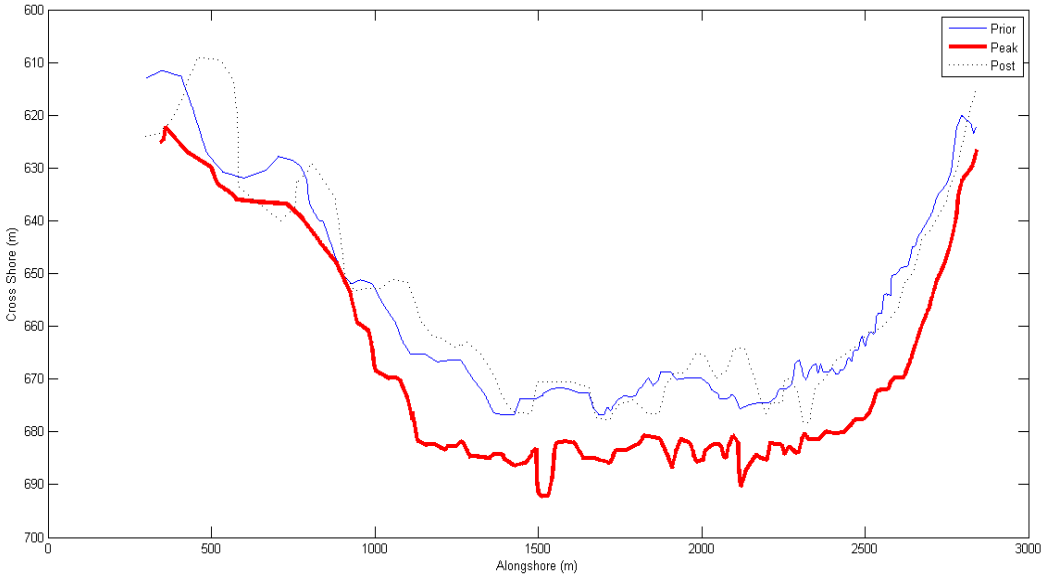

Figure I.9: Storm nine alongshore shoreline positions at Pauanui Beach.

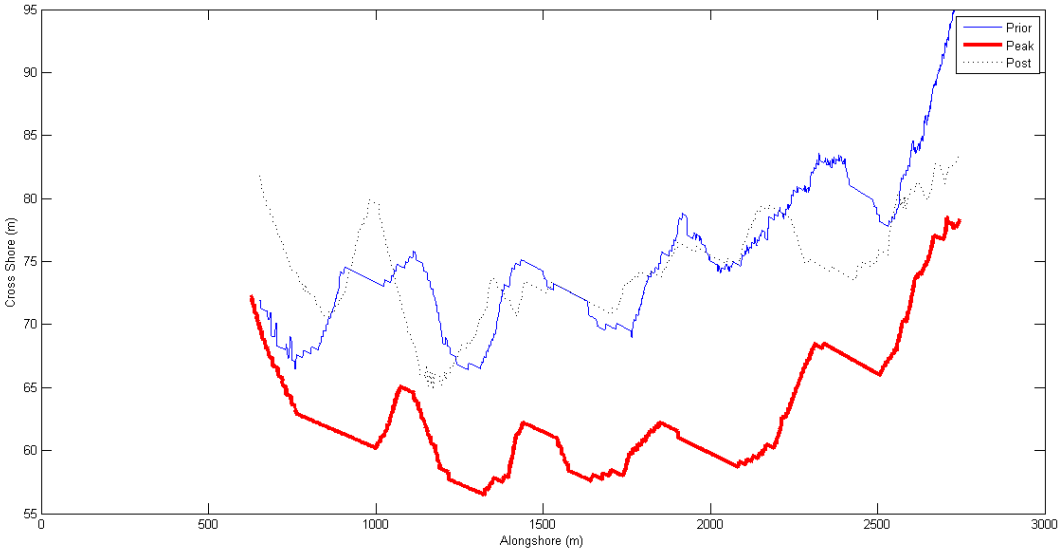

Figure I.10: Storm three alongshore shoreline positions at Tairua Beach.

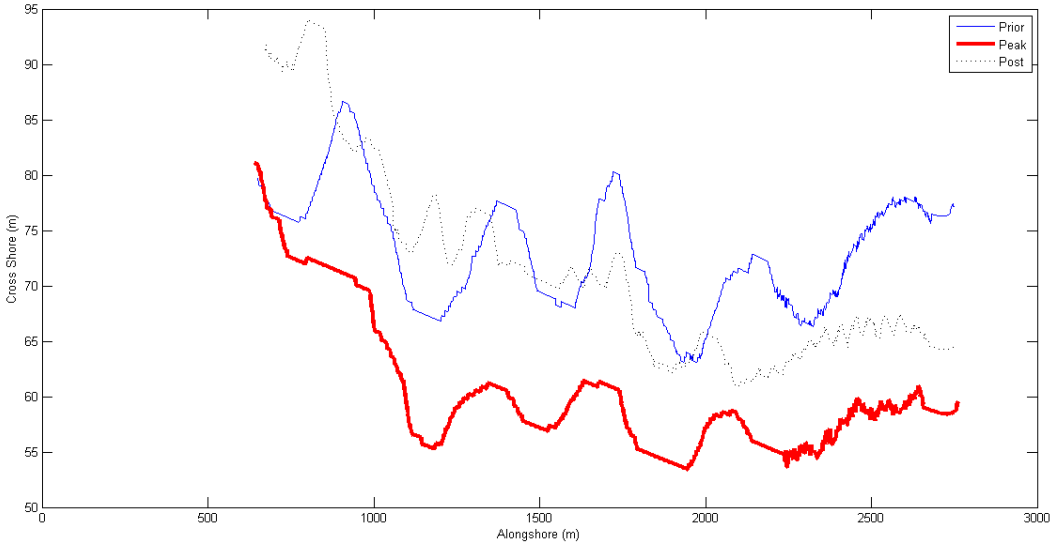

Figure I.11: Storm four alongshore shoreline positions at Tairua Beach.

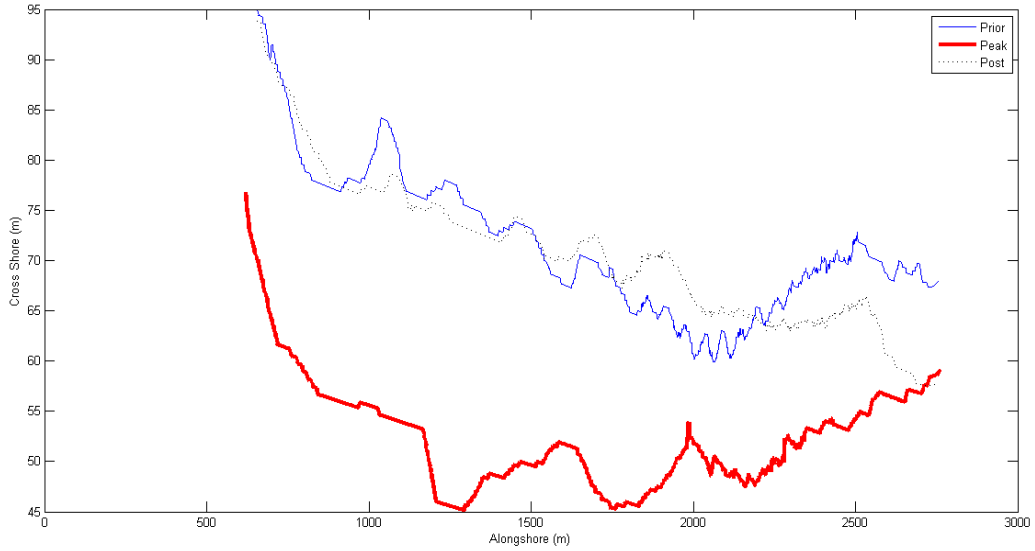

Figure I.12: Storm five alongshore shoreline positions at Tairua Beach.

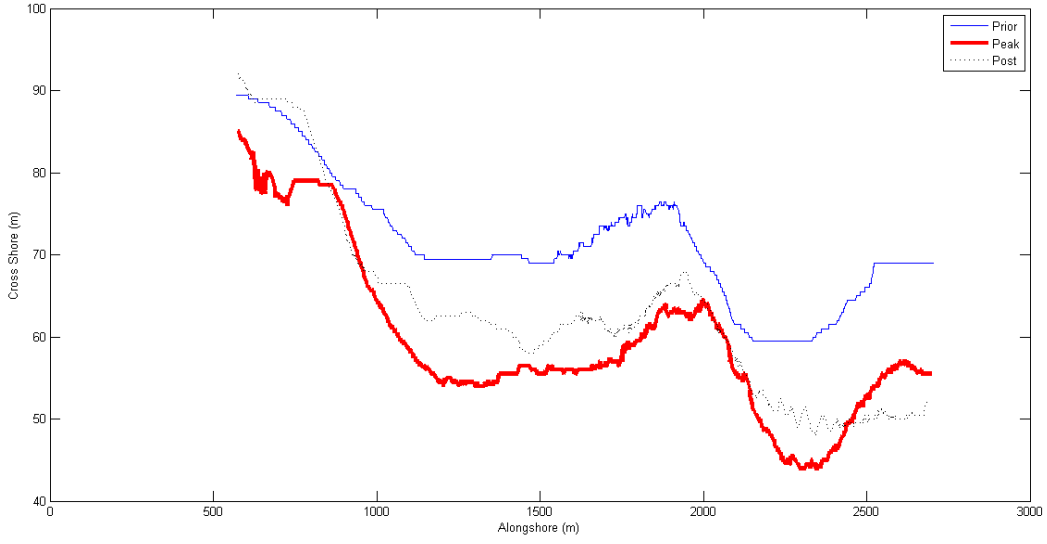

Figure I.13: Storm six alongshore shoreline positions at Tairua Beach.

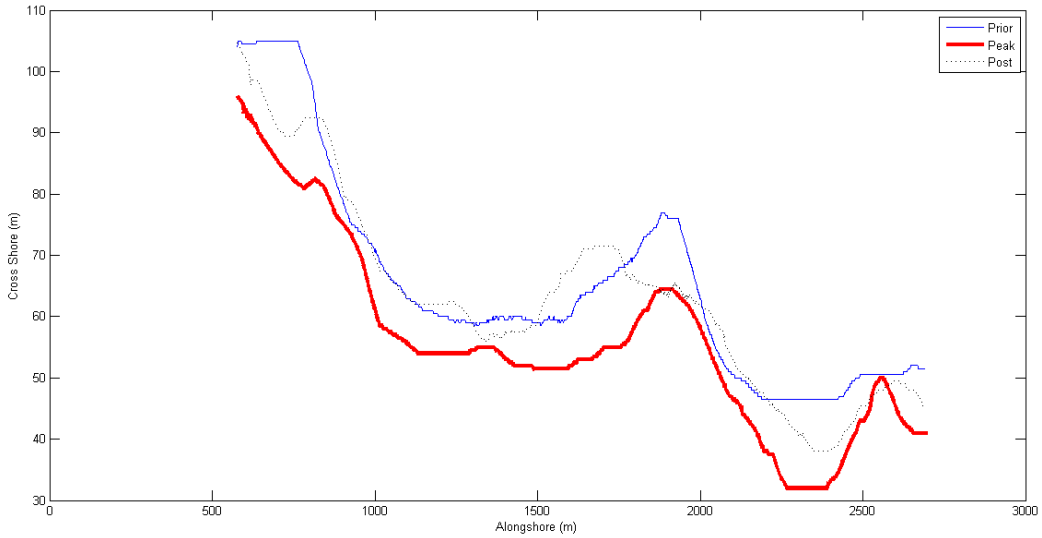

Figure I.14: Storm seven alongshore shoreline positions at Tairua Beach.

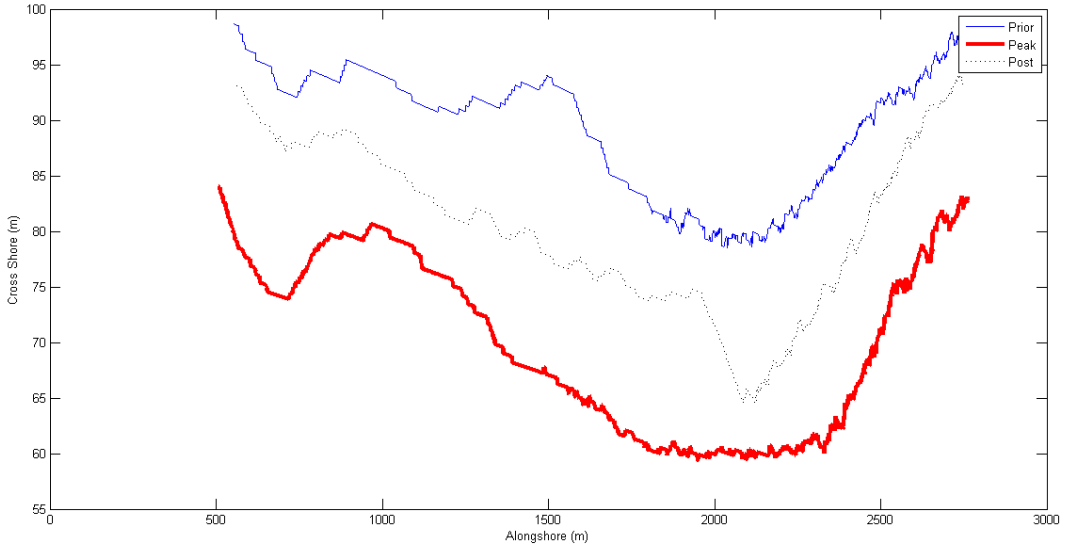

Figure I.15: Storm eight alongshore shoreline positions at Tairua Beach.

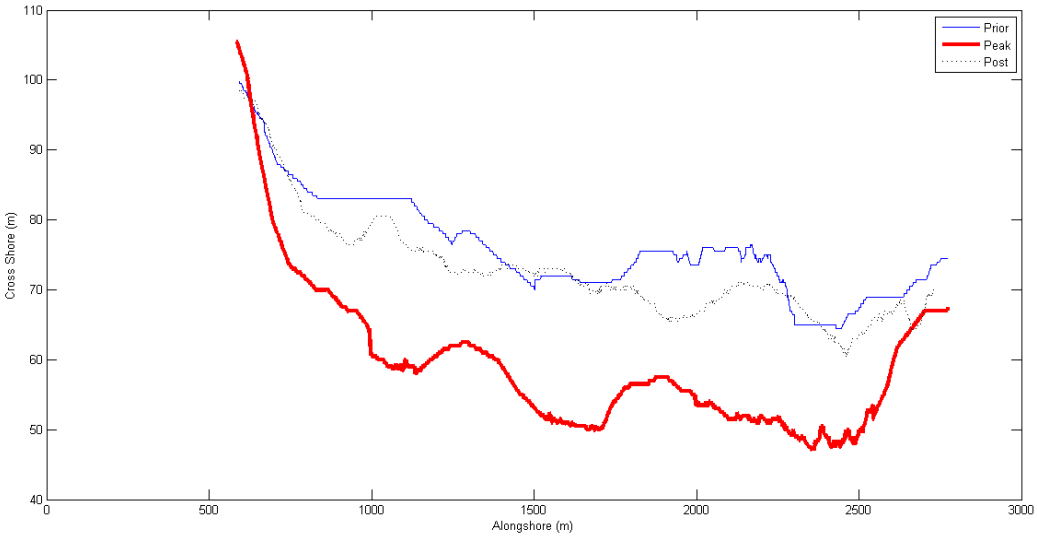

Figure I.16: Storm nine alongshore shoreline positions at Tairua Beach.

Appendix II

Beach Profile Timeseries

Beach profiles are collected at quarterly intervals by Waikato Regional Council at Pauanui Beach. Five profile benchmarks are distributed along the beach as shown in Figure II.1. The northern most profile although included here, is unused during profile analysis as in comparison to the other four, it has a shorter timeseries (begun in 2004). The cross shore beach elevation profiles are provided for all five locations as well as the zero meter contour mark, also referred to as the shoreline position, marked by the thick black line. The locations of each profile are marked on the provided map image, and all cross shore graphs are ordered from North to South according to this image. The y axis shows the cross shore distance with 0m being the most landward location.

Figure II.1: Profile benchmarks along Pauanui Beach as collected by Waikato Regional Council. Taken from Wood (2009).

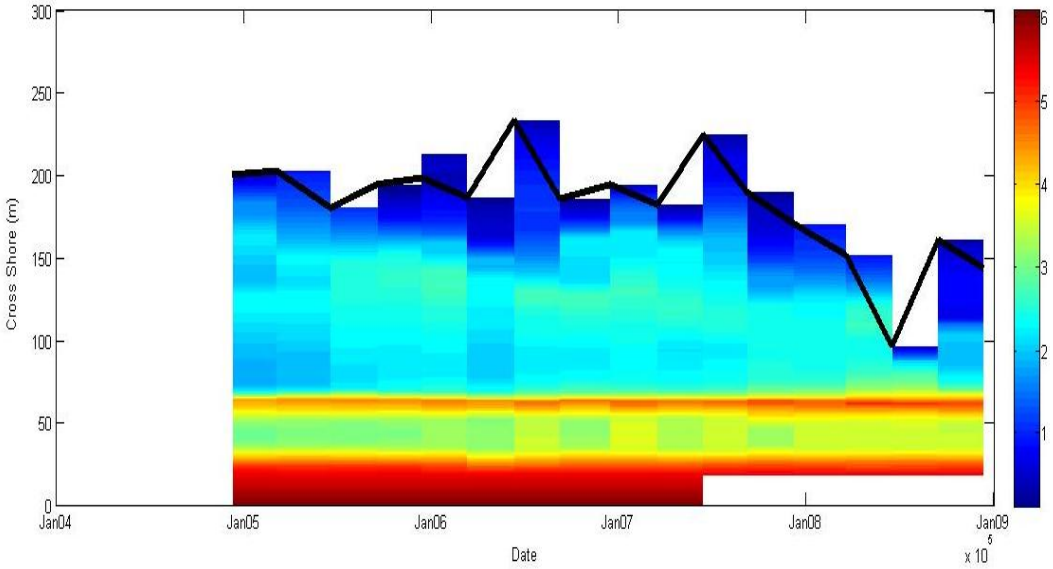

Figure II.2: Cross shore elevation diagram of Pauanui Beach profile CCS72. Colour bar represents the elevation in metres.

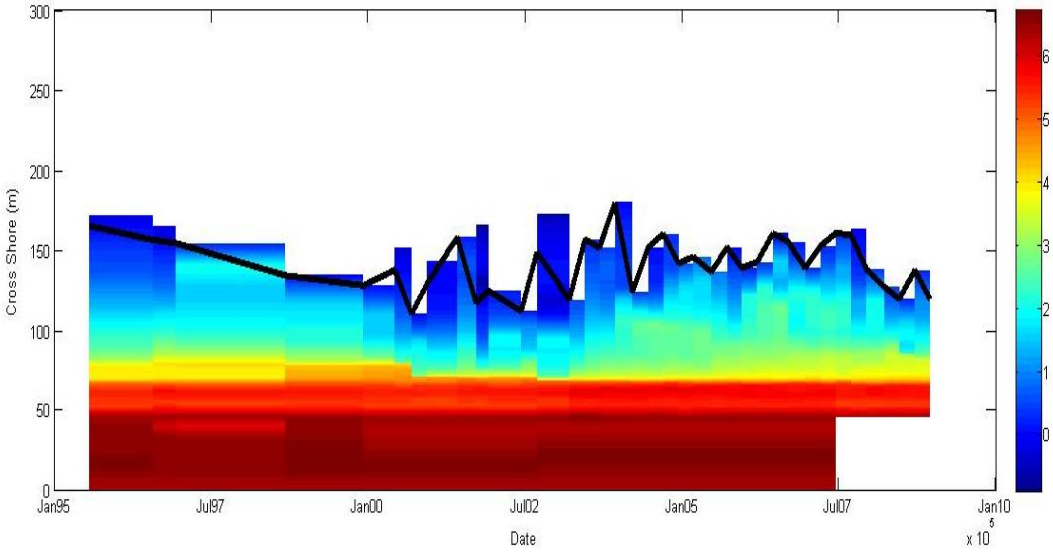

Figure II.3: Cross shore elevation diagram of Pauanui Beach profile CCS38. Colour bar represents the elevation in metres.

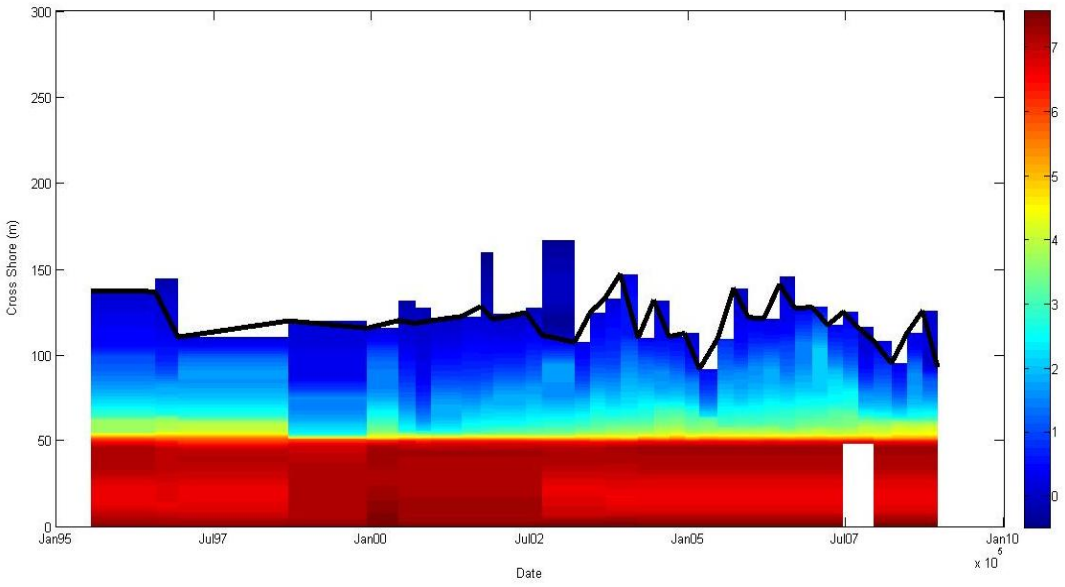

Figure II.4: Cross shore elevation diagram of Pauanui Beach profile CCS39. Colour bar represents the elevation in metres.

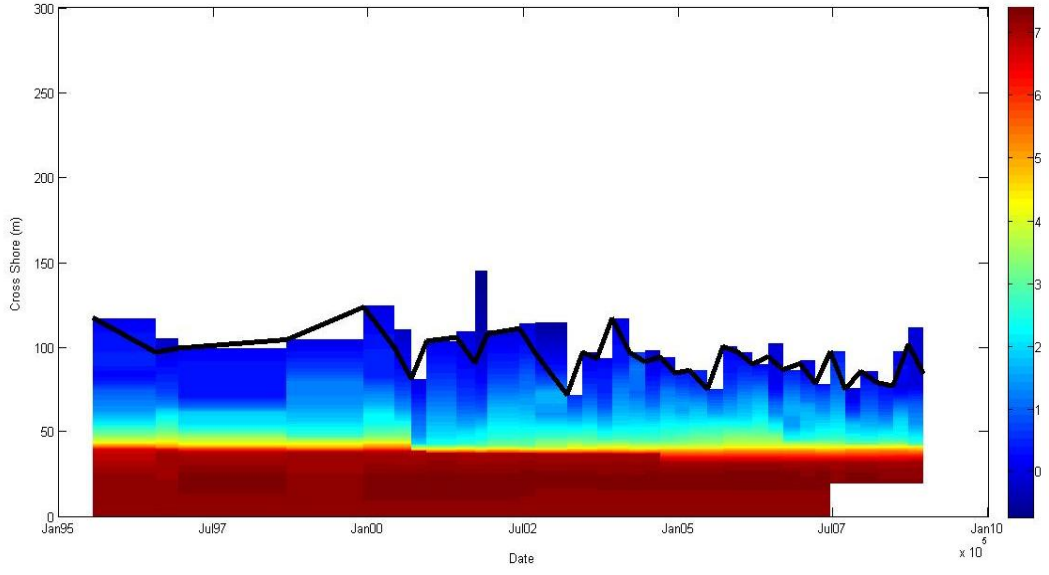

Figure II.5: Cross shore elevation diagram of Pauanui Beach profile CCS40. Colour bar represents the elevation in metres.

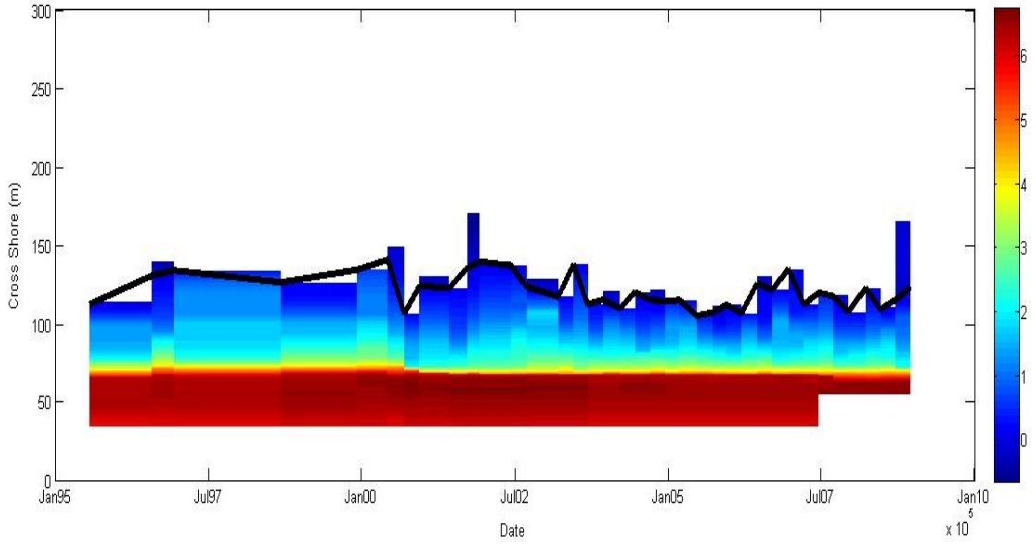

Figure II.6: Cross shore elevation diagram of Pauanui Beach profile CCS70. Colour bar represents the elevation in metres.

Appendix III

Wave Climate Modelling

Wave modelling using SWAN software was completed after unsuccessful attempts using DHI software. A total of 9 model runs were completed that incorporated individual storm characteristics set forth in Table 3-1. Each individual storm was modelled to understand the near shore wave climate, particularly the alongshore variation. Relationships between the alongshore variation in significant wave height, radiation stress and alongshore variation in shoreline position was completed using both Pauanui and Tairua data. Do note that the alongshore extends from the Tairua Harbour entrance (0 m and 0 x-grid) in the north towards the south.

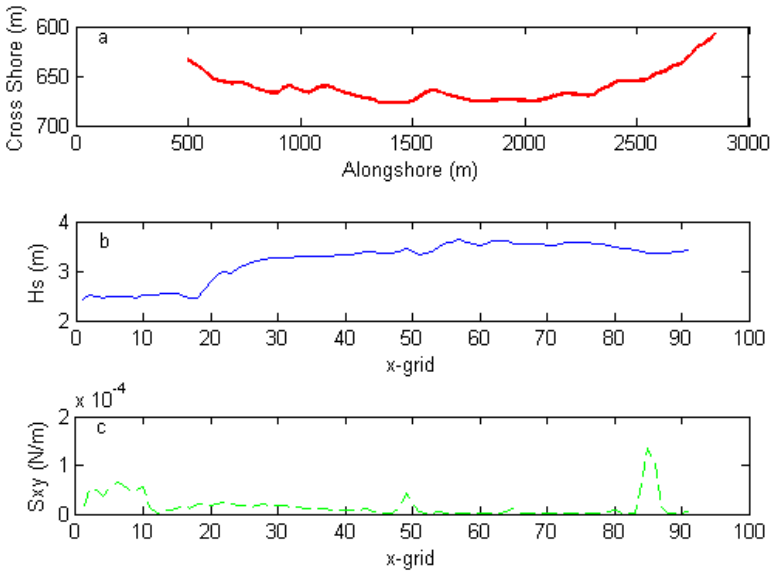

Figure III.1: Comparison of storm one model results for alongshore variation at Pauanui Beach. a) Alongshore shoreline position at Pauanui Beach. b) Significant wave height in the alongshore and c) radiation stress alongshore. X-grid represents the amount of grid cells in the alongshore of the model grid where one grid equals 20 m.

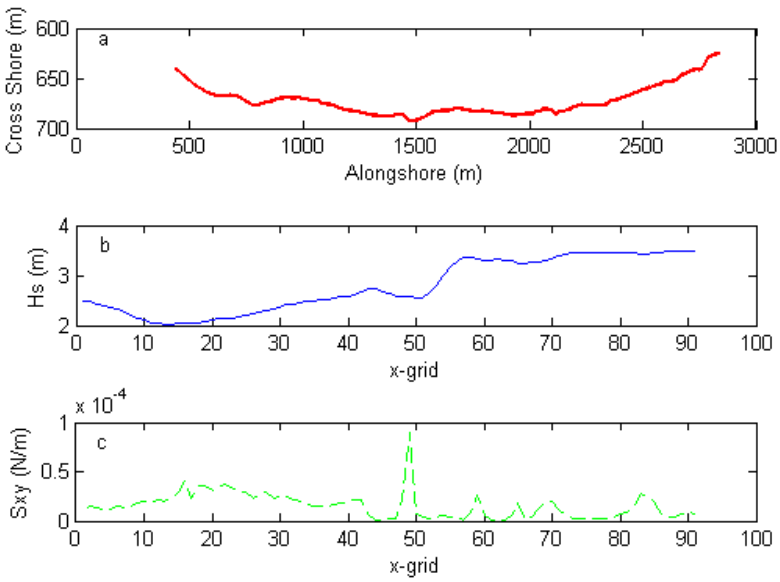

Figure III.2: Comparison of storm two model results for alongshore variation at Pauanui Beach. a) Alongshore shoreline position at Pauanui Beach. b) Significant wave height in the alongshore and c) radiation stress alongshore. X-grid represents the amount of grid cells in the alongshore of the model grid where one grid equals 20 m.

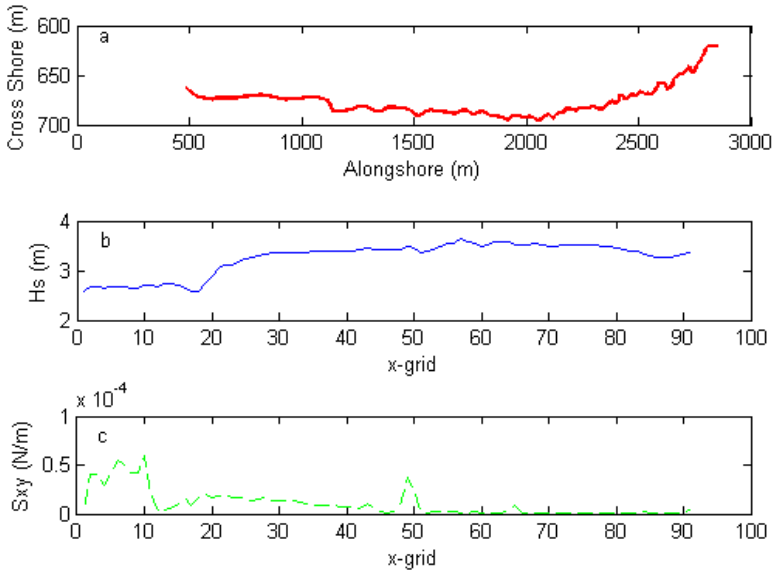

Figure III.3: Comparison of storm three model results for alongshore variation at Pauanui Beach. a) Alongshore shoreline position at Pauanui Beach. b) Significant wave height in the alongshore and c) radiation stress alongshore. X-grid represents the amount of grid cells in the alongshore of the model grid where one grid equals 20 m.

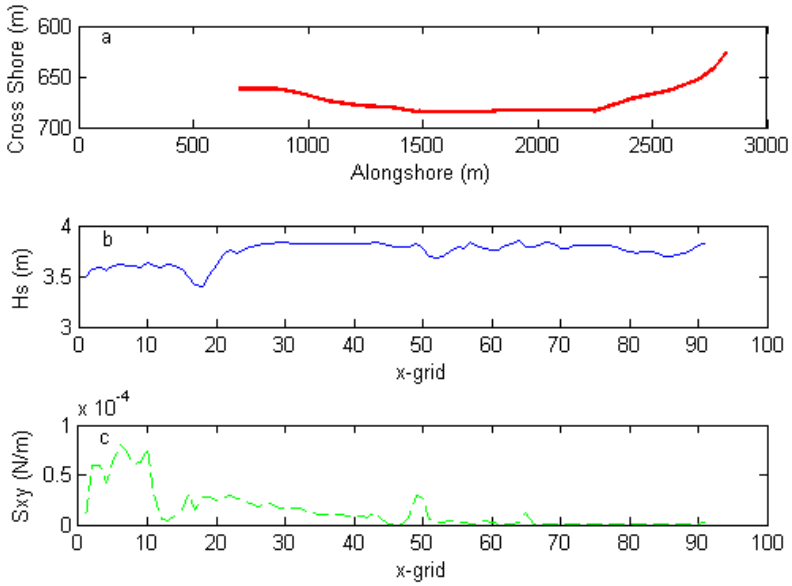

Figure III.4: Comparison of storm four model results for alongshore variation at Pauanui Beach. a) Alongshore shoreline position at Pauanui Beach. b) Significant wave height in the alongshore and c) radiation stress alongshore. X-grid represents the amount of grid cells in the alongshore of the model grid where one grid equals 20 m.

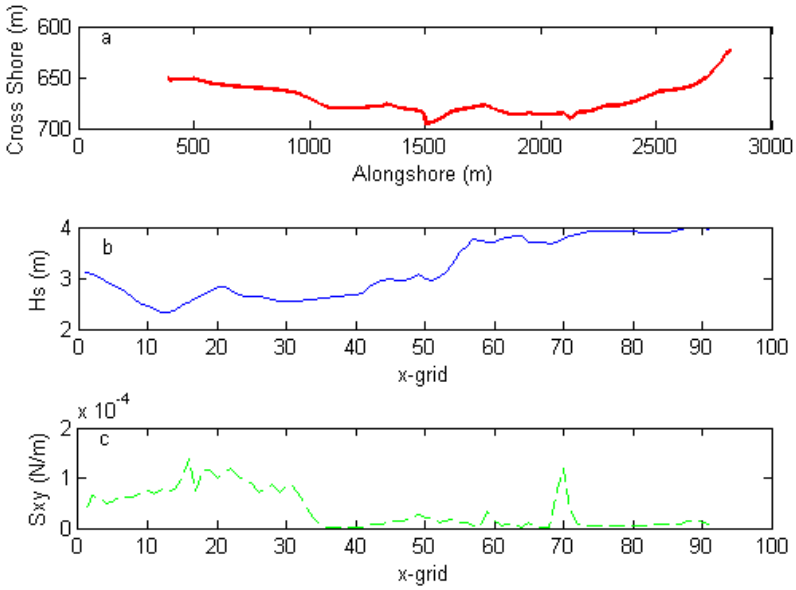

Figure III.5: Comparison of storm five model results for alongshore variation at Pauanui Beach. a) Alongshore shoreline position at Pauanui Beach. b) Significant wave height in the alongshore and c) radiation stress alongshore. X-grid represents the amount of grid cells in the alongshore of the model grid where one grid equals 20 m.

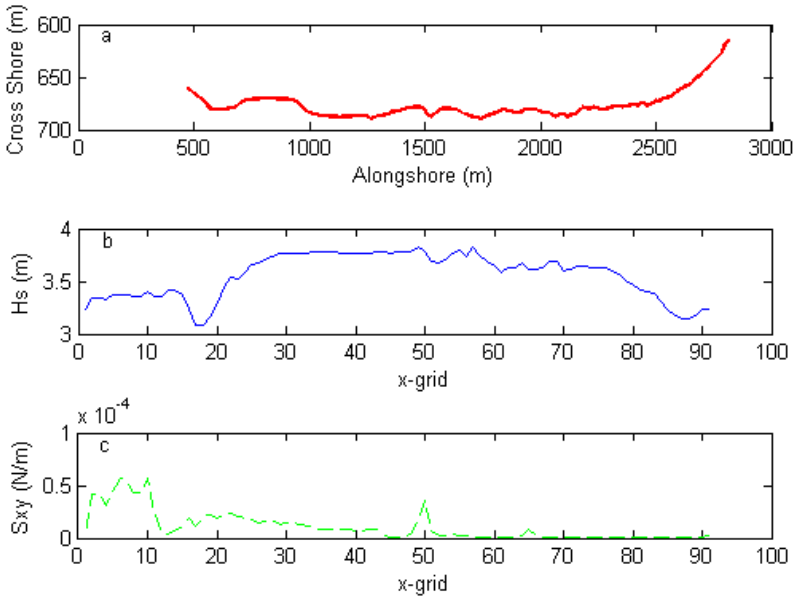

Figure III.6: Comparison of storm six model results for alongshore variation at Pauanui Beach. a) Alongshore shoreline position at Pauanui Beach. b) Significant wave height in the alongshore and c) radiation stress alongshore. X-grid represents the amount of grid cells in the alongshore of the model grid where one grid equals 20 m.

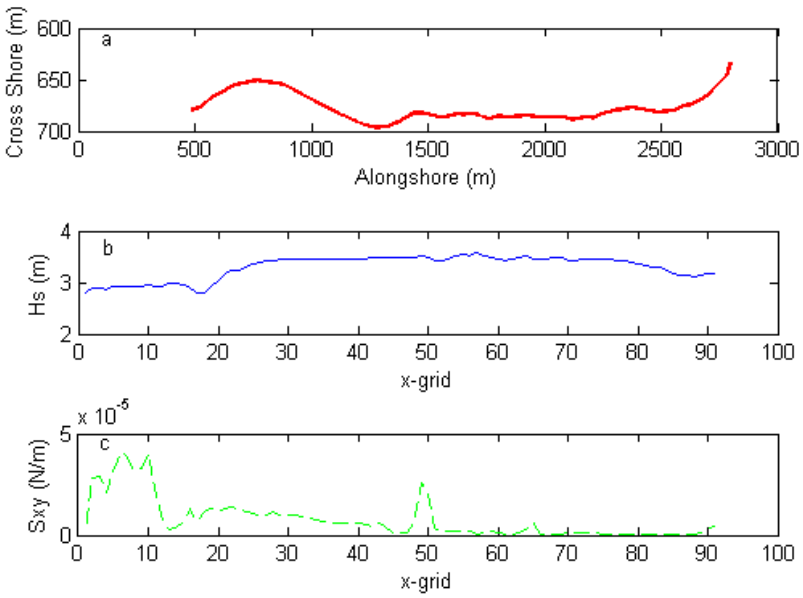

Figure III.7: Comparison of storm seven model results for alongshore variation at Pauanui Beach. **a) Alongshore shoreline position at Pauanui Beach. b) Significant wave height in the alongshore and c) radiation stress alongshore. X-grid represents the amount of grid cells in the alongshore of the model grid where one grid equals 20 m.**

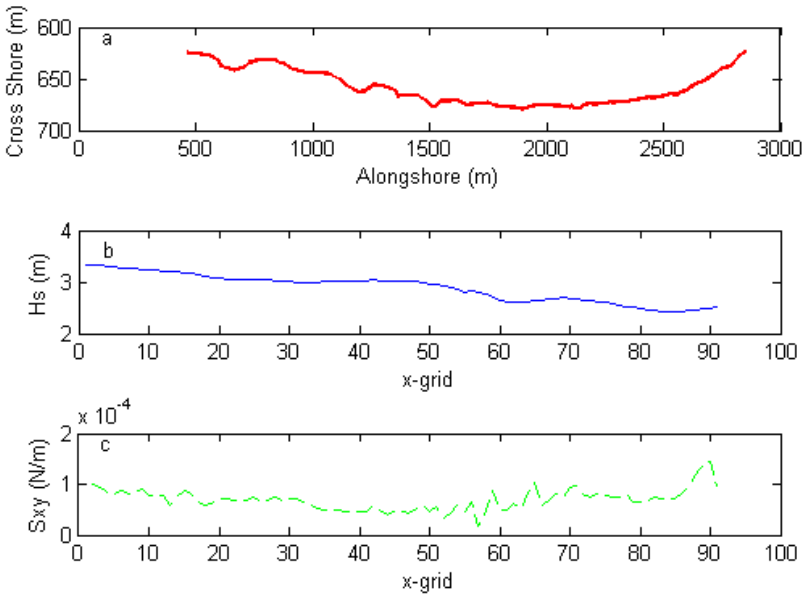

Figure III.8: Comparison of storm eight model results for alongshore variation at Pauanui Beach. a) Alongshore shoreline position at Pauanui Beach. b) Significant wave height in the alongshore and c) radiation stress alongshore. X-grid represents the amount of grid cells in the alongshore of the model grid where one grid equals 20 m.

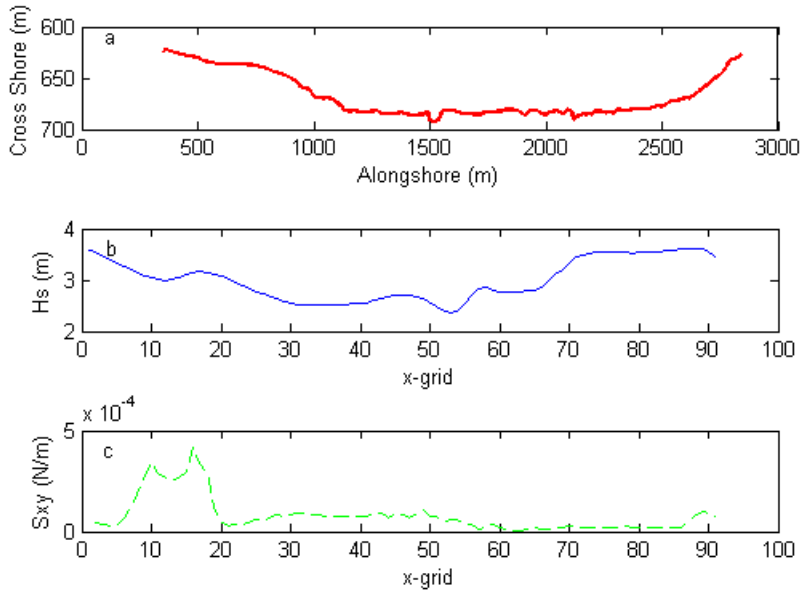

Figure III.9: Comparison of storm nine model results for alongshore variation at Pauanui Beach. a) Alongshore shoreline position at Pauanui Beach. b) Significant wave height in the alongshore and c) radiation stress alongshore. X-grid represents the amount of grid cells in the alongshore of the model grid where one grid equals 20 m.

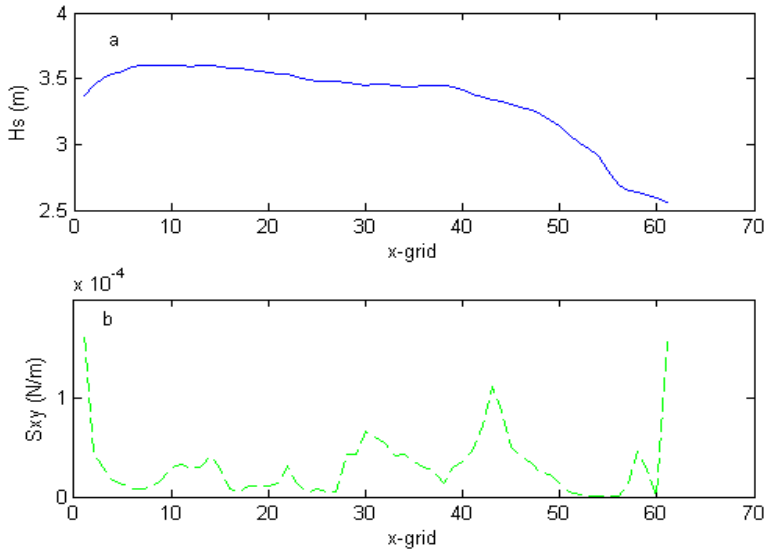

Figure III.10: Comparison of storm one model results for alongshore variation at Tairua Beach. a) Significant wave height in the alongshore. b) Radiation stress alongshore. X-grid represents the amount of grid cells in the alongshore of the model grid where one grid equals 20 m. Due to data gaps no shoreline profile is available.

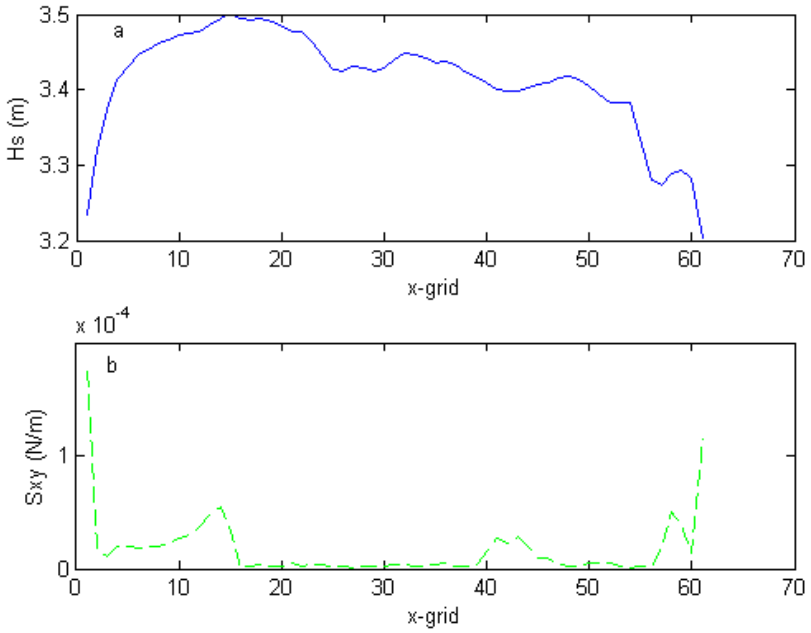

Figure III.11: Comparison of storm two model results for alongshore variation at Tairua Beach. a) Significant wave height in the alongshore. b) Radiation stress alongshore. X-grid represents the amount of grid cells in the alongshore of the model grid where one grid equals 20 m. Due to data gaps no shoreline profile is available.

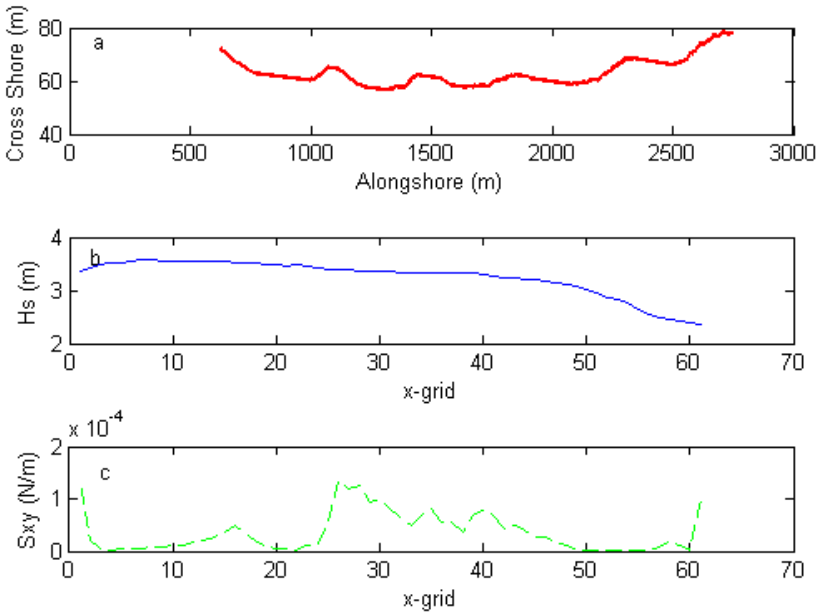

Figure III.12: Comparison of storm three model results for alongshore variation at Tairua Beach. a) Alongshore shoreline position at Pauanui Beach. b) Significant wave height in the alongshore and c) radiation stress alongshore. X-grid represents the amount of grid cells in the alongshore of the model grid where one grid equals 20 m. One alongshore metre on (a) represents 0.5 m.

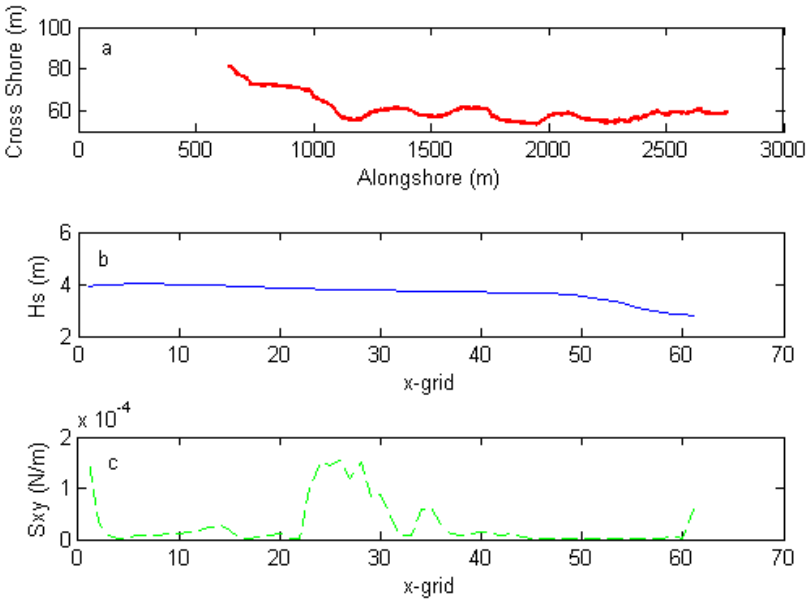

Figure III.13: Comparison of storm four model results for alongshore variation at Tairua Beach. a) Alongshore shoreline position at Pauanui Beach. b) Significant wave height in the alongshore and c) radiation stress alongshore. X-grid represents the amount of grid cells in the alongshore of the model grid where one grid equals 20 m. One alongshore metre on (a) represents 0.5 m.

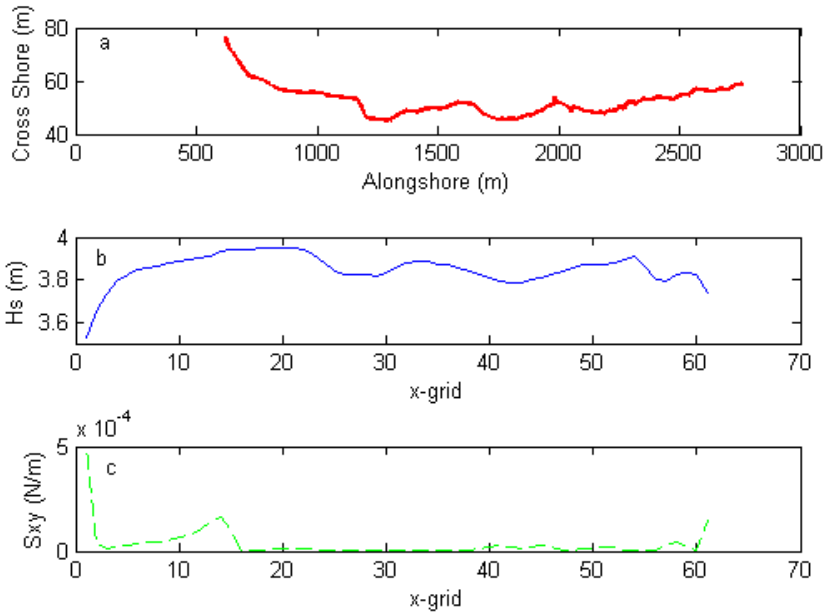

Figure III.14: Comparison of storm five model results for alongshore variation at Tairua Beach. a) Alongshore shoreline position at Pauanui Beach. b) Significant wave height in the alongshore and c) radiation stress alongshore. X-grid represents the amount of grid cells in the alongshore of the model grid where one grid equals 20 m. One alongshore metre on (a) represents 0.5 m.

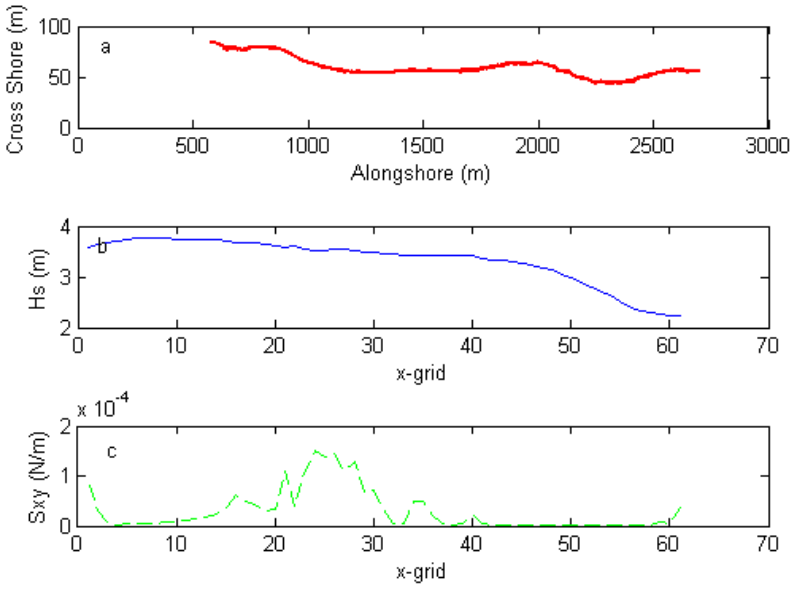

Figure III.15: Comparison of storm six model results for alongshore variation at Tairua Beach. a) Alongshore shoreline position at Pauanui Beach. b) Significant wave height in the alongshore and c) radiation stress alongshore. X-grid represents the amount of grid cells in the alongshore of the model grid where one grid equals 20 m. One alongshore metre on (a) represents 0.5 m.

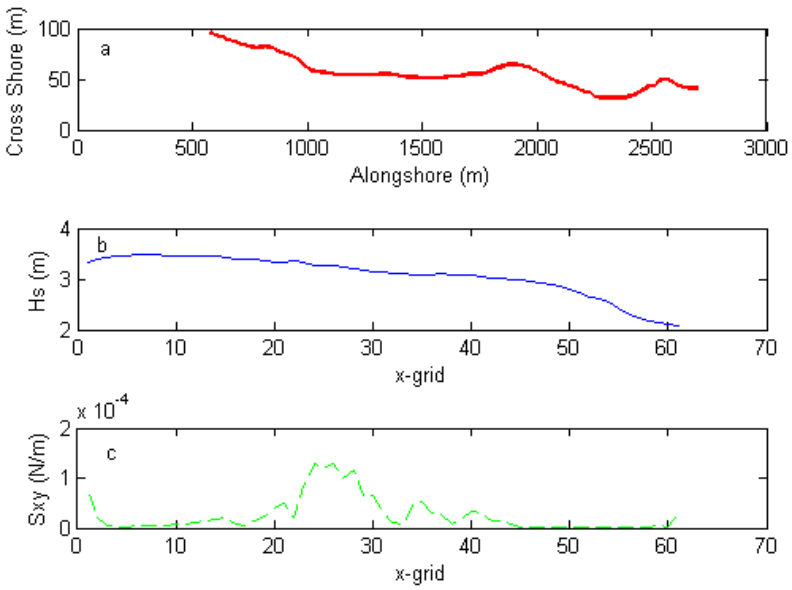

Figure III.16: Comparison of storm seven model results for alongshore variation at Tairua Beach. a) Alongshore shoreline position at Pauanui Beach. b) Significant wave height in the alongshore and c) radiation stress alongshore. X-grid represents the amount of grid cells in the alongshore of the model grid where one grid equals 20 m. One alongshore metre on (a) represents 0.5 m.

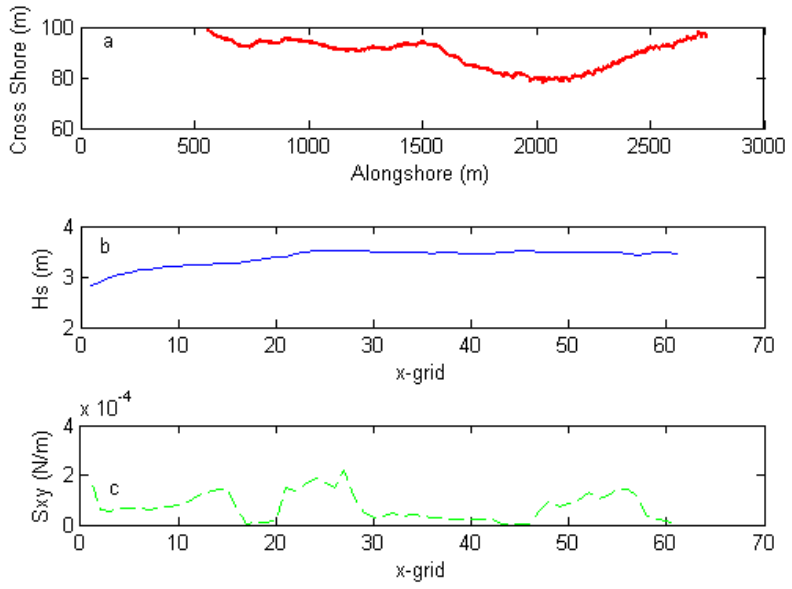

Figure III.17: Comparison of storm eight model results for alongshore variation at Tairua Beach. a) Alongshore shoreline position at Pauanui Beach. b) Significant wave height in the alongshore and c) radiation stress alongshore. X-grid represents the amount of grid cells in the alongshore of the model grid where one grid equals 20 m. One alongshore metre on (a) represents 0.5 m.

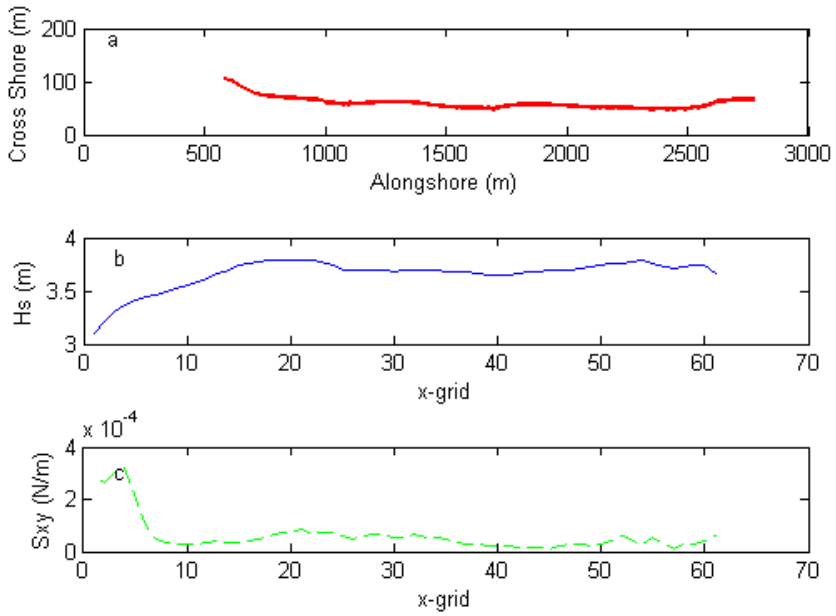

Figure III.18: Comparison of storm nine model results for alongshore variation at Tairua Beach. a) Alongshore shoreline position at Pauanui Beach. b) Significant wave height in the alongshore and c) radiation stress alongshore. X-grid represents the amount of grid cells in the alongshore of the model grid where one grid equals 20 m. One alongshore metre on (a) represents 0.5 m.